Applications of CMOS technology at the ALICE experiment

Domenico Colella
University and INFN Bari
on behalf of the ALICE Collaboration

Contents

Evolution of silicon pixel sensor application in ALICE from LHC Run1 to the future

Contents

Evolution of silicon pixel sensor application in ALICE from LHC Run1 to the future

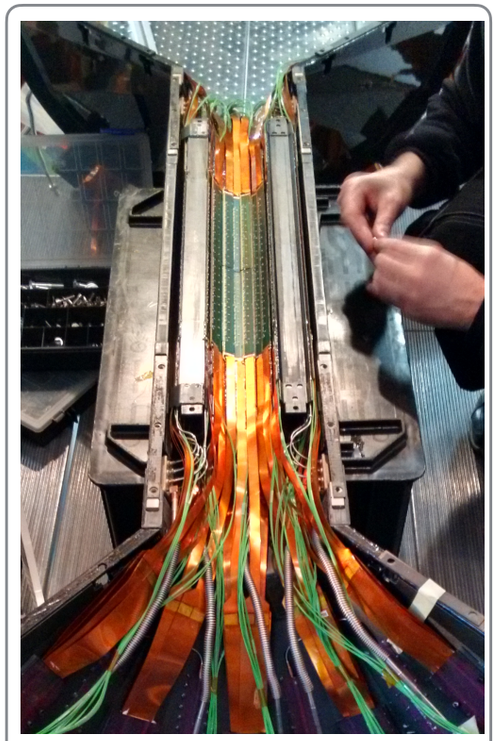

SPD
LHC Run1+2

Contents

Evolution of silicon pixel sensor application in ALICE from LHC Run1 to the future

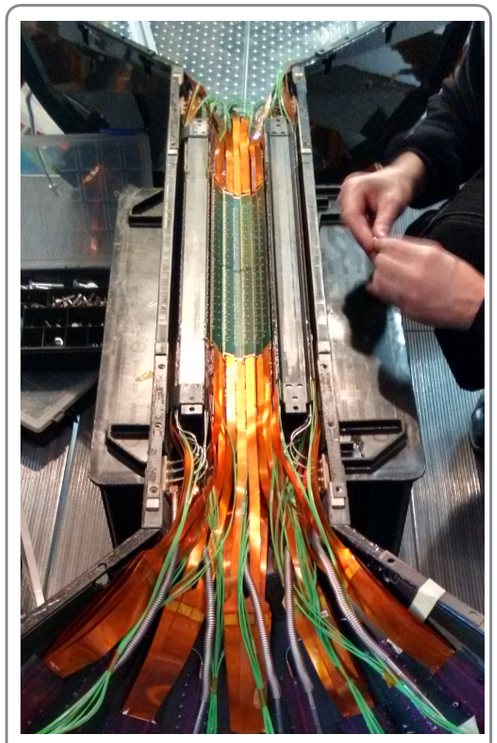

SPD
LHC Run1+2

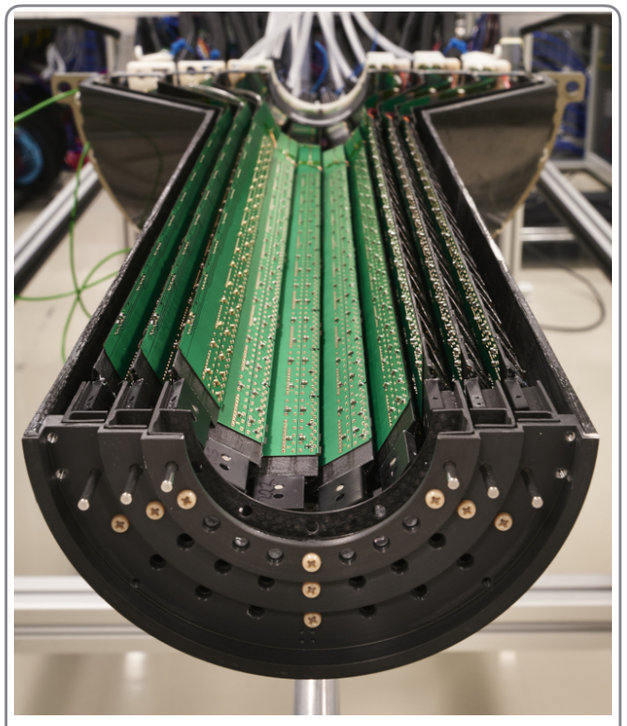

ITS2 + MFT
LHC Run3

Largest MAPS based detector ever built

Contents

Evolution of silicon pixel sensor application in ALICE from LHC Run1 to the future

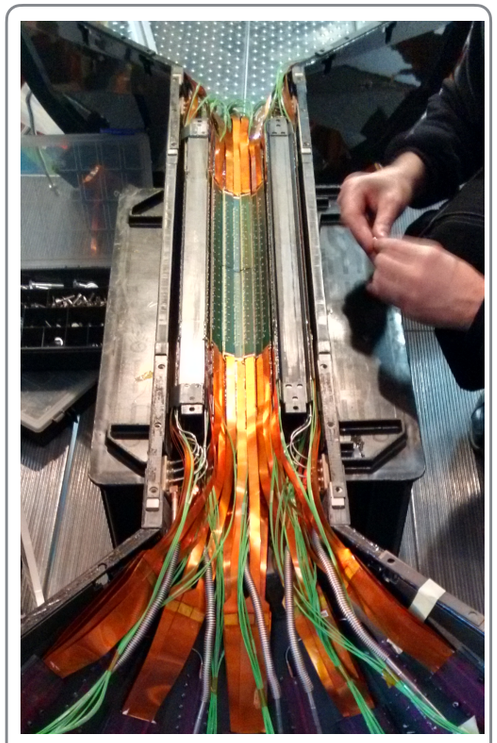

SPD
LHC Run1+2

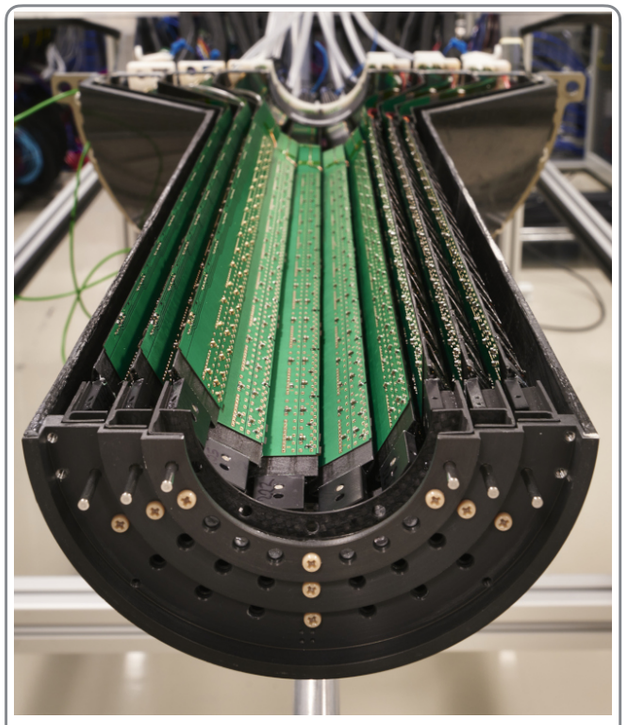

ITS2 + MFT
LHC Run3

Largest MAPS based detector ever built

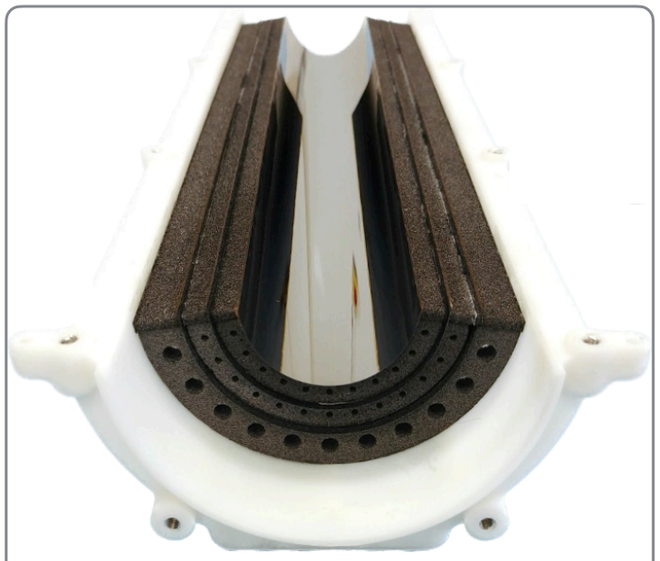

ITS3
LHC Run4

Truly cylindrical detector based on wafer-size sensors in 65 nm CMOS

Contents

Evolution of silicon pixel sensor application in ALICE from LHC Run1 to the future

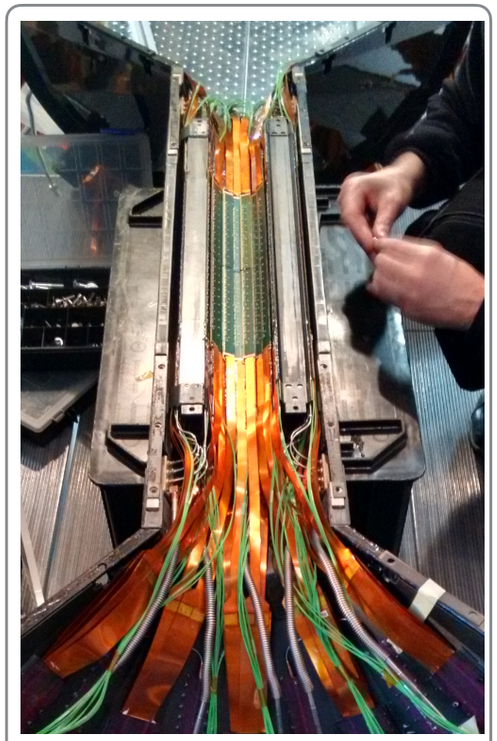

SPD
LHC Run1+2

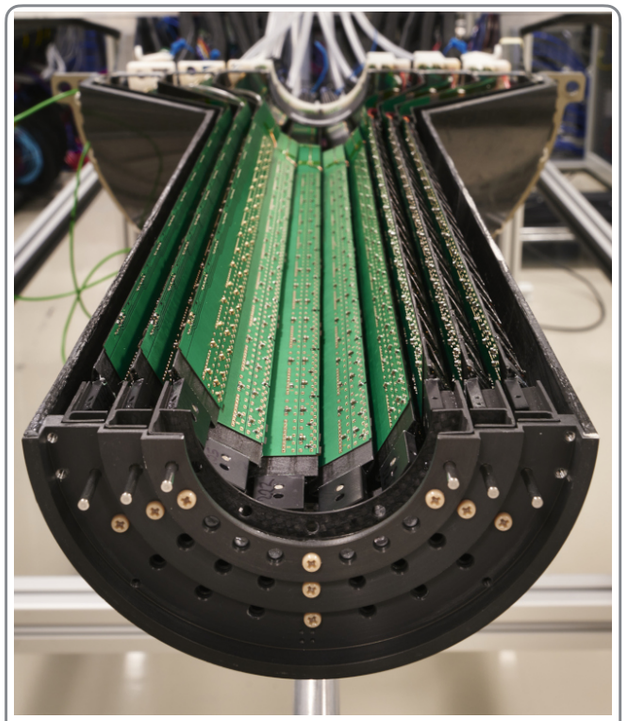

ITS2 + MFT
LHC Run3

Largest MAPS based detector ever built

ITS3
LHC Run4

Truly cylindrical detector based on wafer-size sensors in 65 nm CMOS

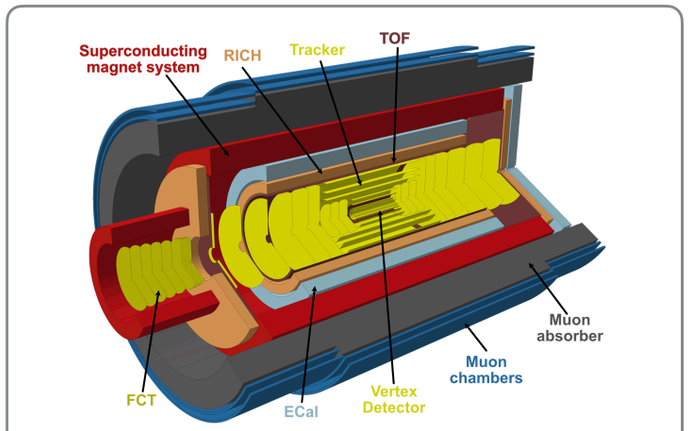

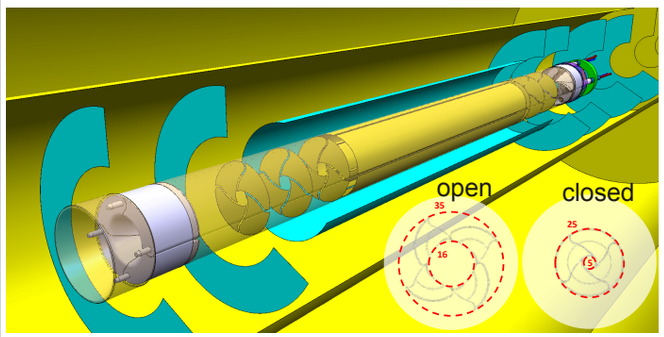

ALICE 3
beyond LHC Run4

Compact all-silicon nearly massless detector

MAPS

(Monolithic Active Pixel Sensor)

for tracking and timing layers

- **ALPIDE leap**
  - ➡ 180 nm CMOS
  - ➡ from partially to fully depleted sensor
- **ITS3 developments**
  - ➡ 65 nm CMOS
  - ➡ stitching technique
  - ➡ sensor bending
- **ALICE3 developments**
  - ➡ in vacuum retractible vertexer
  - ➡ timing performance for TOF

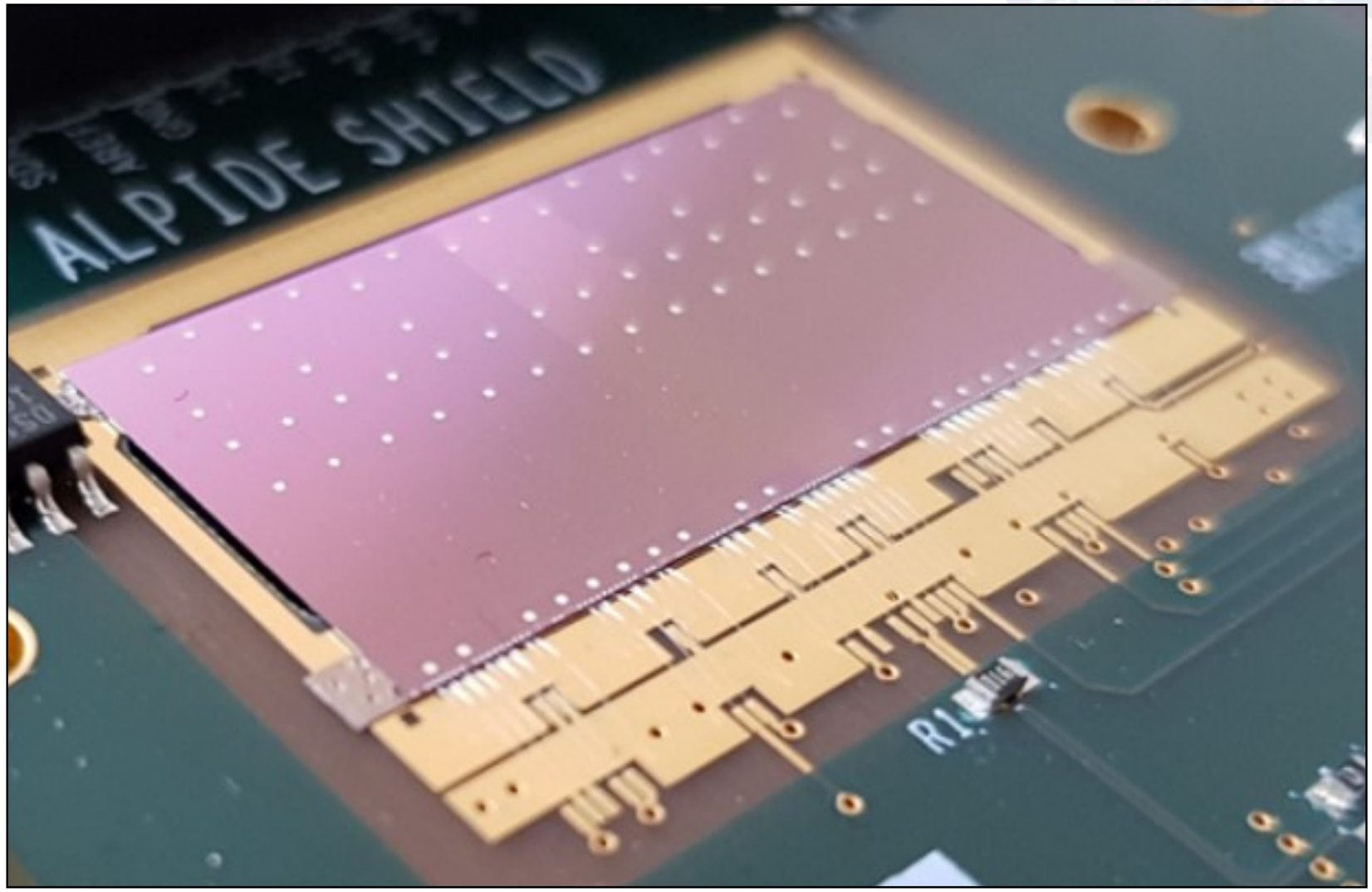

ALPIDE sensor mounted on carrier board

ALICE upgrade for the LS2

ALICE upgrade TDRs
CERN-LHCC-2012-012
CERN-LHCC-2013-024
CERN-LHCC-2013-020
CERN-LHCC-2013-019
CERN-LHCC-2015-006
CERN-LHCC-2015-001

High-precision measurements of rare probes at low p_T requires:

- Improved vertex reconstruction and tracking capabilities
- Gain factor 100 in statistics for minimum-bias trigger
  - the very low S/B ratio prevents selection with hardware trigger
  - read out all interactions up to the maximum LHC Pb-Pb collision rate of 50 kHz

New Inner Tracking System (ITS2)

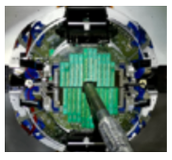

New Muon Forward Tracker (MFT)

New TPC Readout Chambers (ROCs)

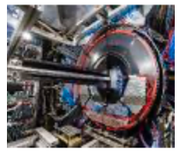

New Fast Interaction Trigger (FIT) detector

Readout upgrade for other detectors

Integrated Online-Offline system (O^2)

ALICE upgrade for the LS2

ALICE upgrade TDRs
CERN-LHCC-2012-012
CERN-LHCC-2013-024
CERN-LHCC-2013-020
CERN-LHCC-2013-019
CERN-LHCC-2015-006
CERN-LHCC-2015-001

High-precision measurements of rare probes at low p_T requires:

- Improved vertex reconstruction and tracking capabilities
- Gain factor 100 in statistics for minimum-bias trigger
  - the very low S/B ratio prevents selection with hardware trigger
  - read out all interactions up to the maximum LHC Pb-Pb collision rate of 50 kHz

New Inner Tracking System (ITS2)

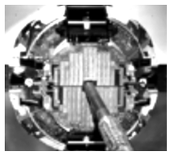

New Muon Forward Tracker (MFT)

New TPC Readout Chambers (ROCs)

New Fast Interaction Trigger (FIT) detector

Readout upgrade for other detectors

Integrated Online-Offline system (O^2)

Inner Tracking System upgrade

Requirements

» Improve impact parameter resolution
- Reduce IP-to-first layer distance (new beam pipe) → *22 mm*
- Reduce material budget → *0.36% X/X_0 (Innermost layers)*
- Reduce pixel size → *~30 x 30 μm²*

» Improve tracking efficiency and p_T resolution at low p_T
- Increase granularity → *from 6 to 7 layers, all pixels*
- Increase readout capabilities → *from 1 kHz to 100 kHz*

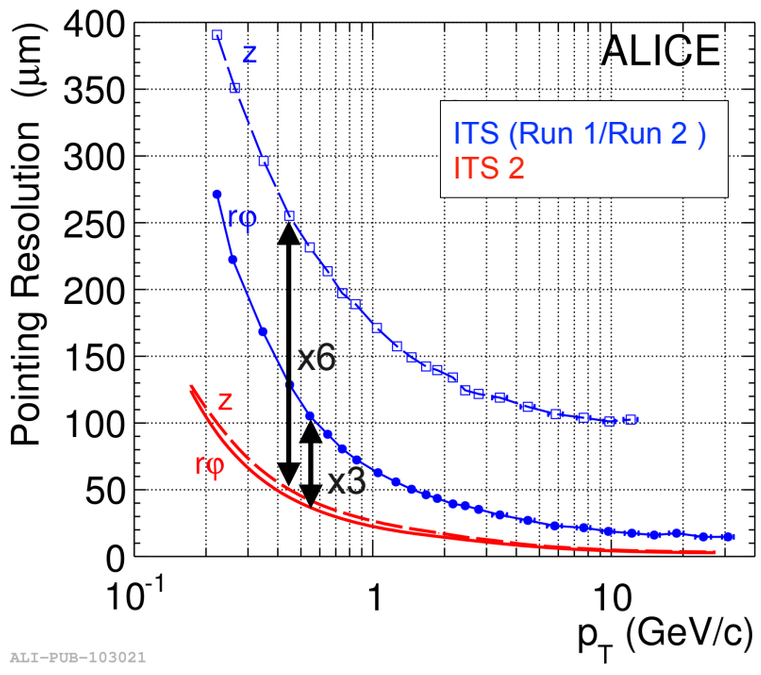

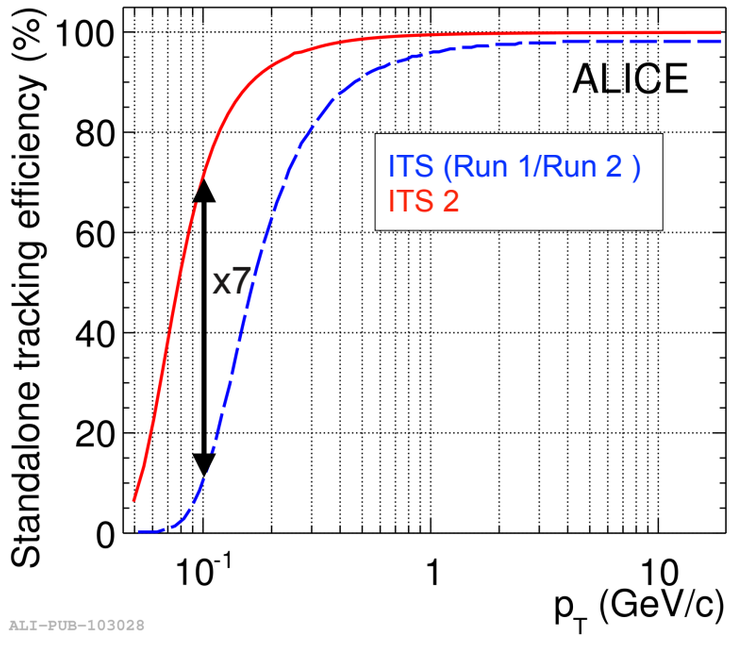

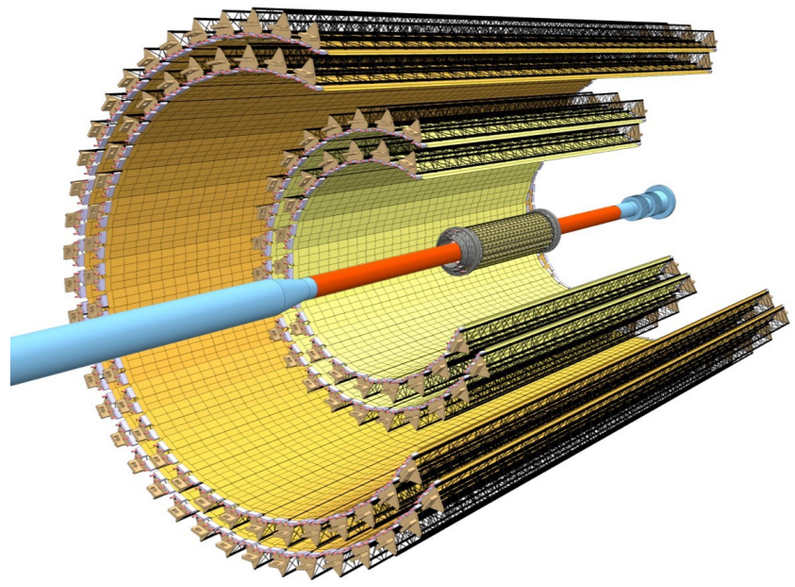

10 m² active silicon area
12.5×10⁹ pixels

Inner Tracking System upgrade

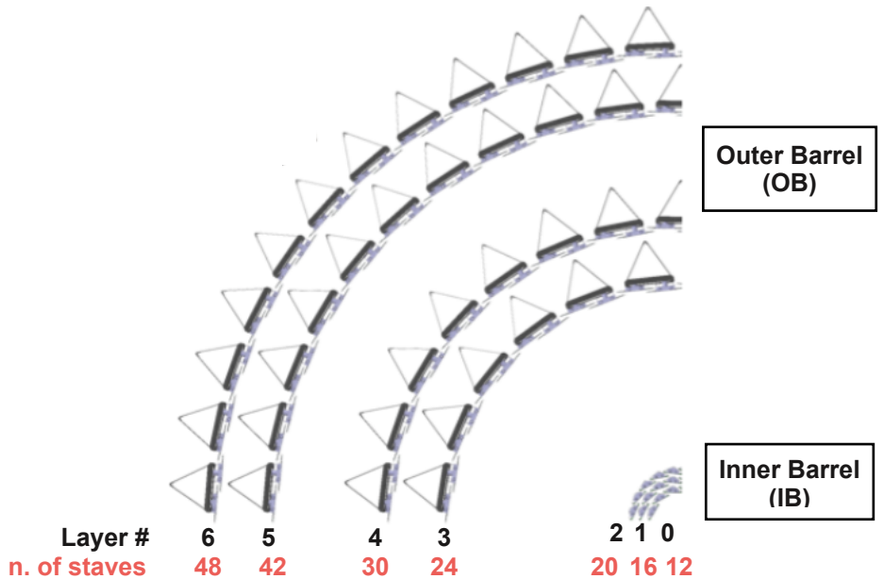

<u>7-layer barrel geometry based on MAPS</u>

» Inner Barrel (IB) : 3 layers
» Outer Barrel (OB) : 4 layers
» r coverage: (min) 22 – (max) 394 mm
» η coverage: (min) 1.3 – (max) 2.5

Inner Barrel stave

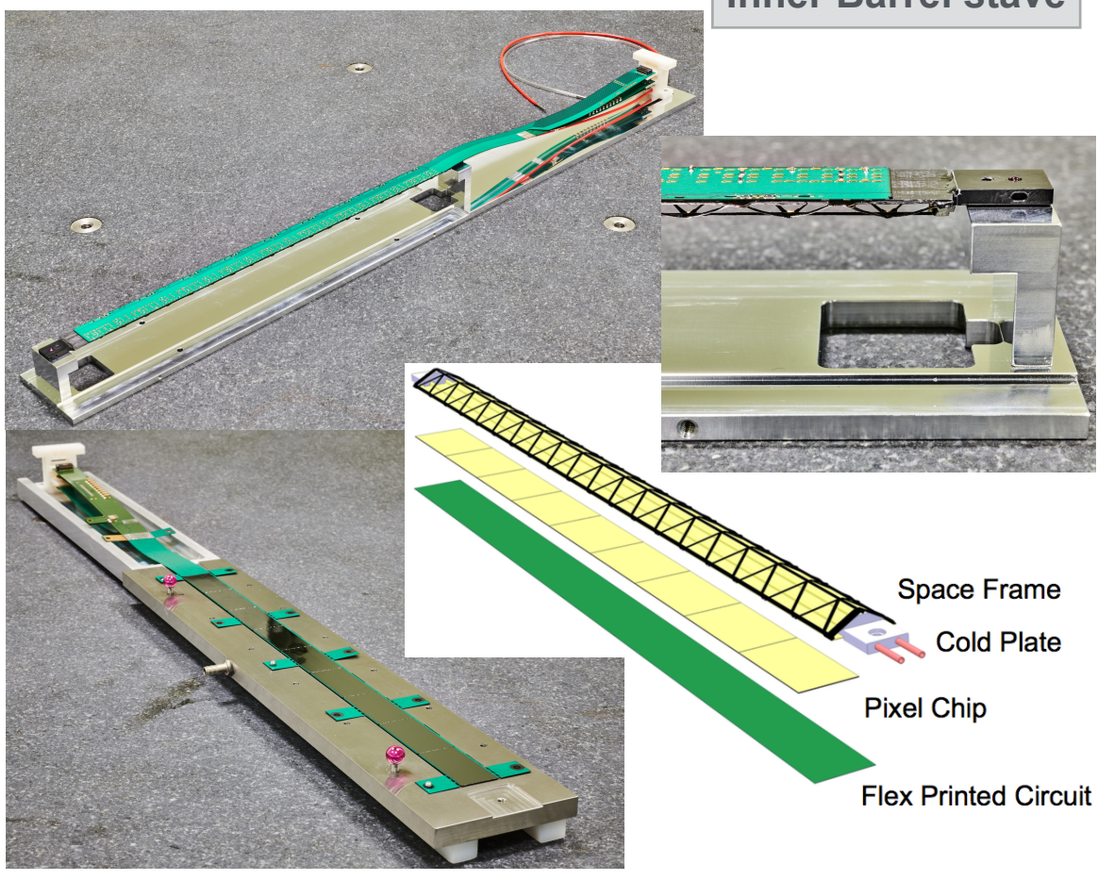

Outer Barrel stave

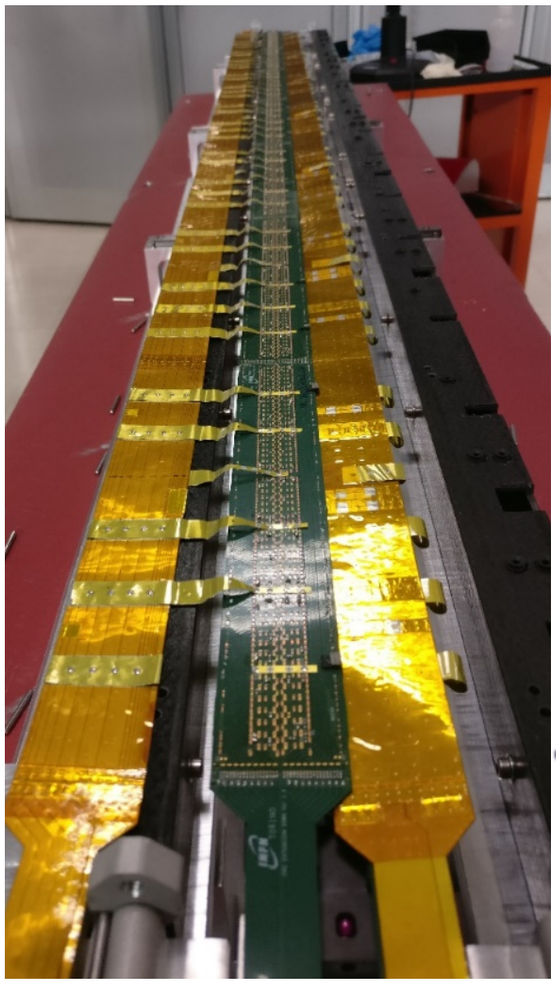

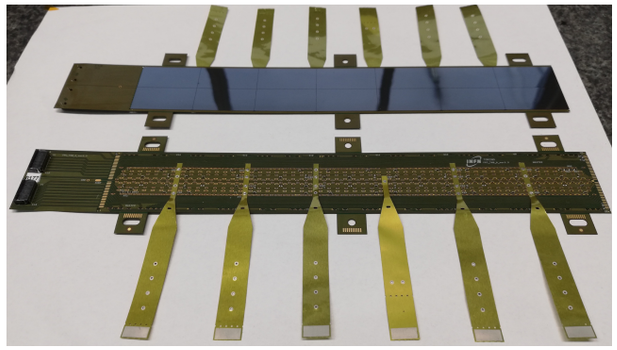

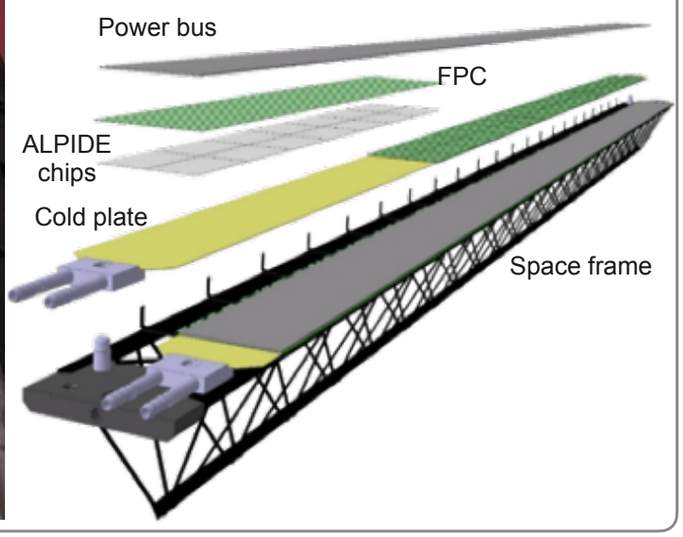

Inner Tracking System upgrade

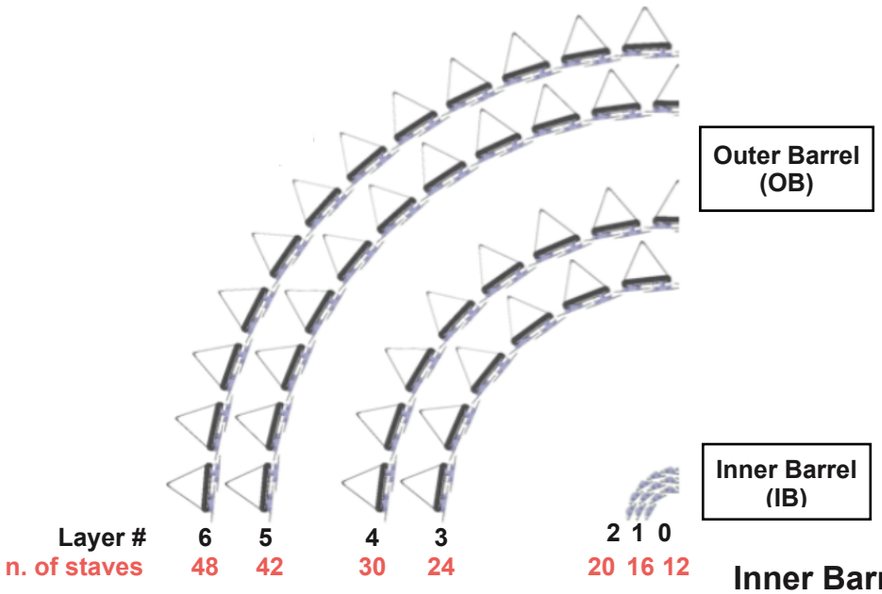

<u>7-layer barrel geometry based on MAPS</u>

» Inner Barrel (IB) : 3 layers
» Outer Barrel (OB) : 4 layers
» r coverage: (min) 22 – (max) 394 mm
» η coverage: (min) 1.3 – (max) 2.5

Inner Barrel Top

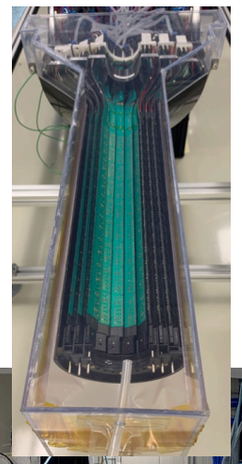

Inner Barrel Bottom

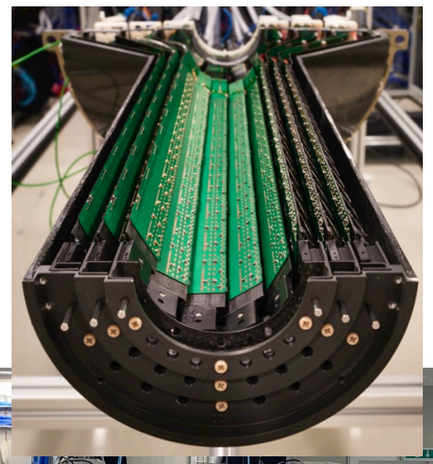

Outer Barrel Top

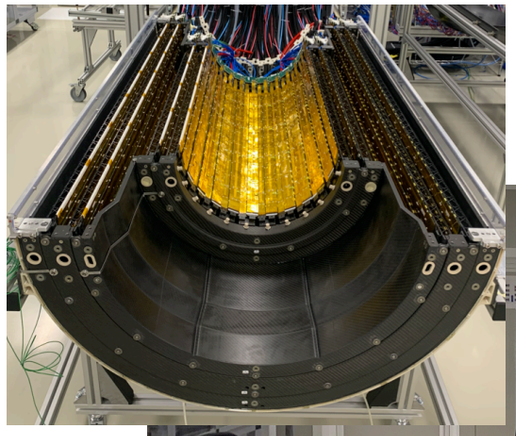

Outer Barrel Bottom

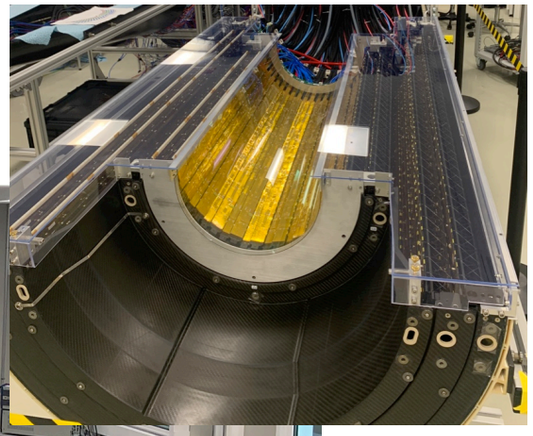

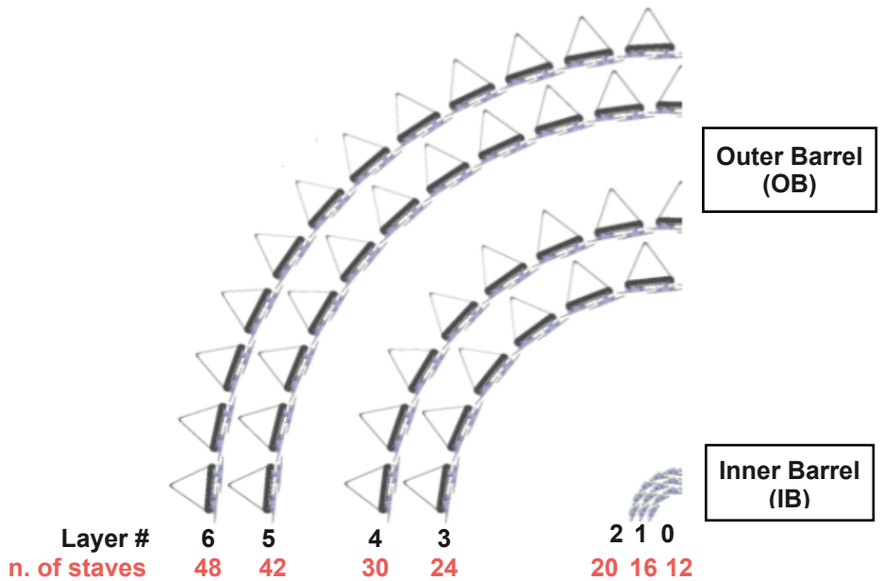

Inner Tracking System upgrade

7-layer barrel geometry based on MAPS

» Inner Barrel (IB) : 3 layers
» Outer Barrel (OB) : 4 layers
» r coverage: (min) 22 – (max) 394 mm
» η coverage: (min) 1.3 – (max) 2.5

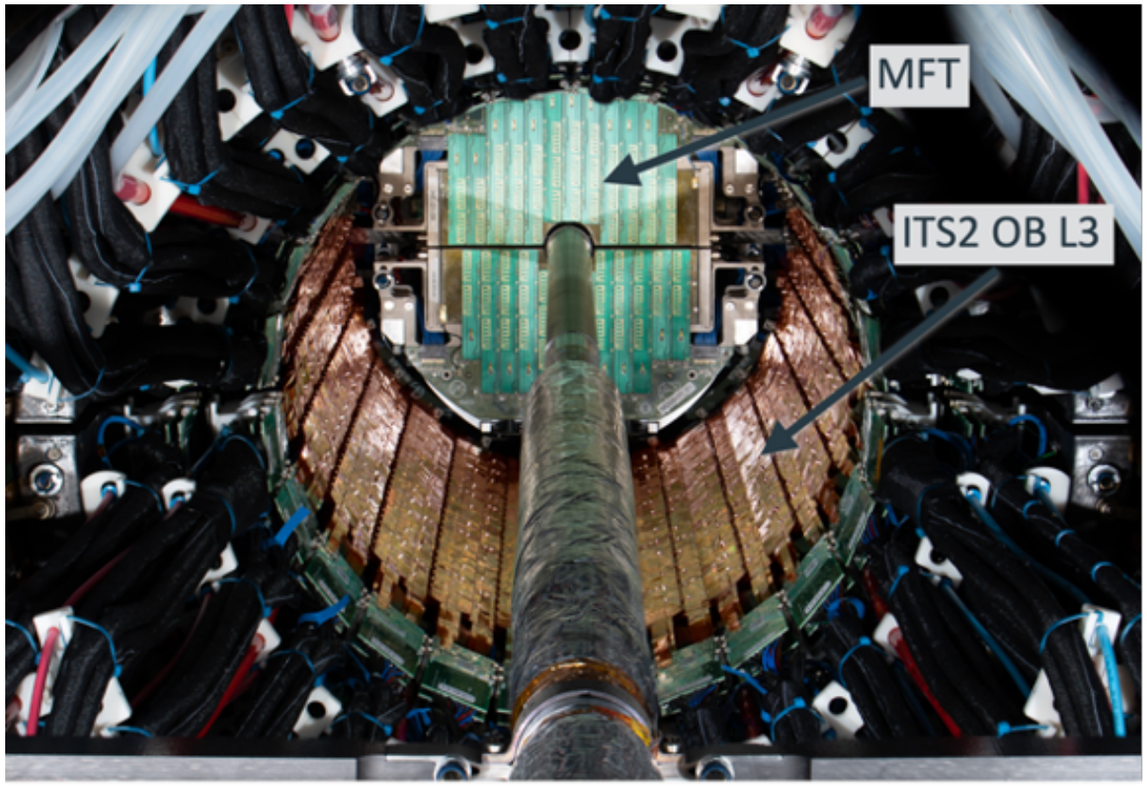

ITS Outer Barrel surrounding the beam pipe, MFT in the back

ITS Inner Barrel Bottom and Outer Barrel

Inner Tracking System upgrade

2012 ← Research & Development
- Conceptual Design Report: Sep '12
- Technical Design Report: Nov '13

Dec '16 ← Detector construction and assembly
- ~72000 chips —> ~2600 Hybrid Integrated Circuits (HICs) —> ~280 staves
- > 10 production sites worldwide
- ~ 30 institutes involved

May '19 ← On-surface commissioning w/ final services
- 24/7 operation with ~200 shifters from ~30 institutes
- Calibration runs, cosmic muon data taking
- Key to spot potential issues early
- Valuable input for the planning of the installation

Dec '20

Jan '21 ← Services installation in the cavern

Mar '21 ← Outer Barrel installation

May '21 ← Inner Barrel installation

Jul '21 ← Verification of the detector

← Global commissioning

Oct '21 ← Pilot beam test

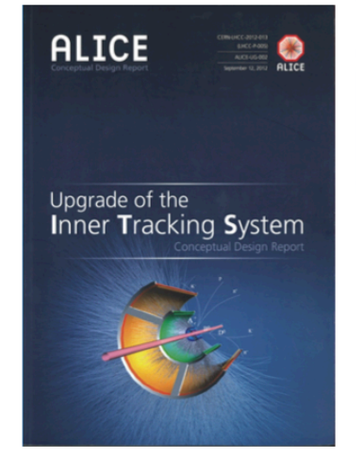

Conceptual Design Report

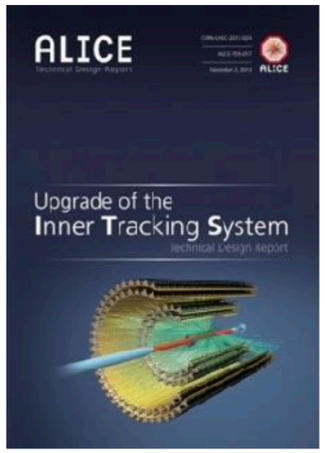

Technical Design Report

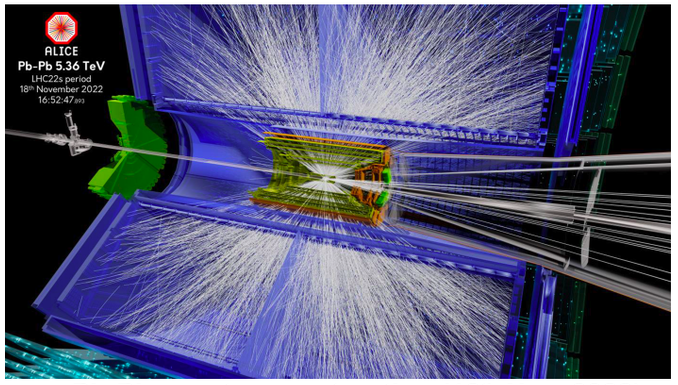

Pb-Pb event reconstruction (18th Nov. 2022)

Ten years from conceptual design to first event reconstruction and almost 30 institutes from more than 10 countries involved!

180 nm CMOS technology: sensor details

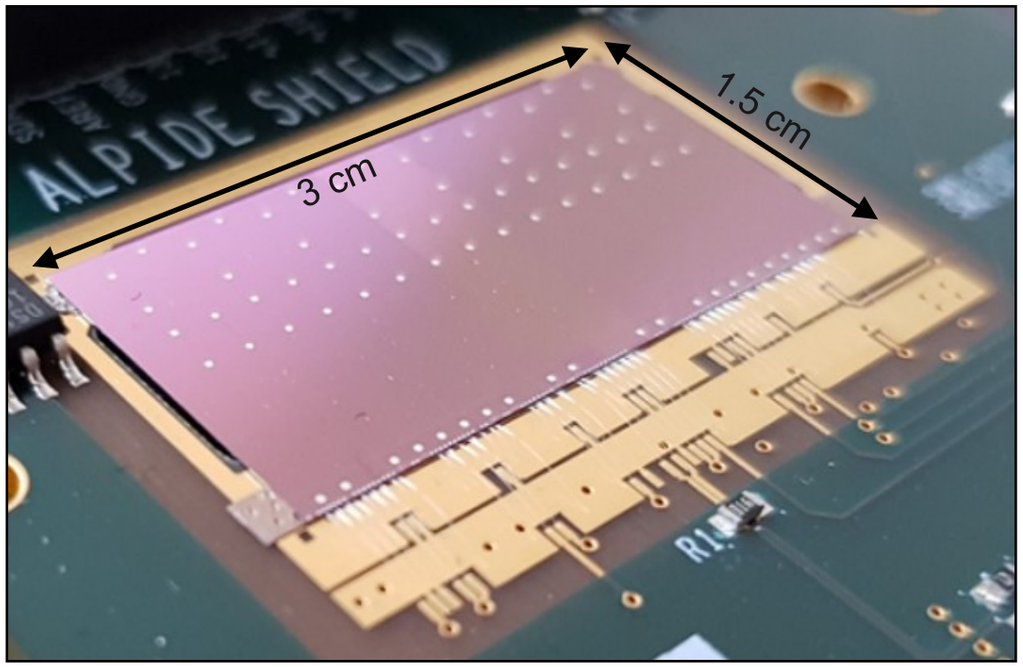

J. NIMA 765 (2014) 177–182

» MAPS development for ALICE ITS2 detector @LHC (2021) → **ALPIDE**

- pixel dimensions: 28 x 28 μm²
- matrix: 512 × 1024 pixels (524k)
- CMOS technology: TowerJazz 0.18 μm
- power budget: 40 mW/cm²

- Detection layer: 25 μm high-resistivity (> 1 kΩcm) epitaxial layer
- DEEP P-WELL to shield CMOS circuitry and avoid loss of efficiency
  → charge collected from the non-depleted zone by diffusion and prone to trapping after irradiation
- Total thickness: 50 μm

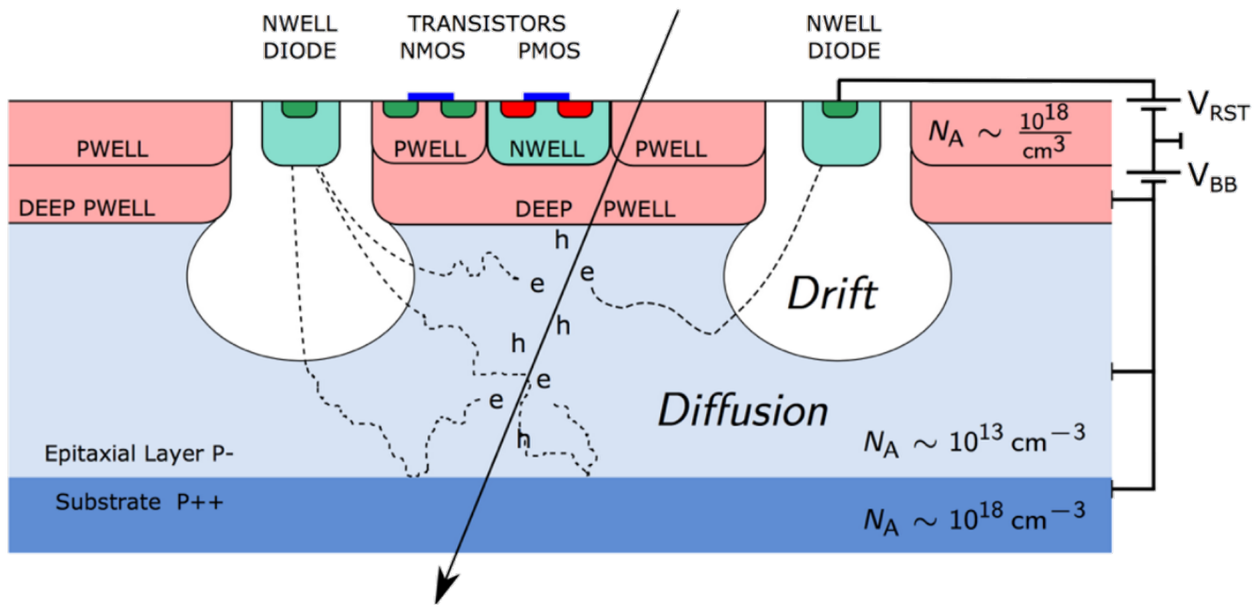

180 nm CMOS technology: sensor details

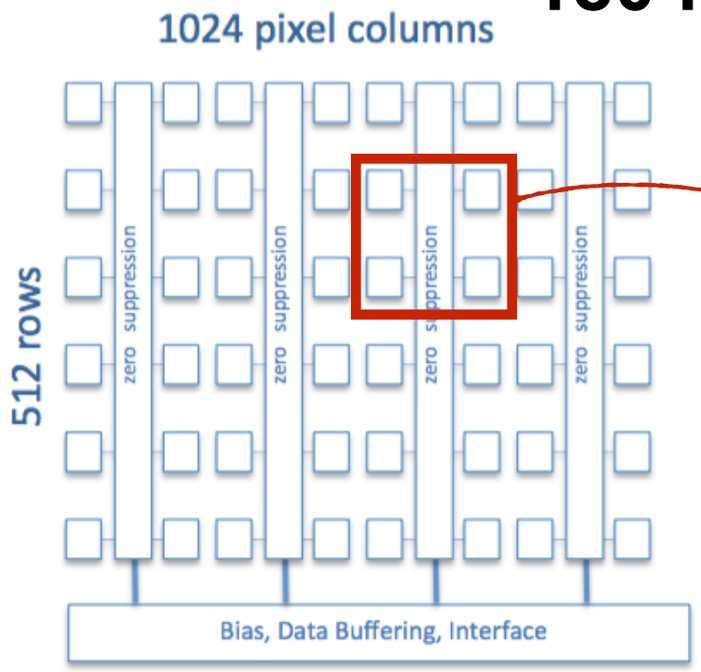

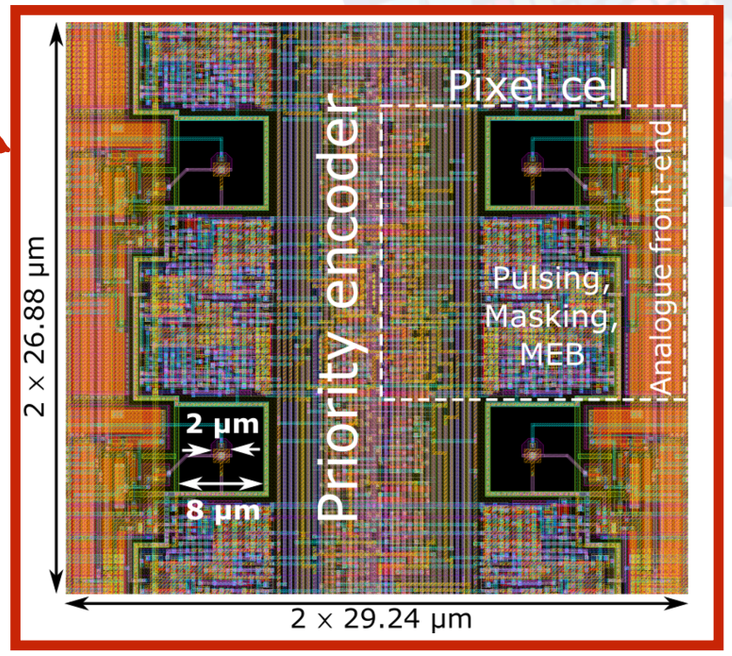

» In-pixel front-end
- Analog signal formation
  (9 transistors, full-custom)
- Multiple-event memory: 3 stages
  (62 transistors, full-custom)
- Configuration: pulsing & masking registers
  (31 transistors, full-custom)
- Testing: analogue & digital pulse circuitry
  (17 transistors, full-custom)

O(200) transistors / pixel

Single pixel readout mechanism

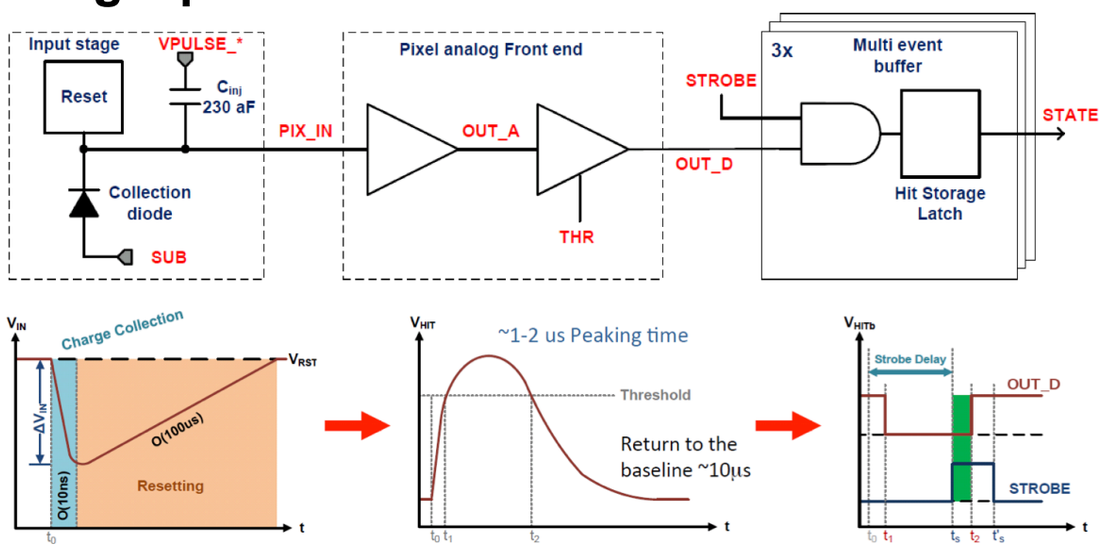

180 nm CMOS technology: sensor details

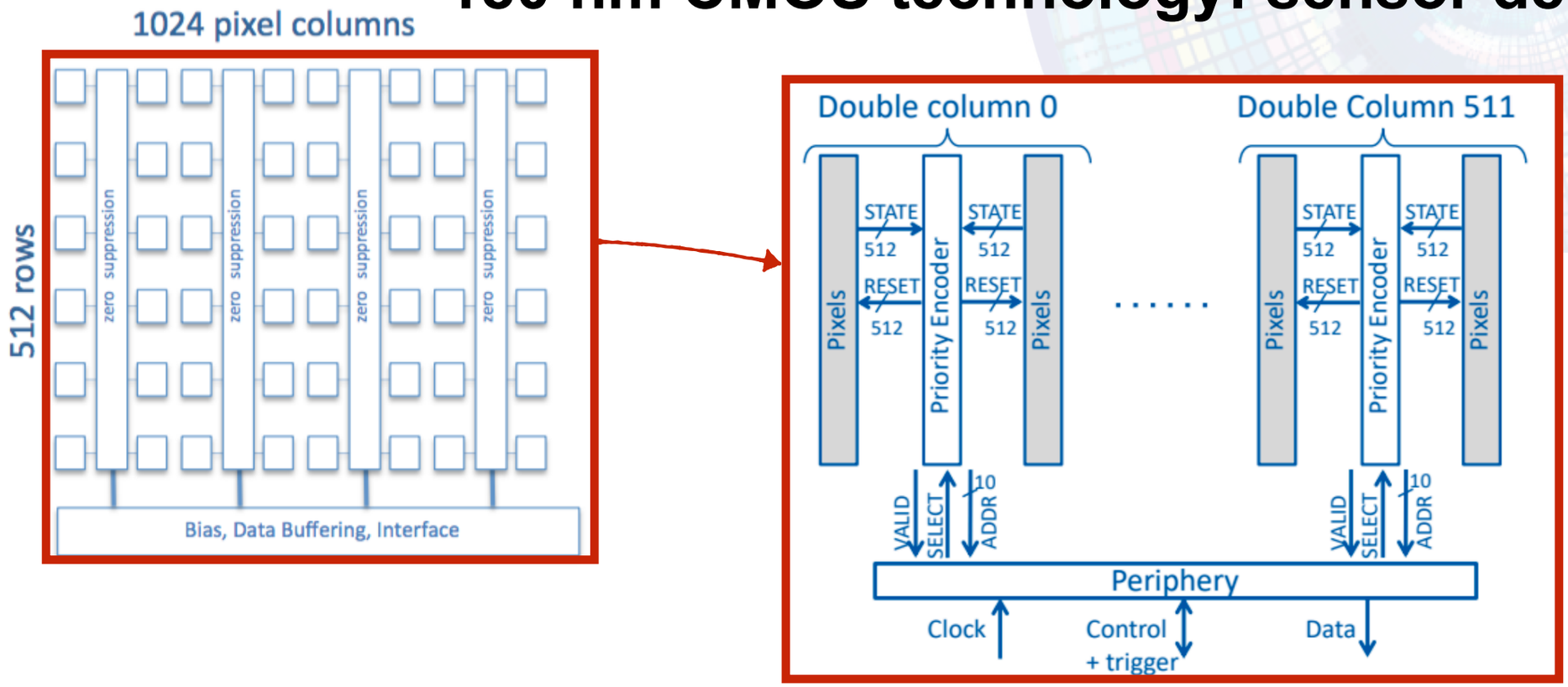

» Pixel matrix read-out
- Fully integrated in the sensor
- Global shutter and zero suppression realised through priority encoding
- Single pixel multi-event memory and global strobing allow triggered or continuous read-out

Rolling Shutter

Global Shutter

Sensor performances

» Low fake-hit rate: ≪10^{-6} hits/pixel/event
» Radiation tolerance:
  • TID: > 270 krad
  • NIEL: > $1.7 \cdot 10^{13}$ 1 MeV n_{eq}/cm^2
» Spatial resolution: ~5 µm

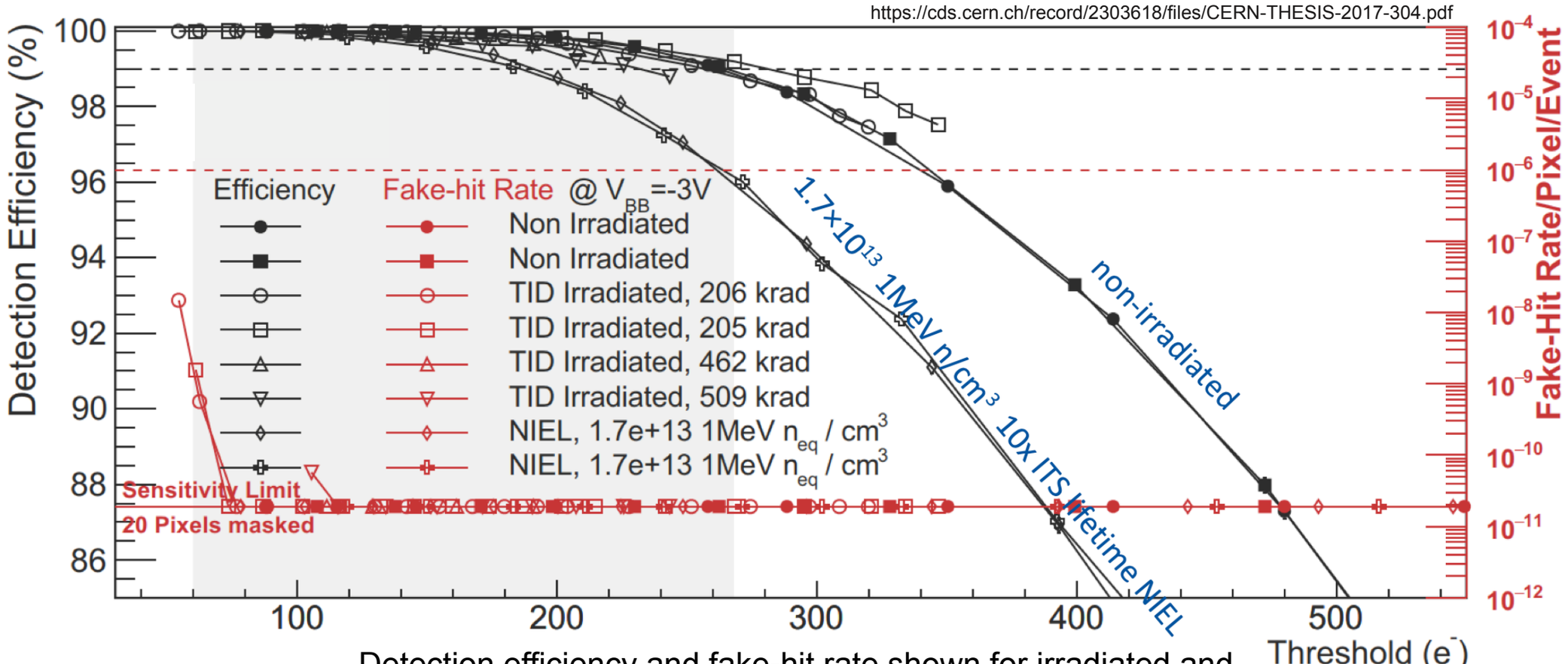

Detection efficiency and fake-hit rate shown for irradiated and non-irradiated sensors as a function of the applied threshold

Sensor performances

» Fake-hit rate measured during ITS2 commissioning: 10^{-10} hits/pixel/event, after masking 100 noisy pixels over 10^8 total pixels

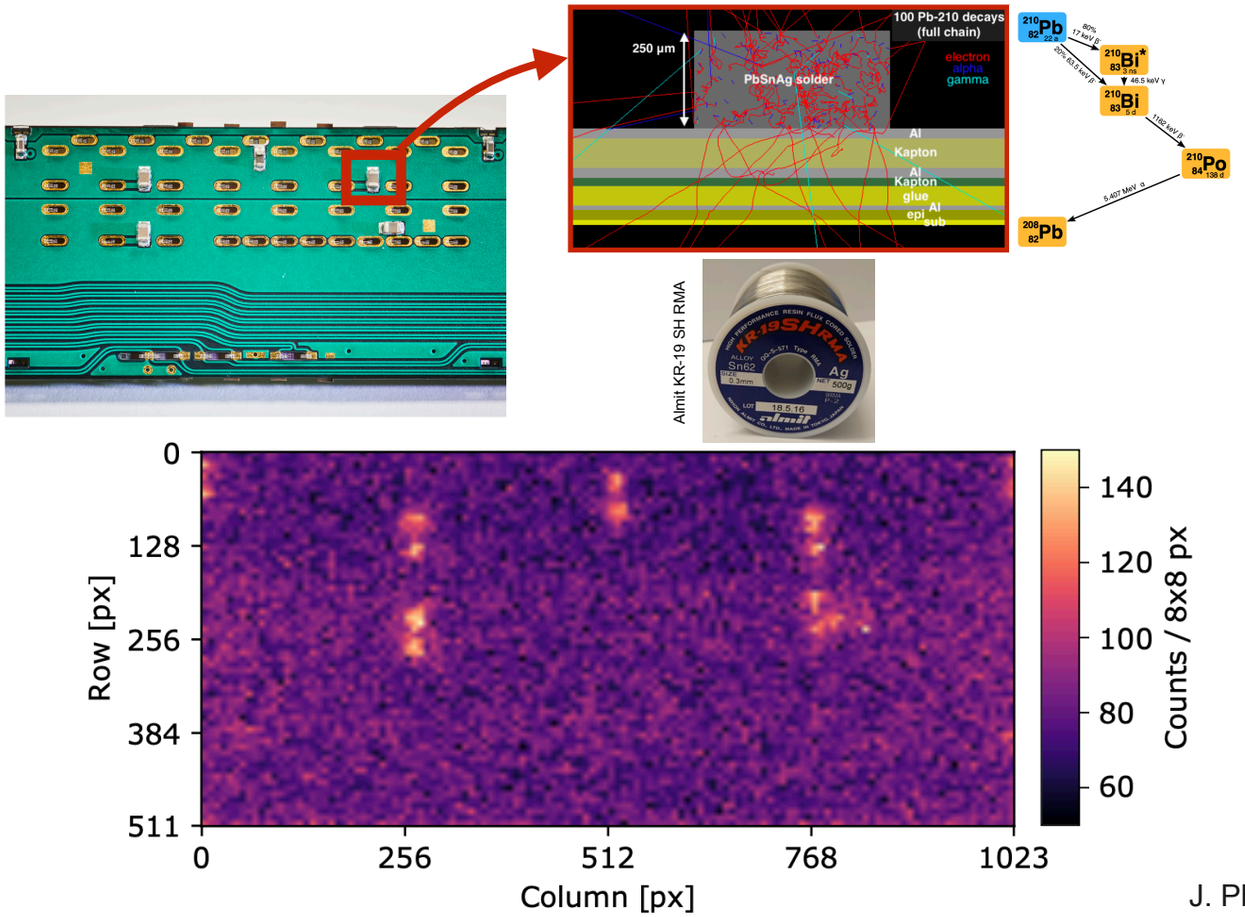

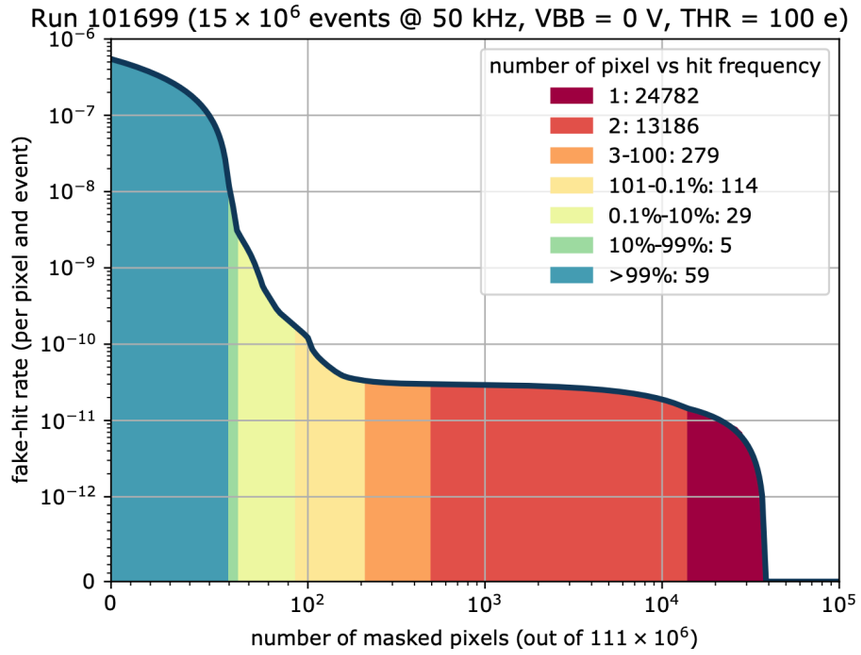

» Noise pattern on ITS2 modules → ^{210}Pb radioactive decay from solder used to mount decoupling capacitors

- Simulation demonstrated that β-particles from the ^{210}Bi (^{210}Pb daughter) can penetrate the FPC and reach the sensor

J. Phys.: Conf. Ser. 2374 012062

Other ALPIDE applications

» ALICE Muon Forward Tracker (MFT)
- Based on the same ALPIDE sensors
- Add vertex capability at forward muon arm

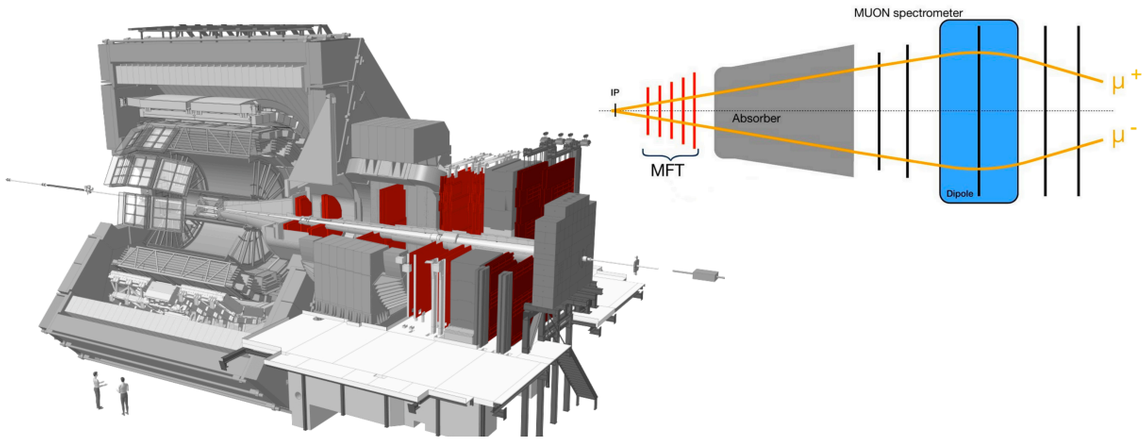

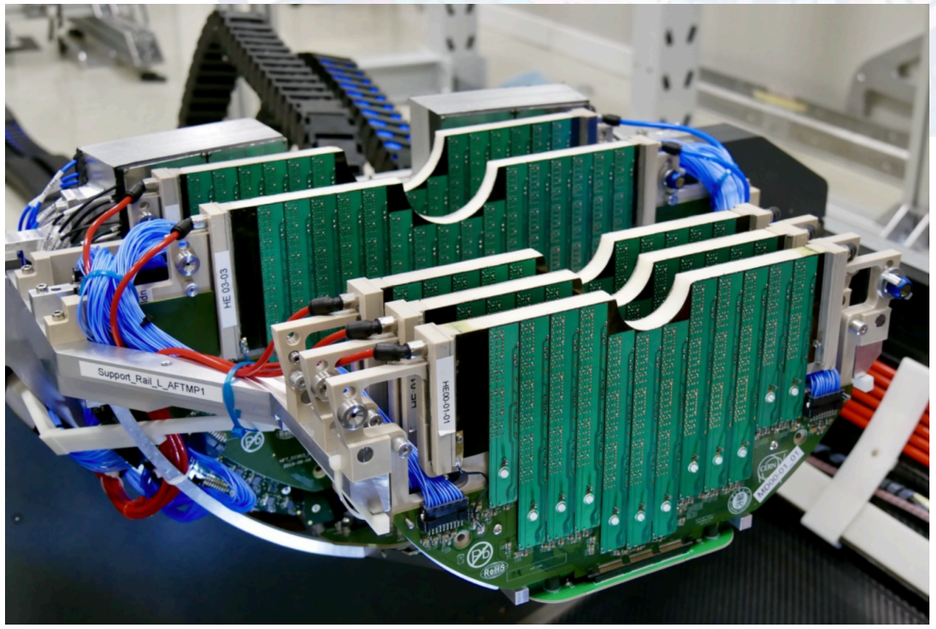

» ALICE Forward Calorimeter (FoCal)
- Measure gluon density in proton/nuclei collisions at small x and Q value
- To be installed during LHC LS3
- ALPIDEs used to provide spatial resolution in the FoCal-E

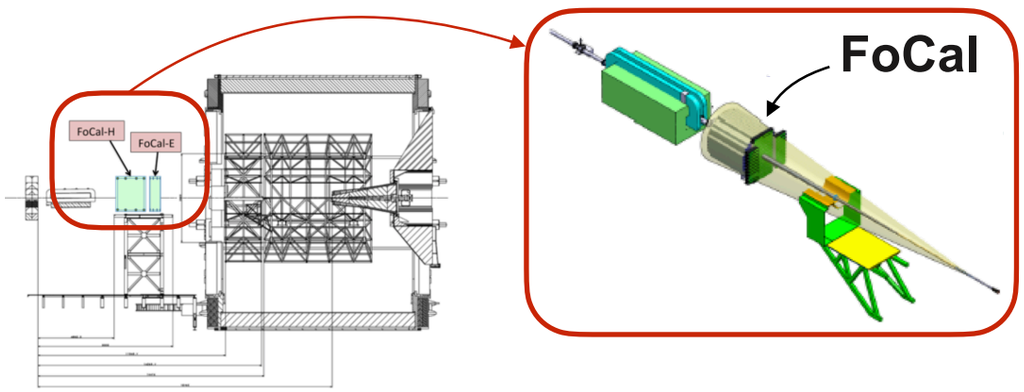

At z ~ 7 m from IP, 3.2 < η < 5.8

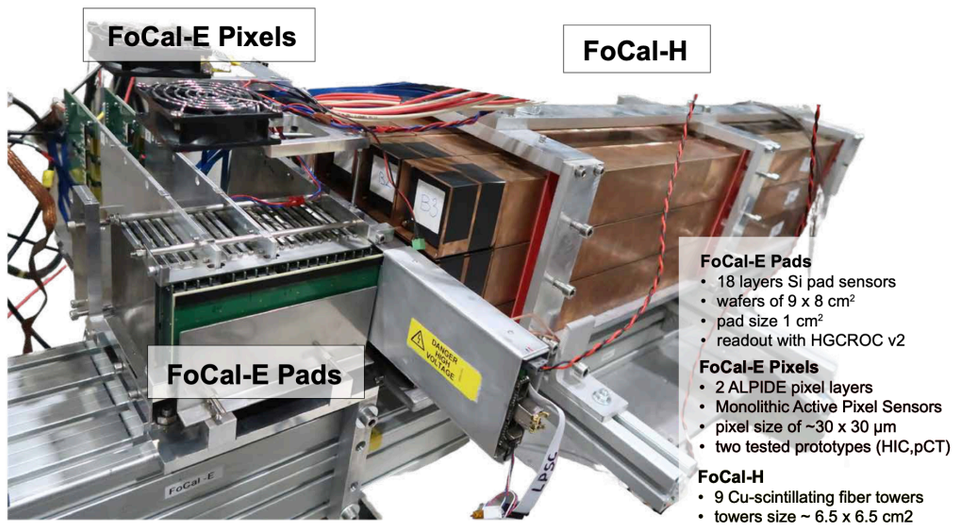

FoCal-E Pads
- 18 layers Si pad sensors
- wafers of 9 x 8 cm²
- pad size 1 cm²
- readout with HGCROC v2

FoCal-E Pixels
- 2 ALPIDE pixel layers
- Monolithic Active Pixel Sensors
- pixel size of ~30 x 30 μm
- two tested prototypes (HIC,pCT)

FoCal-H
- 9 Cu-scintillating fiber towers
- towers size ~ 6.5 x 6.5 cm2
- length ~110 cm
- readout with CAEN DT5202

FoCal prototype tested in electron/hadron beams at SPS in Nov. 2022 and May 2023!

Other ALPIDE applications

» sPHENIX MVTX @RHIC
- Replica of the ITS2-IB detector

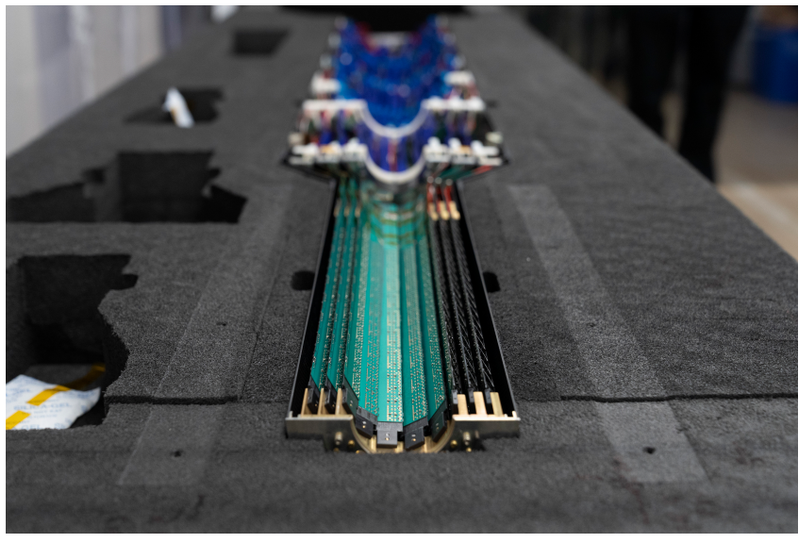

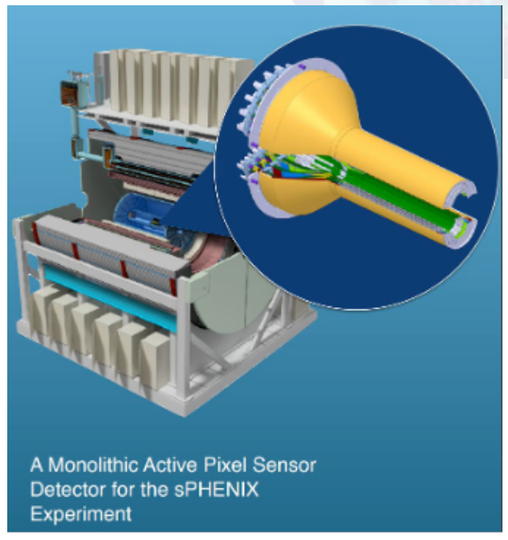

… and many more, also in medical applications

Technology improvements: toward fully depleted sensor

» **Standard** process: partially depleted epitaxial layer
→ doesn't allow full charge collection by drift, mandatory for more extreme radiation tolerance
- Operational up to 10^{13} 1 MeV n_{eq}/cm^2

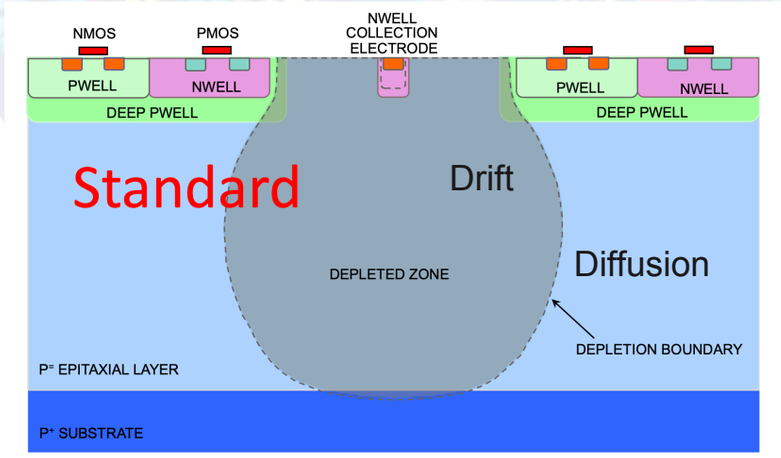

Technology improvements: toward fully depleted sensor

» **Standard** process: partially depleted epitaxial layer → doesn't allow full charge collection by drift, mandatory for more extreme radiation tolerance
  • Operational up to 10^{13} 1 MeV n_{eq}/cm^2

» **Modified** process: toward fully depleted epitaxial layer (still keepings small collection electrode) → planar junction separated from the collection electrode in the epitaxial layer through a low dose deep *n*-type implant
  • Operational up to: 10^{14} 1 MeV n_{eq}/cm^2

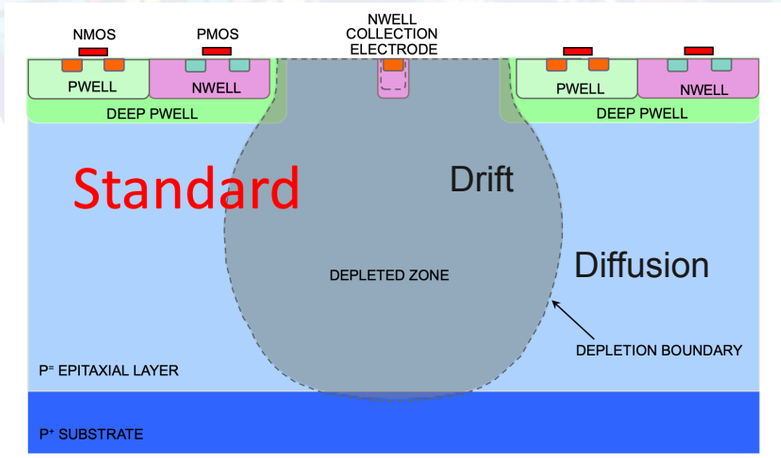

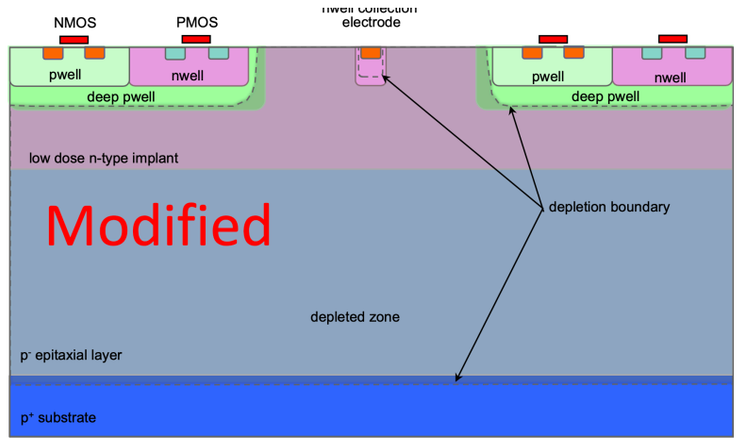

J. NIMA 871 (2017) 90–96
J. NIMA 958 (2020) 162404

Technology improvements: toward fully depleted sensor

» **Standard** process: partially depleted epitaxial layer → doesn't allow full charge collection by drift, mandatory for more extreme radiation tolerance
  • Operational up to 10^{13} 1 MeV n_{eq}/cm^2

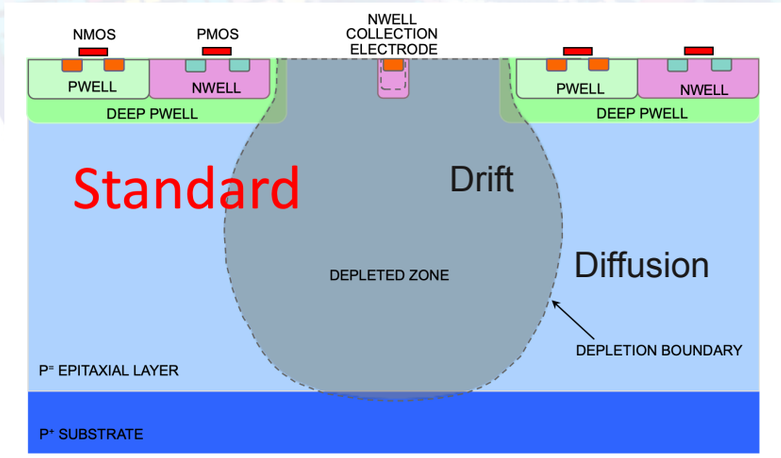

» **Modified** process: toward fully depleted epitaxial layer (still keepings small collection electrode) → planar junction separated from the collection electrode in the epitaxial layer through a low dose deep *n*-type implant
  • Operational up to: 10^{14} 1 MeV n_{eq}/cm^2
  • Electric field reaches a minimum in the pixel corners → degraded efficiency after irradiation

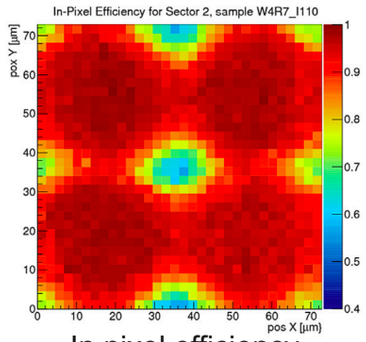

In pixel efficiency in a 2x2 matrix MALTA sensor

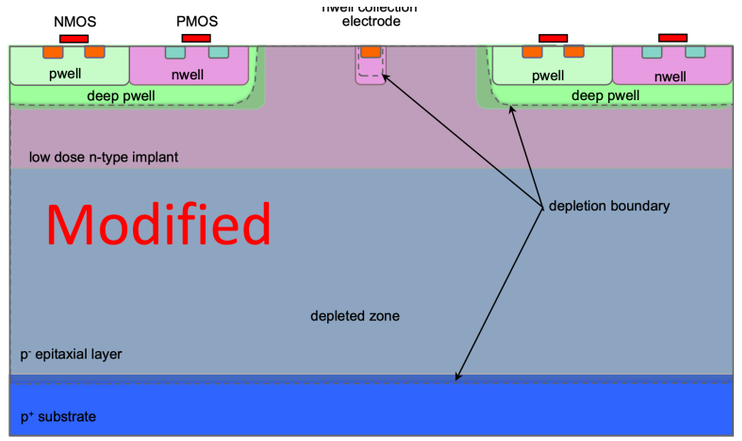

J. NIMA 871 (2017) 90–96
J. NIMA 958 (2020) 162404

Technology improvements: toward fully depleted sensor

» **Standard** process: partially depleted epitaxial layer → doesn't allow full charge collection by drift, mandatory for more extreme radiation tolerance
- Operational up to 10^{13} 1 MeV n_{eq}/cm^2

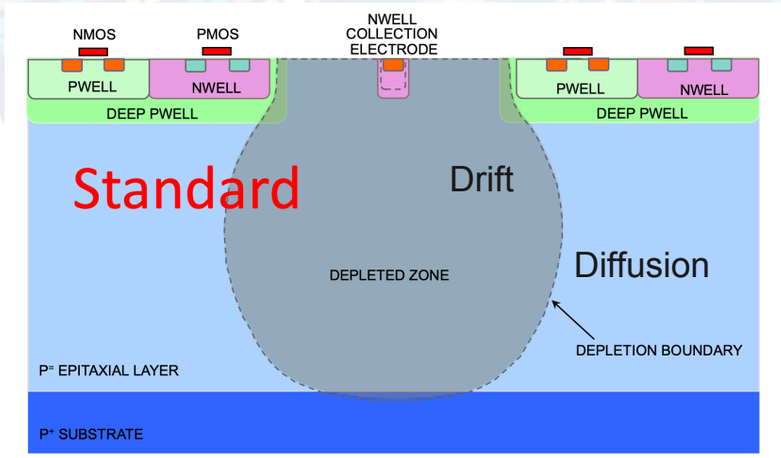

» **Modified** process: toward fully depleted epitaxial layer (still keepings small collection electrode) → planar junction separated from the collection electrode in the epitaxial layer through a low dose deep *n*-type implant
- Operational up to: 10^{14} 1 MeV n_{eq}/cm^2
- Electric field reaches a minimum in the pixel corners → degraded efficiency after irradiation

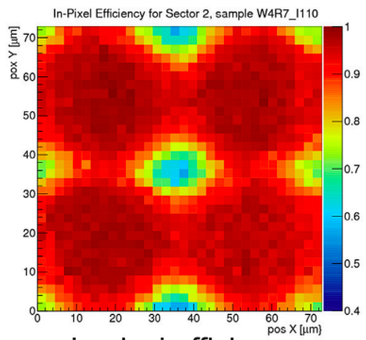

In pixel efficiency in a 2x2 matrix MALTA sensor

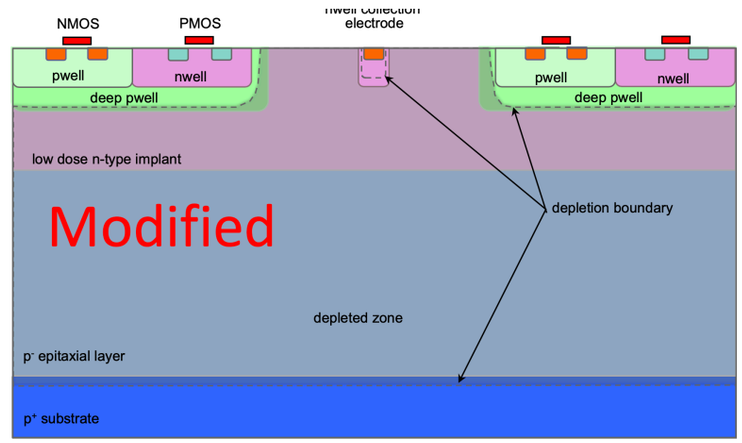

J. NIMA 871 (2017) 90–96
J. NIMA 958 (2020) 162404

» **Modified with gap** process: a gap in the deep n-implant increases the lateral electric field at the pixel borders
- Operational up to: 10^{15} 1 MeV n_{eq}/cm^2

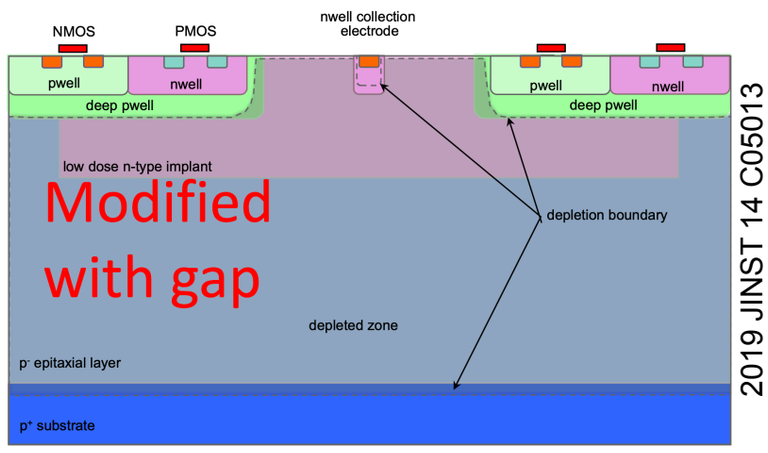

2019 JINST 14 C05013
2020 JINST 15 P0200

Technology improvements: toward fully depleted sensor

» **Standard** process: partially depleted epitaxial layer → doesn't allow full charge collection by drift, mandatory for more extreme radiation tolerance
- Operational up to 10^{13} 1 MeV n_{eq}/cm^2

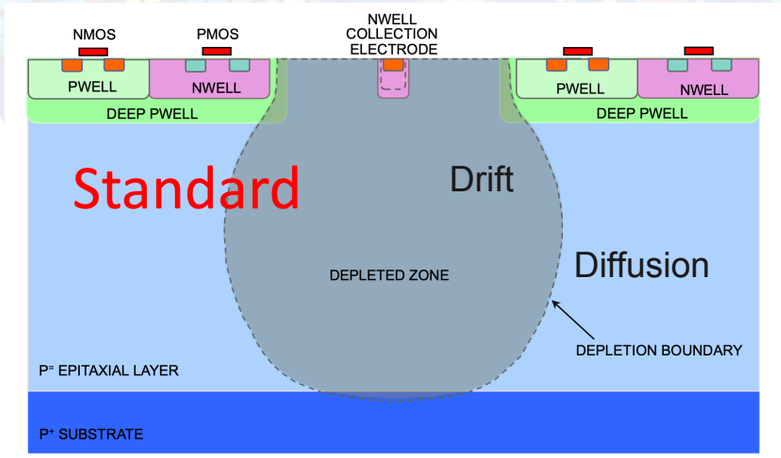

» **Modified** process: toward fully depleted epitaxial layer (still keepings small collection electrode) → planar junction separated from the collection electrode in the epitaxial layer through a low dose deep *n*-type implant
- Operational up to: 10^{14} 1 MeV n_{eq}/cm^2
- Electric field reaches a minimum in the pixel corners → degraded efficiency after irradiation

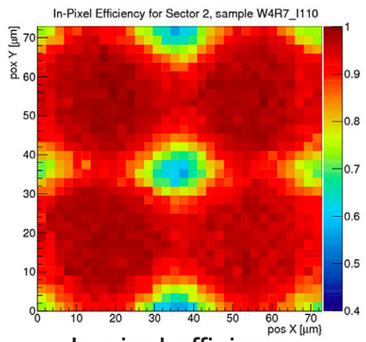

In pixel efficiency in a 2x2 matrix MALTA sensor

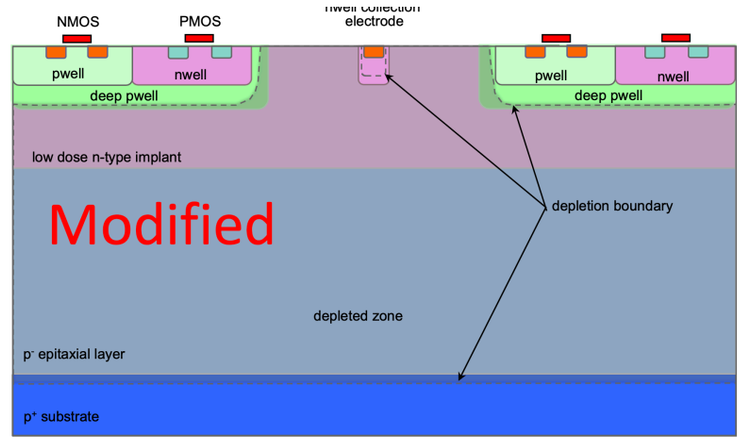

J. NIMA 871 (2017) 90–96
J. NIMA 958 (2020) 162404

» **Modified with gap** process: a gap in the deep n-implant increases the lateral electric field at the pixel borders
- Operational up to: 10^{15} 1 MeV n_{eq}/cm^2

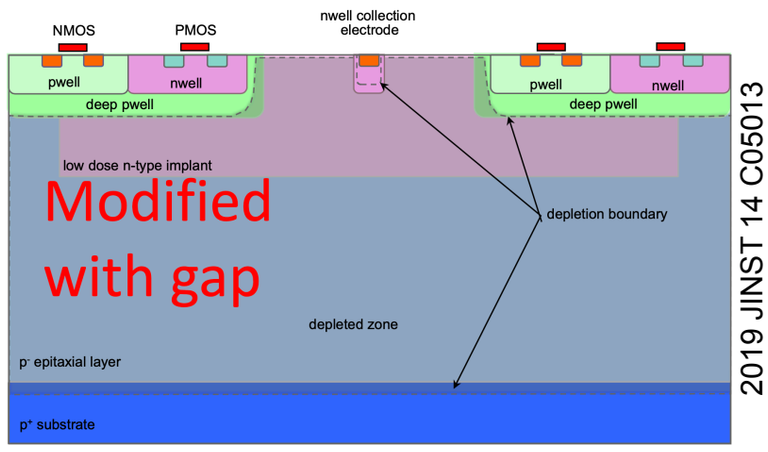

2019 JINST 14 C05013
2020 JINST 15 P0200

Modified process further pursued with MALTA, CLICpix, FastPix, ITS3…

Optimisation in 65 nm CMOS: https://doi.org/10.22323/1.420.0083

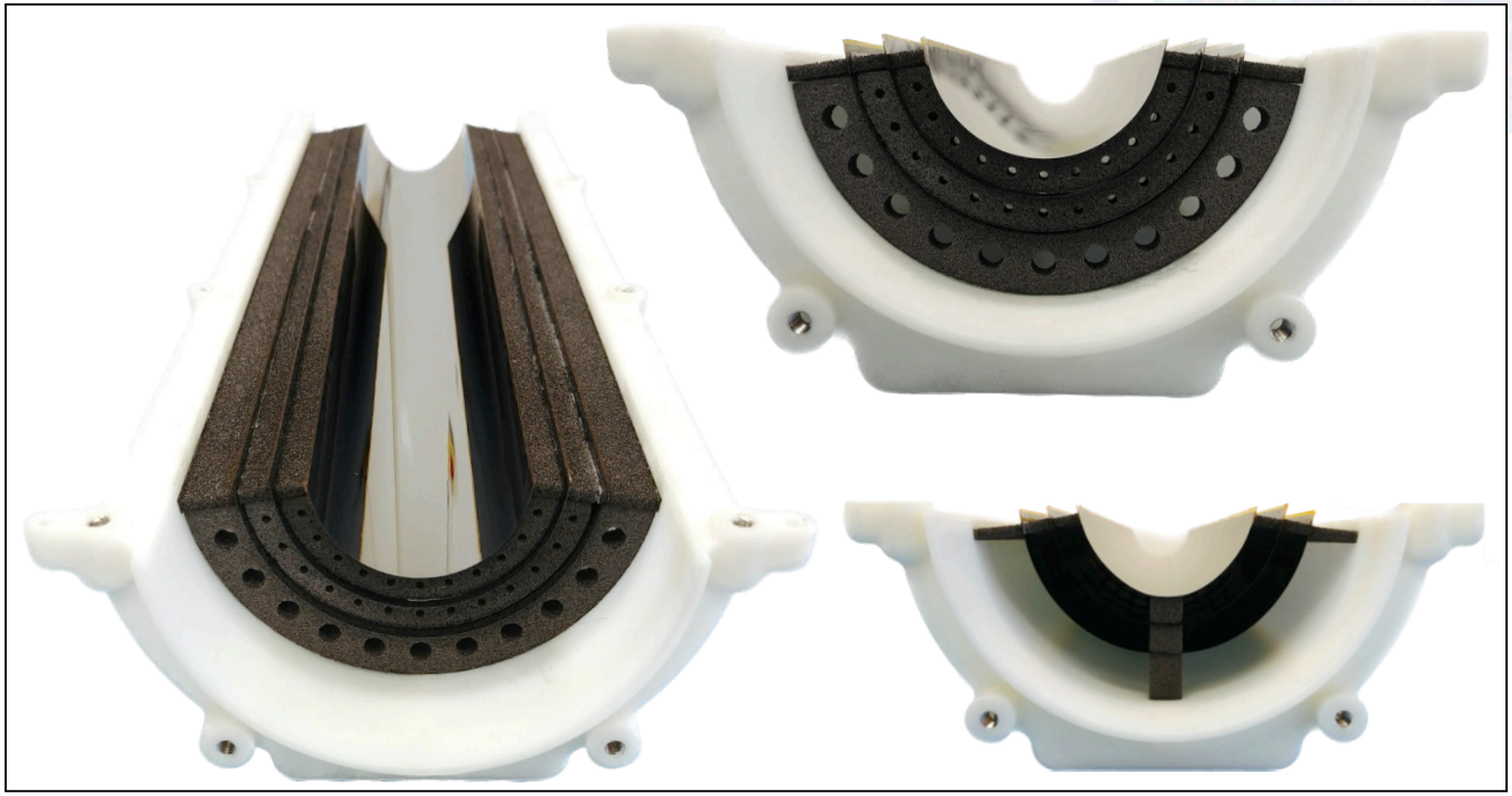

Large dimension silicon pieces bent in cylindrical shape at ITS3 target radii

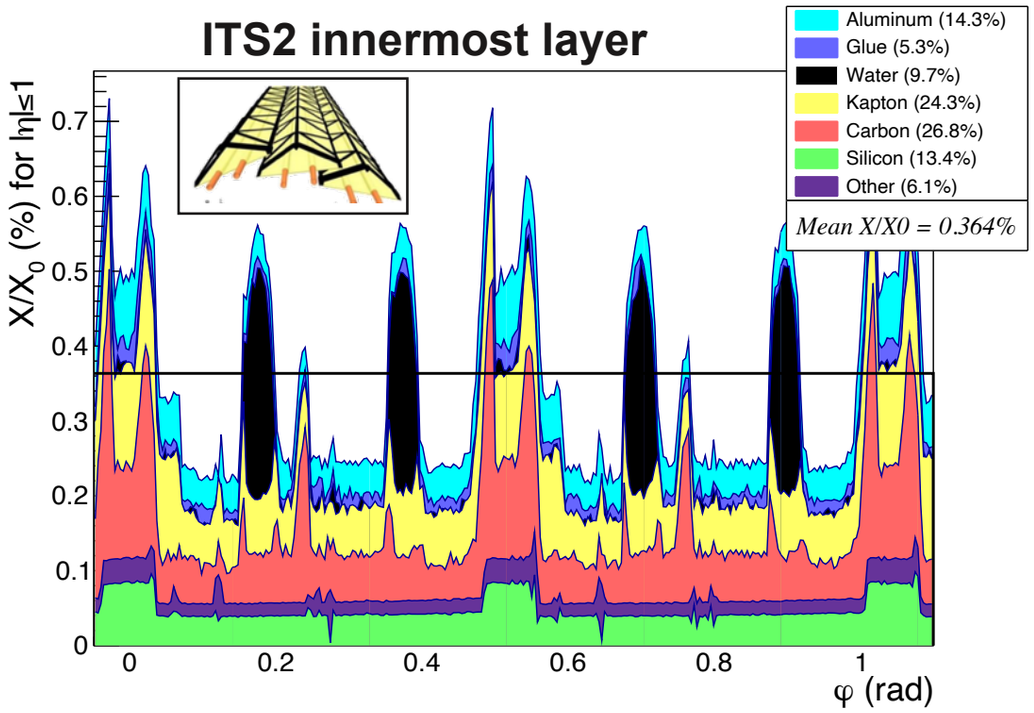
ITS2 innermost layer
Aluminum (14.3%)
Glue (5.3%)
Water (9.7%)
Kapton (24.3%)
Carbon (26.8%)
Silicon (13.4%)
Other (6.1%)
Mean X/X0 = 0.364%
X/X0 (%) for |η|≤1
0
0.1
0.2
0.3
0.4
0.5
0.6
0.7
0
0.2
0.4
0.6
0.8
1
φ (rad)

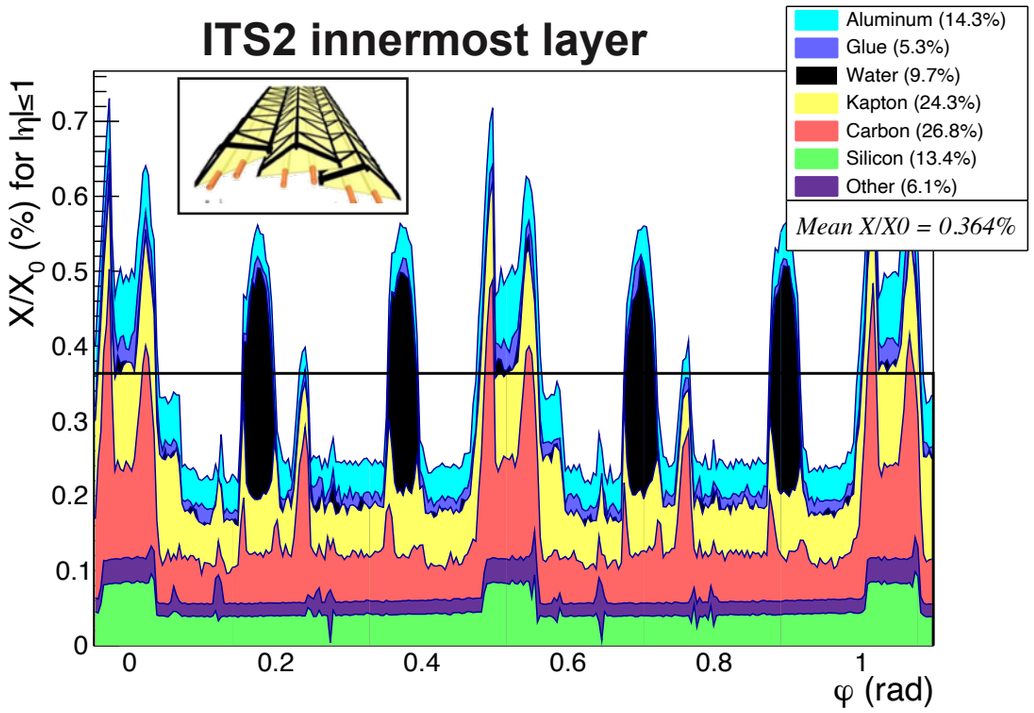
ITS2 innermost layer
Aluminum (14.3%)
Glue (5.3%)
Water (9.7%)
Kapton (24.3%)
Carbon (26.8%)
Silicon (13.4%)
Other (6.1%)
Mean X/X0 = 0.364%
X/X0 (%) for |η|≤1
φ (rad)

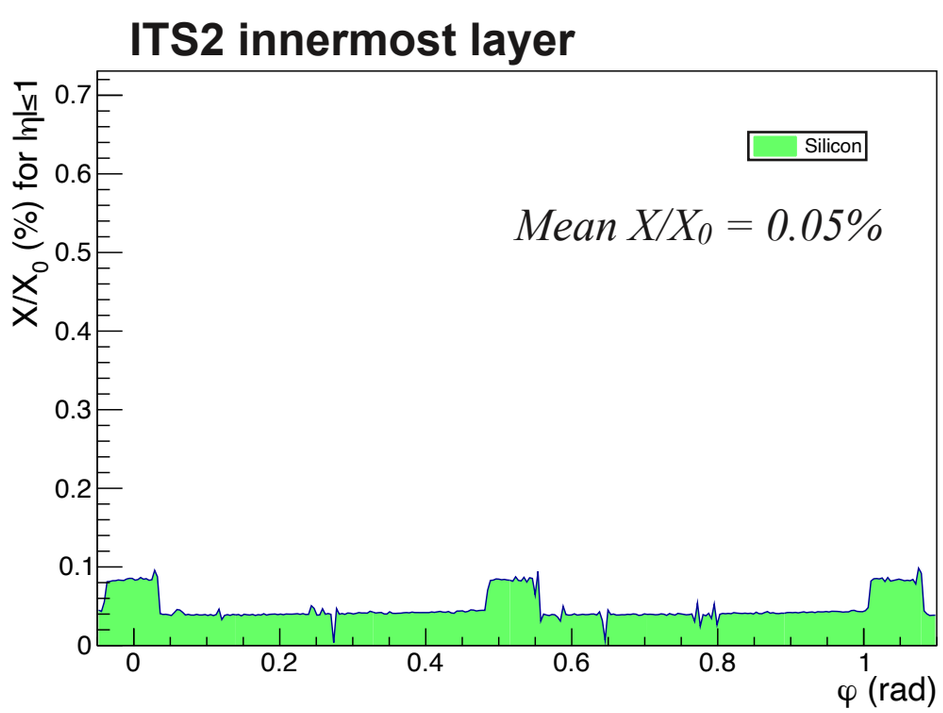
ITS2 innermost layer
Silicon
Mean X/X0 = 0.05%
X/X0 (%) for |η|≤1
φ (rad)

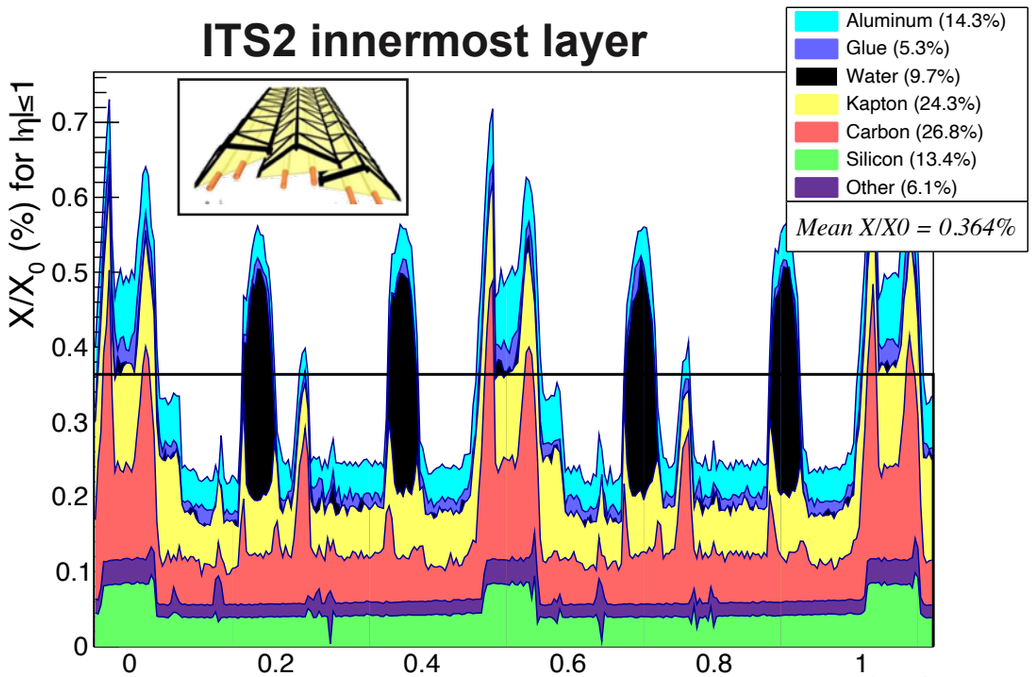

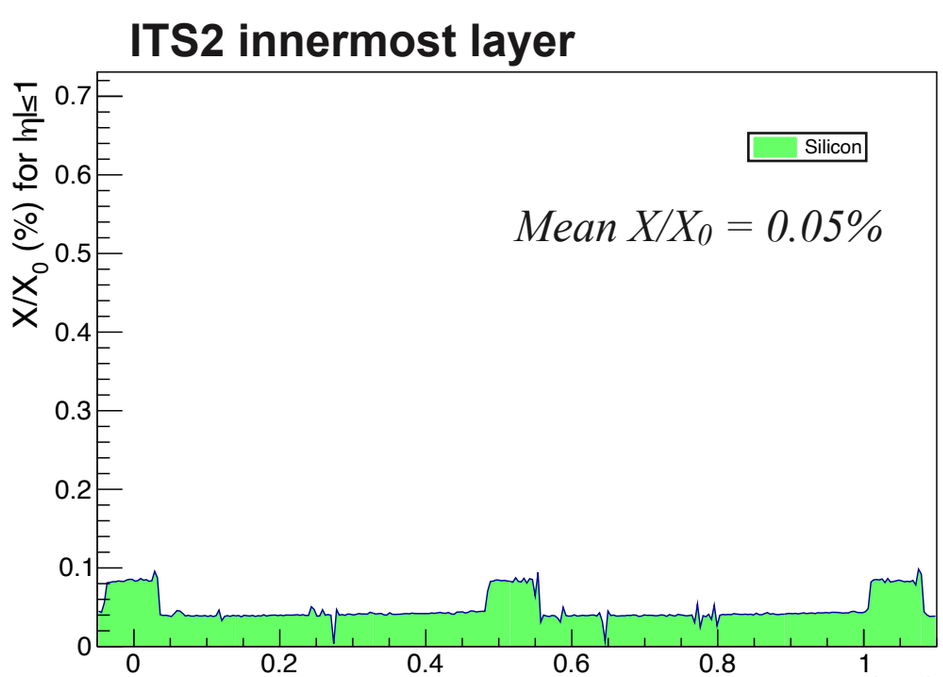

First fully cylindrical detector based on wafer-size dimension MAPS sensors

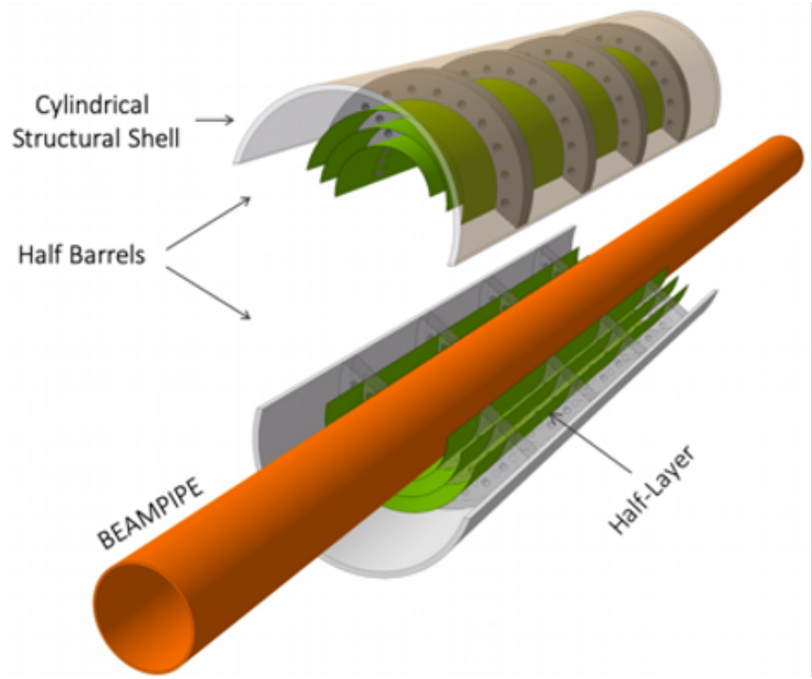

Letter of Intent for an ALICE ITS Upgrade in LS3: https://cds.cern.ch/record/2703140

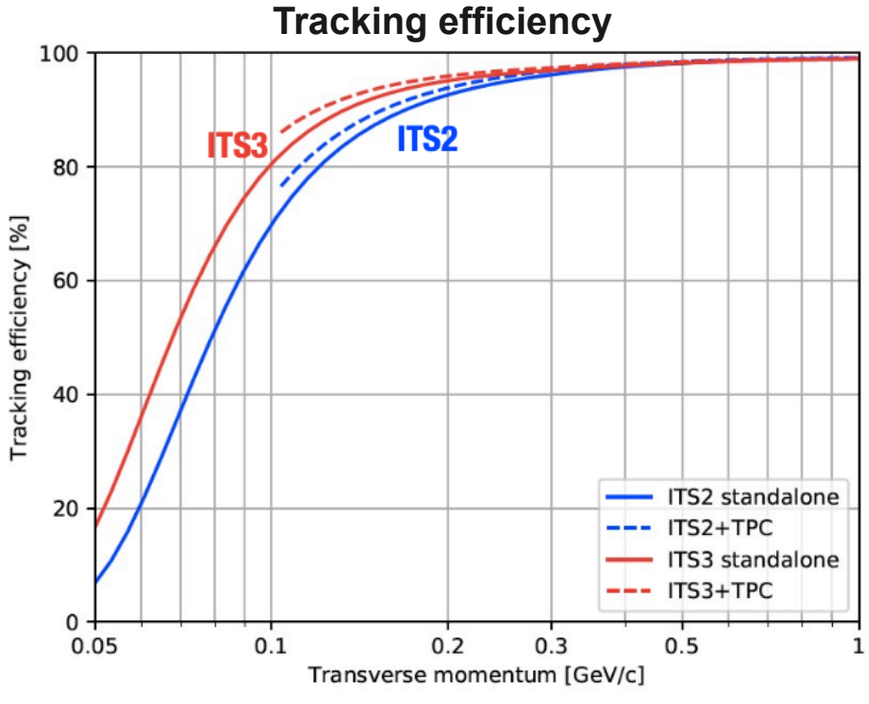

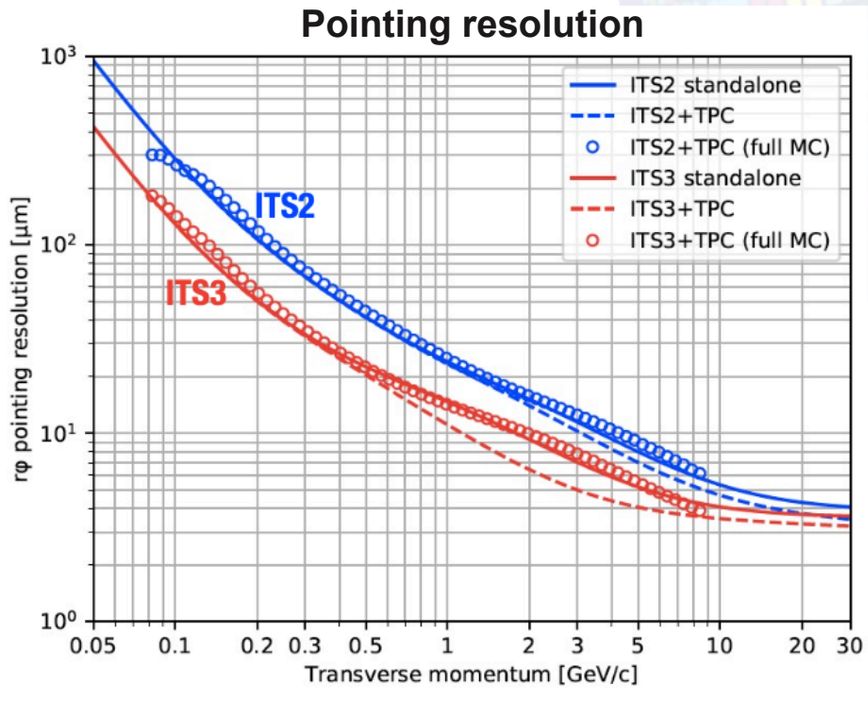

Improved pointing resolution and tracking efficiency for low momenta (×2 at all p_T)

Study of the enhancement of charm quarks in heavy-ion collisions

» Λ_C^+ and D_S^+ used to study baryon and strangeness enhancement (compared to D^0)

» Ξ_C might set very powerful constraints to test HF coalescence models

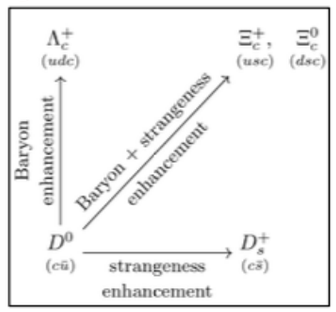

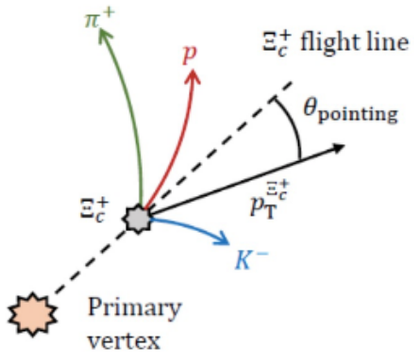

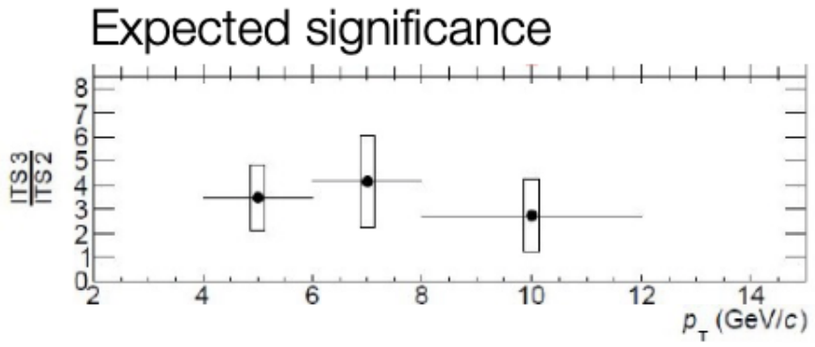

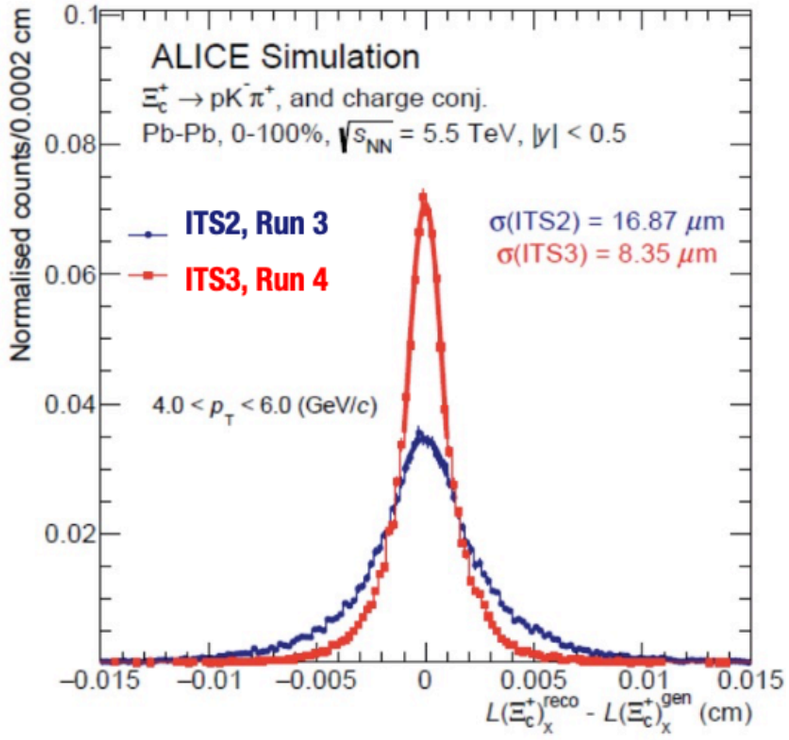

Key ingredients

» Wafer-scale chips (up to ~28x10 cm^2)
→ fabricated using stitching (to connect metal traces)

» MAPS sensor based on 65 nm CMOS technology
→ TPSCo largest (300 mm) wafer in this node
→ potentially smaller pixel size (with same in-pixel integrated electronics)
→ potentially low power consumption

» Chips bent in cylindrical shape
→ sensor thickness ≤ 50 μm
→ ultra light carbon foam structures

» Air cooling
→ power consumption limits to be established

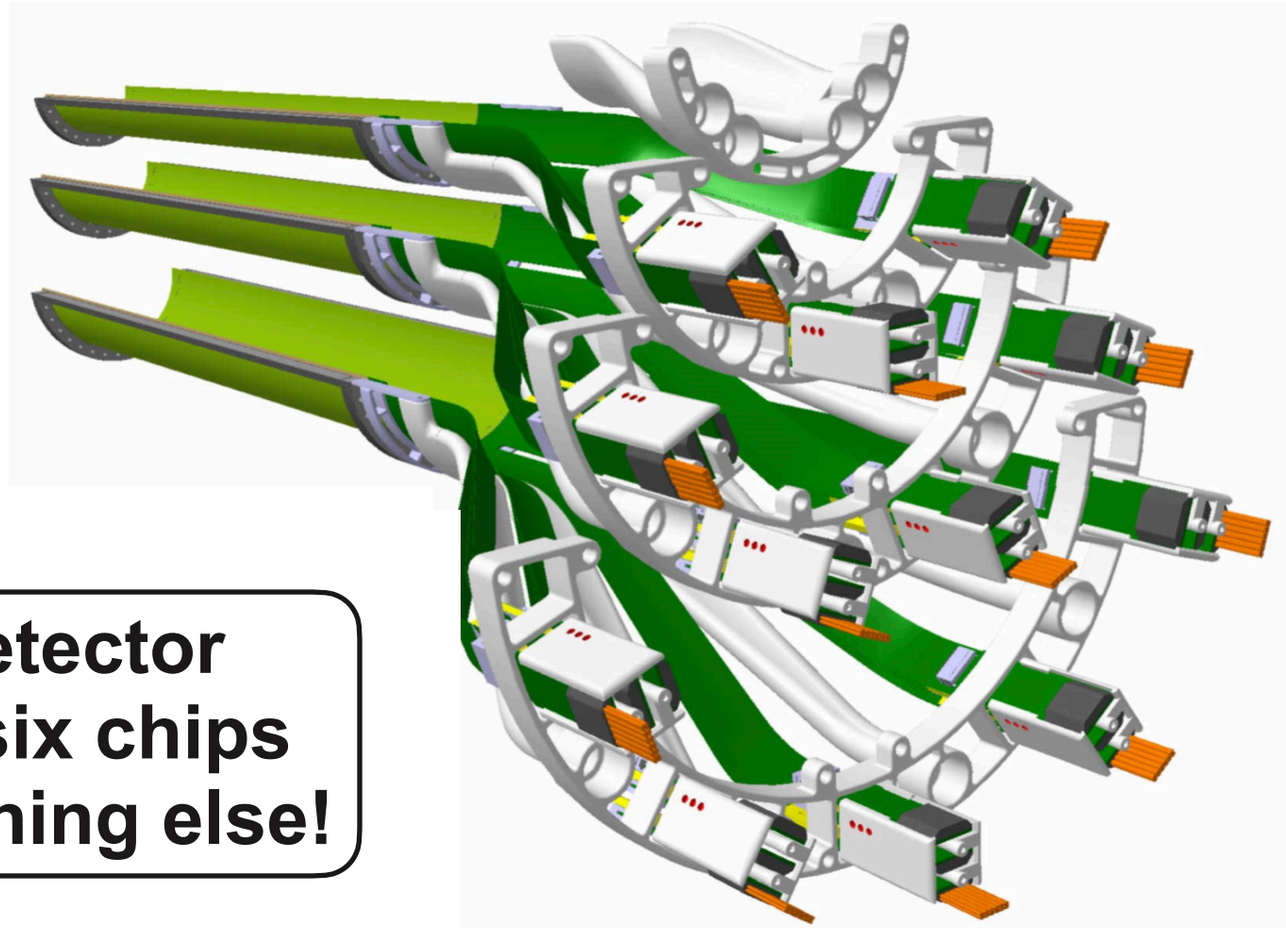

The whole detector will comprise six chips and barely anything else!

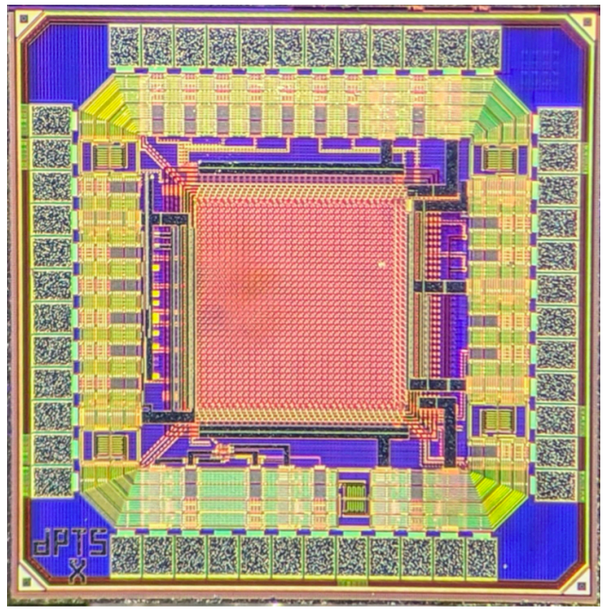

65 nm CMOS

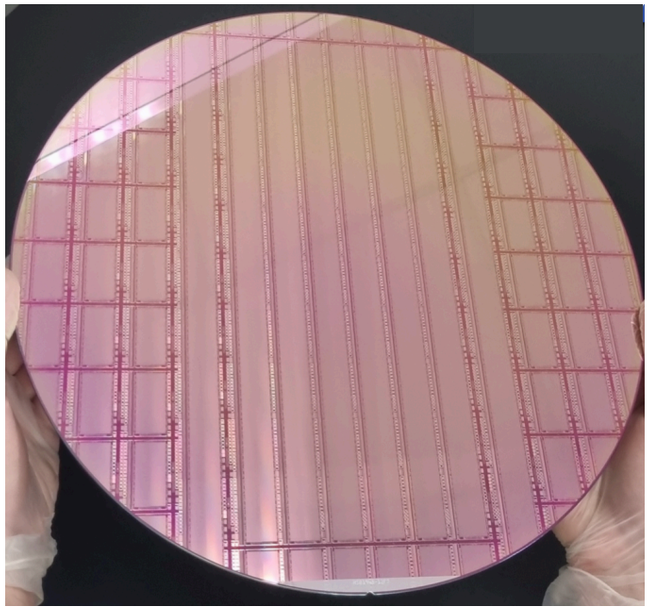

Stitching technique

Bending silicon

ALPIDE leap

ITS3 developments

ALICE3 developments

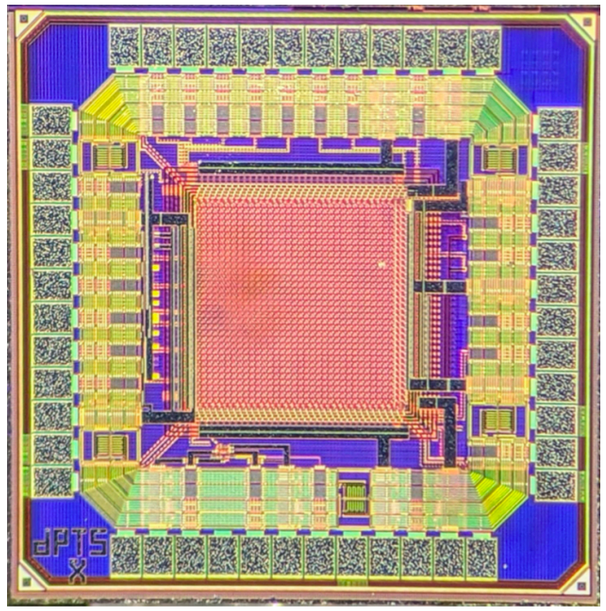

65 nm CMOS

ALICE Inner Tracking System Upgrade: characterization of first chips fabricated in 65 nm CMOS technology
(A. Trifirò)
Wed. 17:00 - E1 session

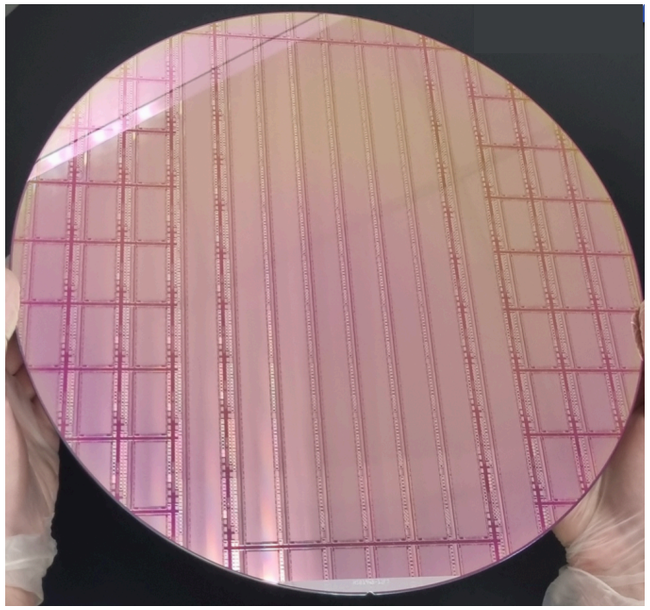

Stitching technique

The ALICE Inner Tracking System Upgrade
(V. Sarritzu)
Wed. 11:20 - D1 session

Bending silicon

ALICE ITS3:
how to integrate a large dimension MAPS sensor in a bent configuration detector
(D. Colella)
Wed. 12:20 - D1 session

65 nm CMOS technology qualification

» First test structures submission (MLR1) for 65 nm in December 2020
- 10 transistor test structures (3 x 15 mm²)
- 60 chips (1.5 x 1.5 mm²)
  - Analog and digital blocks
  - Pixel prototype: APTS, CE65, DPTS

» Main goals:
- Learn technology features
- Characterise charge collection
- Validate radiation tolerance

» Testing since September 2021
- Huge effort shared among many institutes
- Laboratory tests with ^{55}Fe source
- Beam tests @ PS, SPS, Desy, MAMI

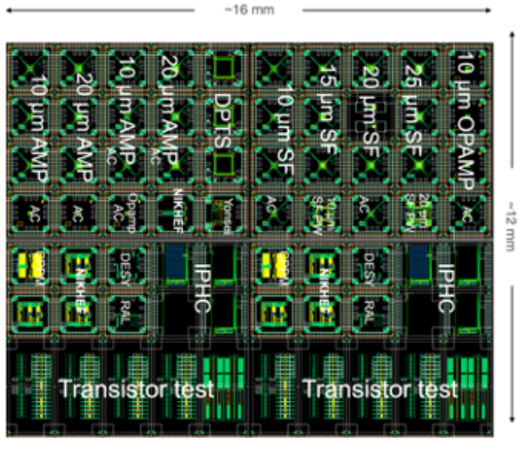

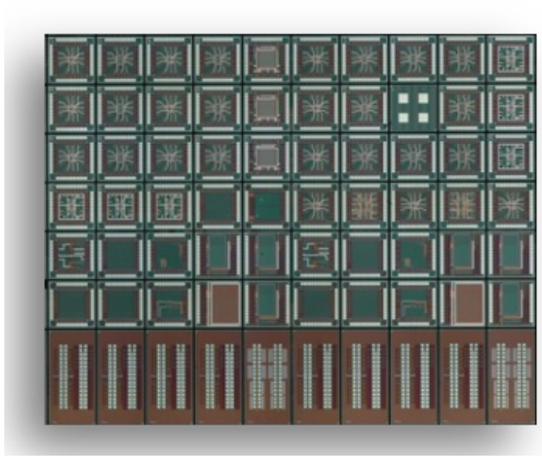

APTS

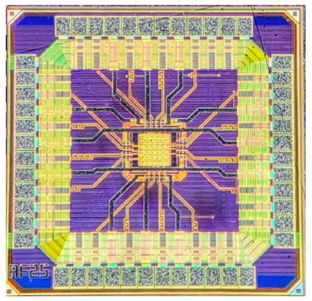

- 6x6 pixel matrix
- Direct analogue readout of central 4x4 submatrix
- Two types of output drivers:
  1. Traditional source follower (APTS-SF)
  2. Very fast OpAmp (APTS-OA)
- 4 pixel pitches: 10, 15, 20, 25 µm

CE65

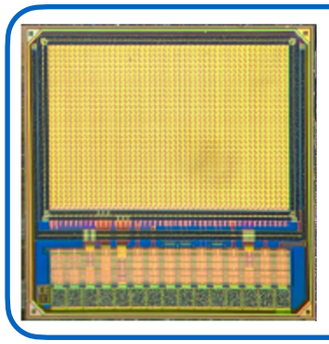

- 64x32 and 48x32 pixel matrix
- Rolling shutter readout (50 µs integration)
- 3 in-pixel architectures:
  1. AC-coupling
  2. DC-coupling
  3. Source follower
- 2 pixel pitches: 15, 25 µm

DPTS

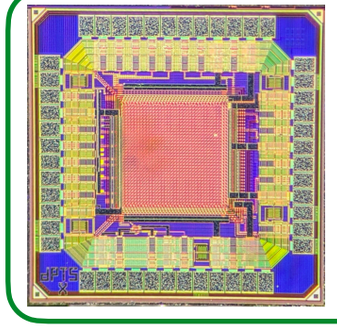

- 32x32 pixel matrix
- Asynchronous digital readout
- Time-over-threshold information
- Pixel pitch: 15 µm

65 nm CMOS technology qualification

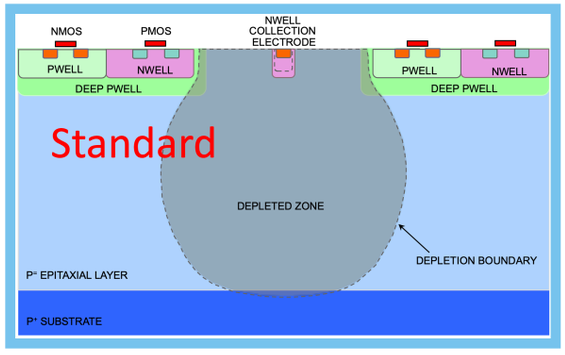

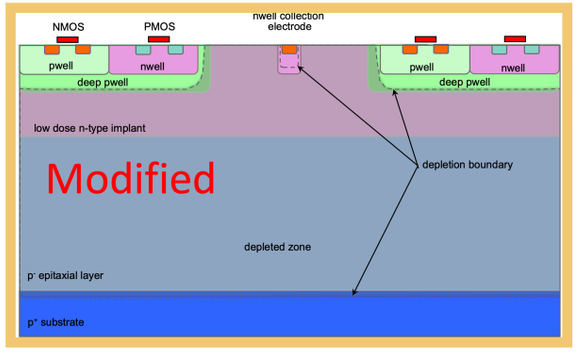

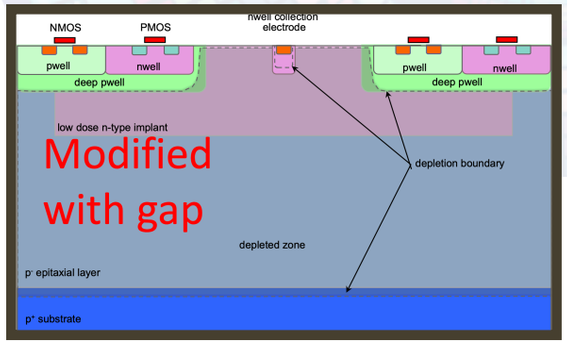

» Moving from *Standard* to *Modified with gap* process, the fraction of charge collected by the seed pixel increases

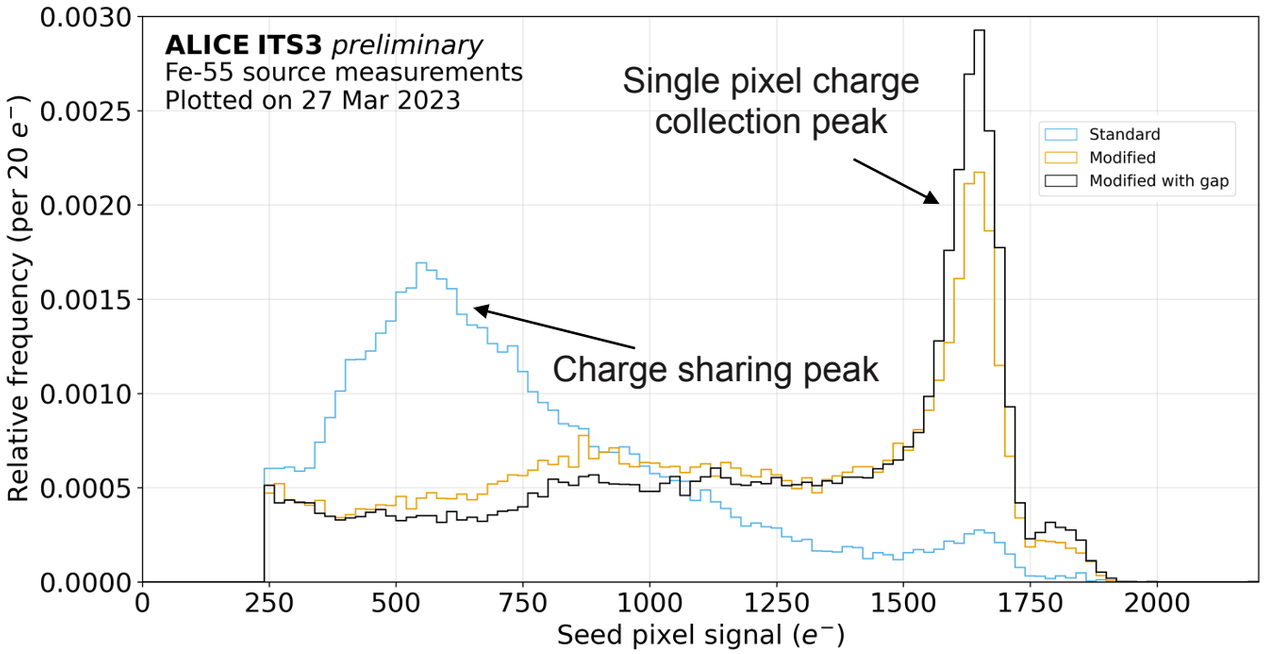

» Moving from *Standard* to *Modified with gap* process, the efficiency degrading limit (< 99%) moves to higher threshold

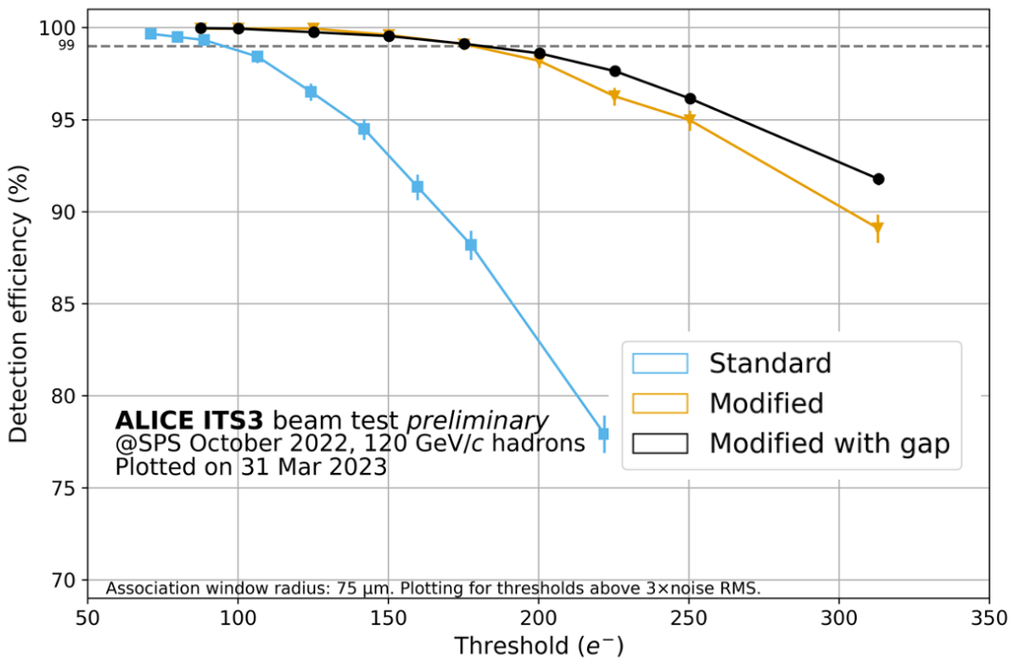

65 nm CMOS technology qualification

» **Pixel pitch**

→ For m*odified with gap* process charge collection doesn't depend on pixel pitch (10, 15, 20 and 25 µm)

» **Radiation hardness**

→ full digital sensor implementation does satisfies ALICE ionising (10 kGy) and non-ionising (10^{13} 1 MeV n_{eq} cm^{-2}) dose for LHC Run 4

→ can be operated at the temperature of +20ºC (99% efficiency) after 10^{15} 1 MeV n_{eq} cm^{-2} and inefficiency comes from particle track away from the collection diode

65 nm CMOS TPSCo technology fully validated for ALICE application!

Wafer-size sensors: 2D stitching

» Chip size limited by field of exposure of photolithography equipment (~20 x 20 mm²)
» **Stitching** technique allow sensor size exceeding the photolithography limitations
- Building blocks are integrated in the photolithography mask as different mask regions
- During photo-lithographic patterning, wafers are selectively exposed onto adjacent locations according to a pre-established pattern → very accurate translation and alignment required
- Metal traces are used to create connections (power distribution and buses for control/data readout) across adjacent matrices (repeated units)

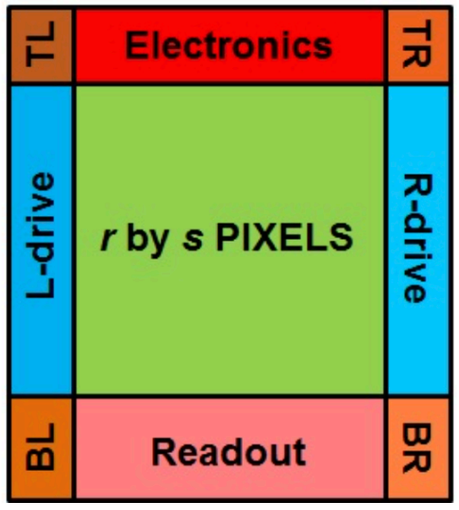

Sketch of an image sensor design

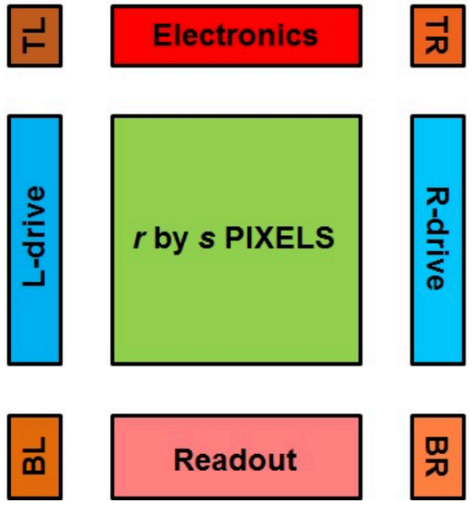

Isolated building blocks put separately on the reticle

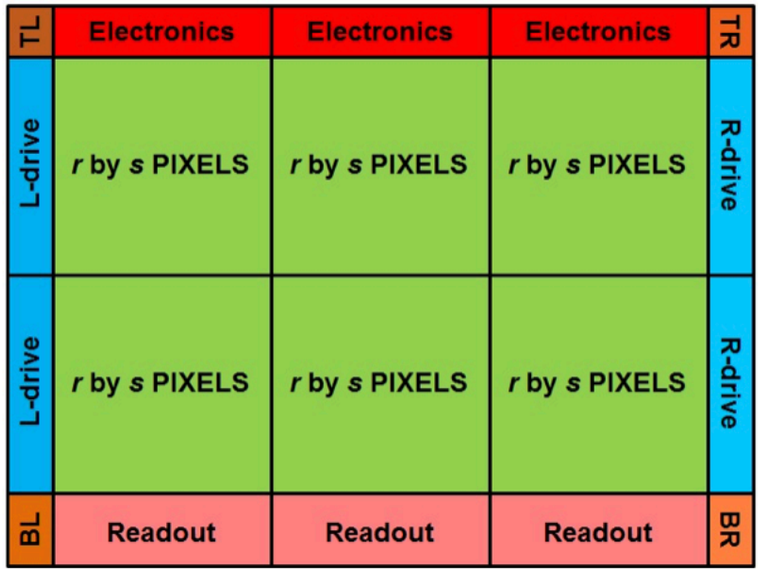

Extending the size of the sensor beyond the reticle field of view

Tower Semiconductor Ltd, Stitching design rules for forming interconnect layers, US Patent 6225013B1 (2001)

Wafer-size sensors: 2D stitching

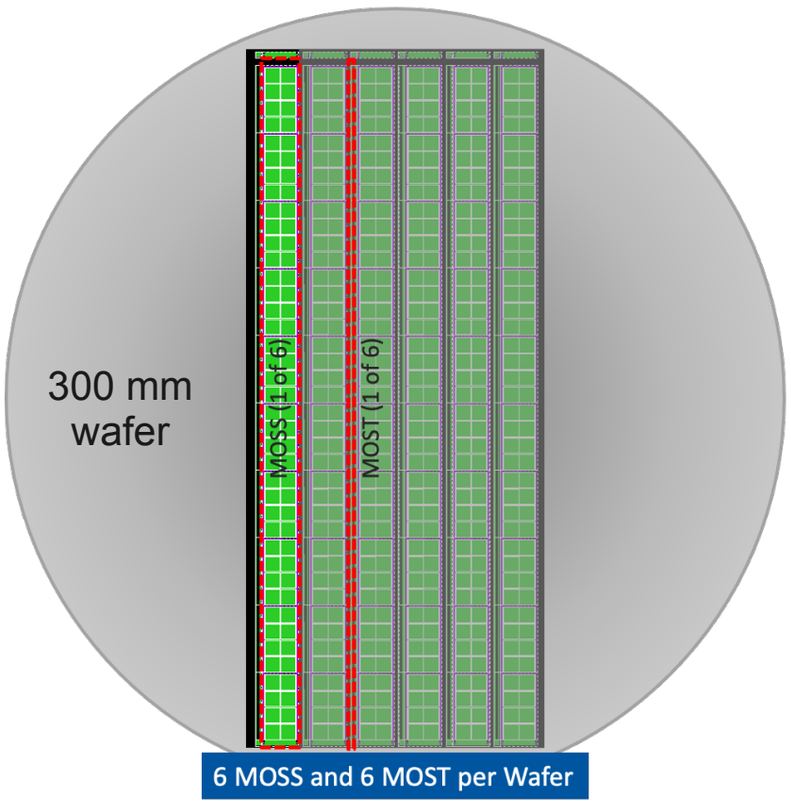

» Two stitched sensor prototypes (ER1):
- **Mo**nolithic **S**titched **S**ensor (**MOSS**)
  - Size: 1.4 x 25.9 cm² - 6.72 MPixels
  - Pitches: 22.5 x 22.5 µm² and 18 x 18 µm²
  - Conservative design: separated powered sub-matrices
- **Mo**nolithic **S**titched **S**ensor with **T**iming (**MOST**)
  - Size: 0.25 x 25.9 cm² - 0.9 MPixels
  - Pitch: 18 x 18 µm²
  - More dense design: global power network

» Primary goals
- Learn stitching technique to make a particle detector
- Interconnect power and signals on wafer scale sensor
- Learn about yield

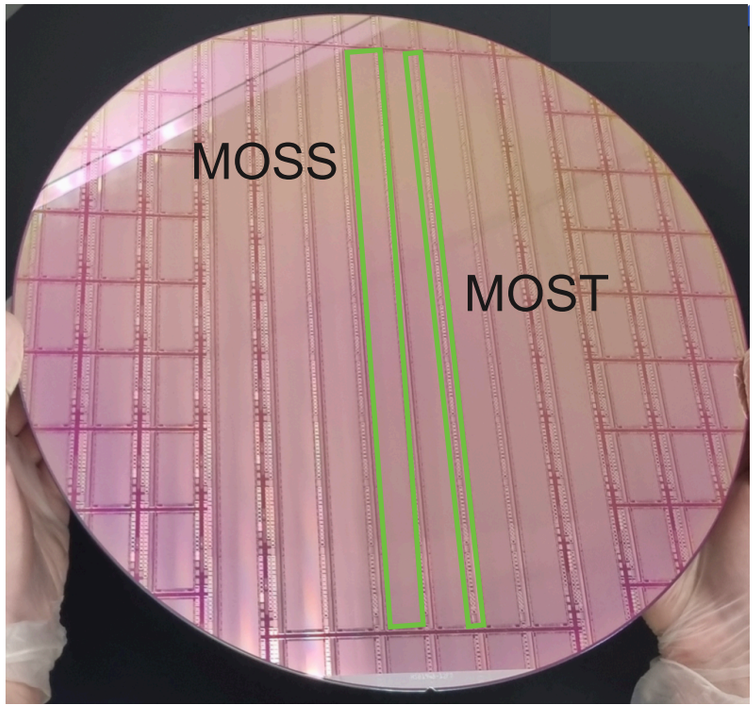

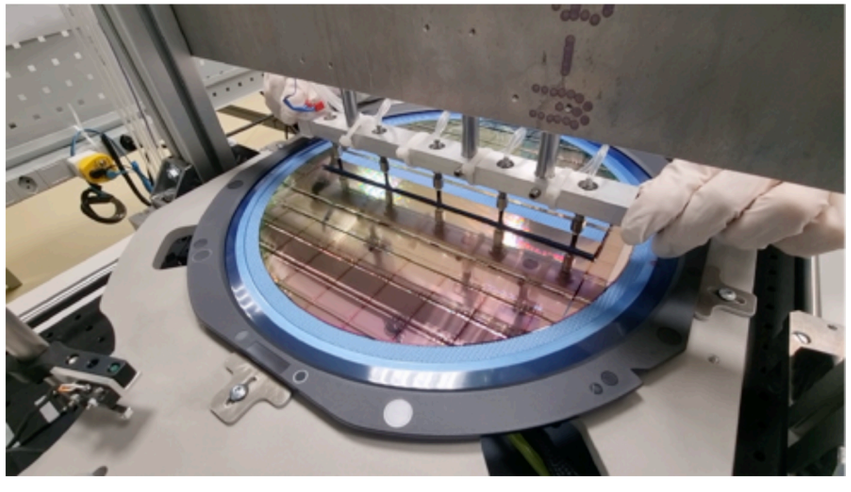

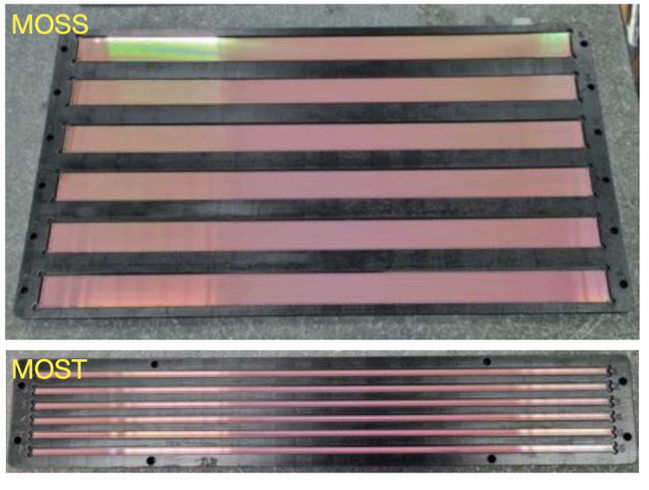

Wafer-size sensors: 2D stitching

Left Endocarp (Side A)
Standalone

Reticle (Mask)

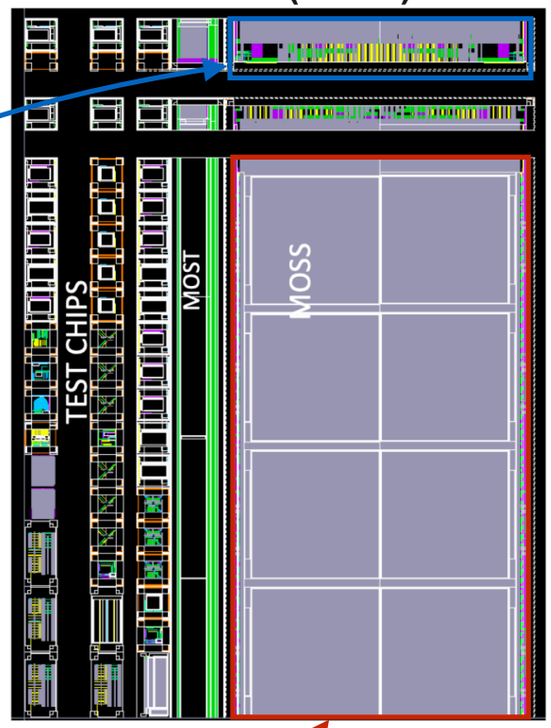

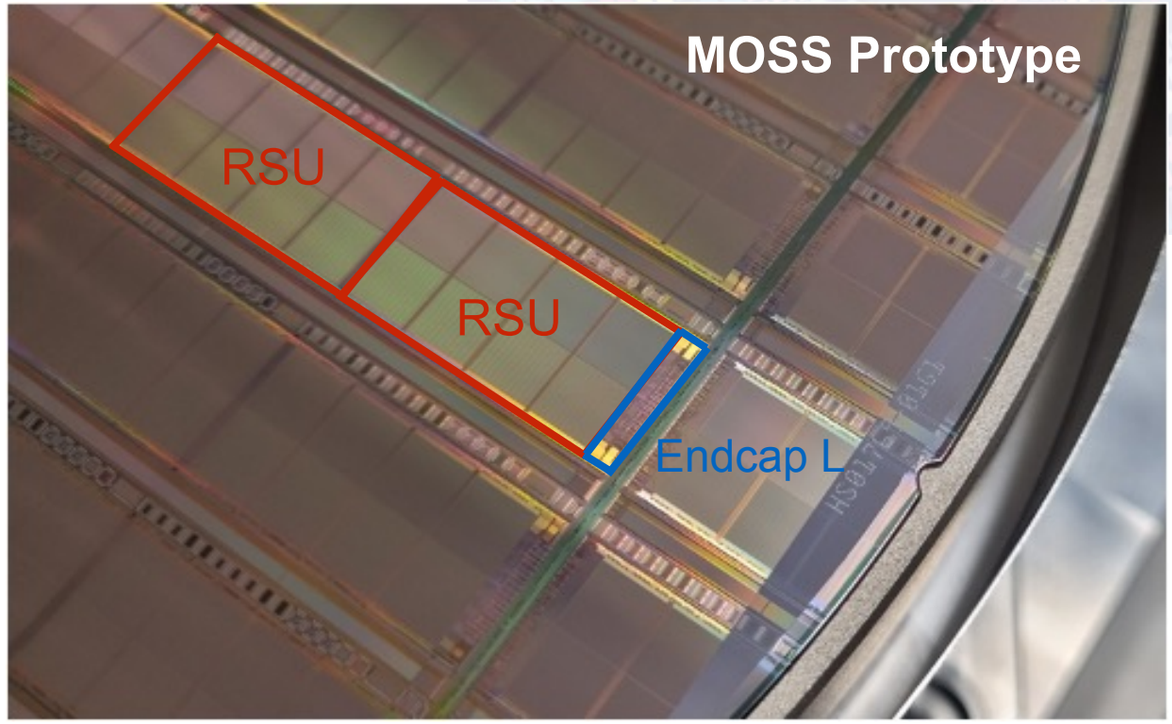

Repeated Sensor Unit (RSU)
Standalone functional unit with independent periphery, I/Os and powering

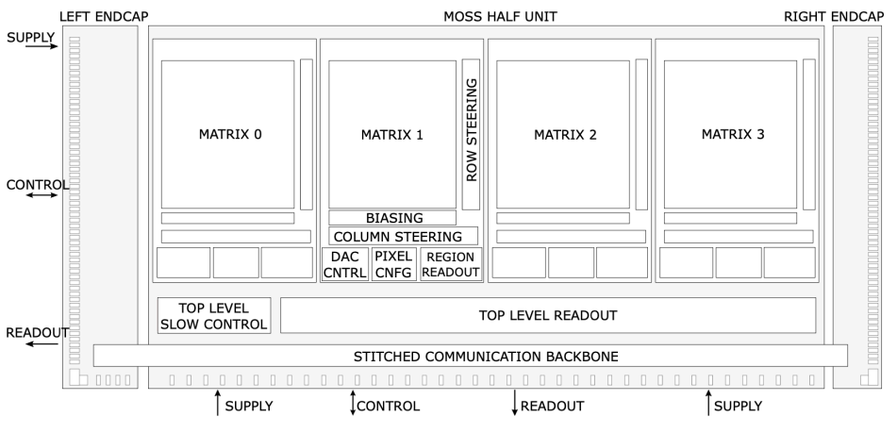

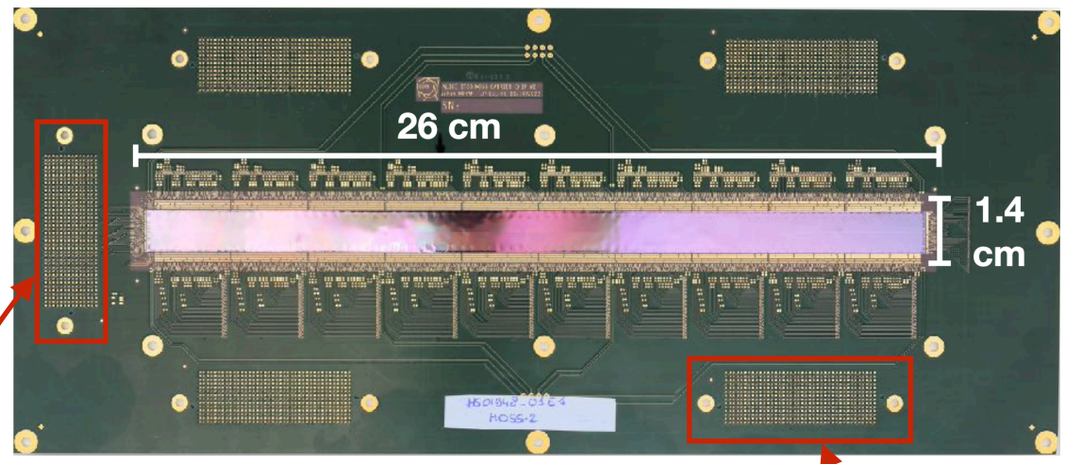

Short edge - testing full stitched sensor simultaneously

Long edge - each 10 RSUs can be tested independently

Wafer-size sensors: 2D stitching

» MOSS qualification
- **First successful contact and readout on May!**
  - using dedicated probe card on wafer
- **First operation in a telescope under beam in August!**
  - correlation with reference planes already visible

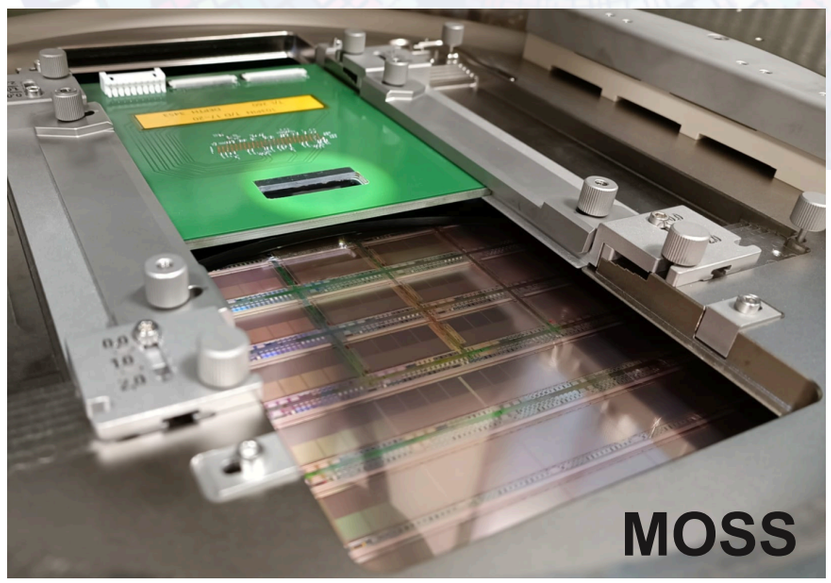

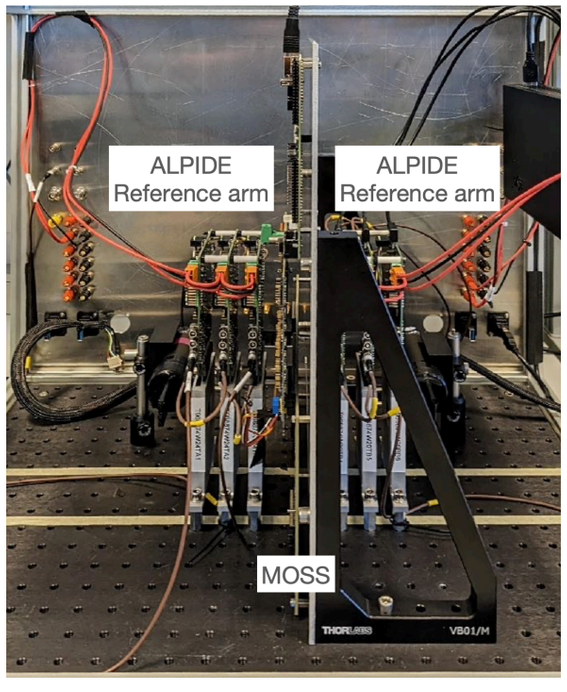

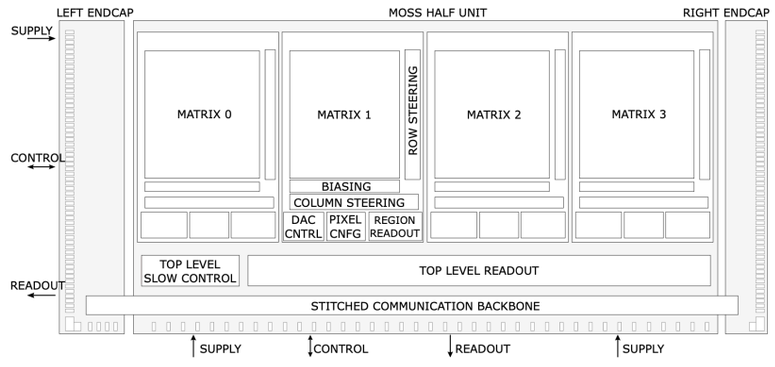

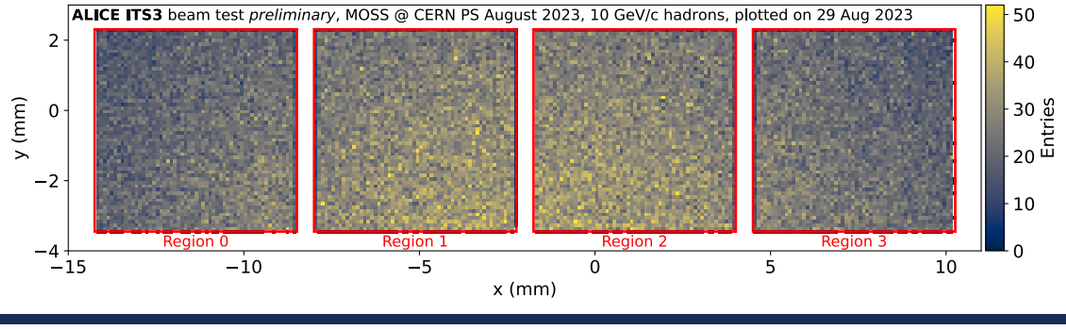

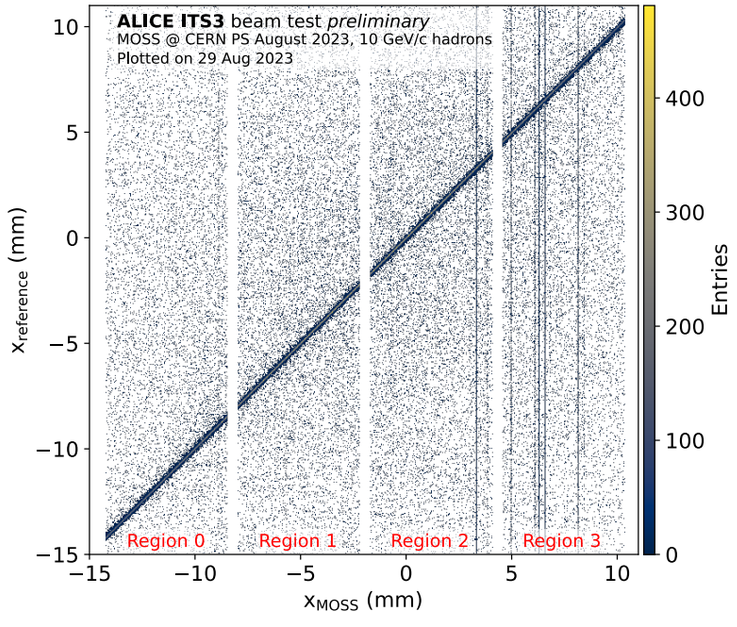

Wafer-size sensors: 2D stitching

Really exciting initial results from first stitching sensor!

» Path to the final sensor for ITS3:

- ER1 validation during 2023
- submission of ER2, compliant with ITS3 requirements, beginning 2024
- submission of final sensor (ER3) in 2025

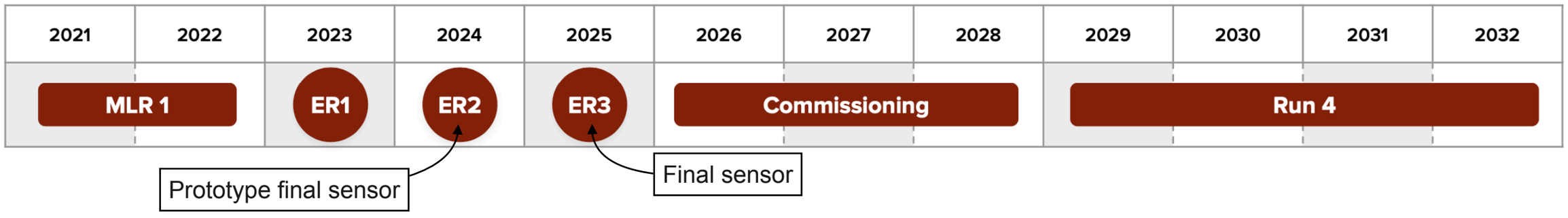

Bending effect on MAPS

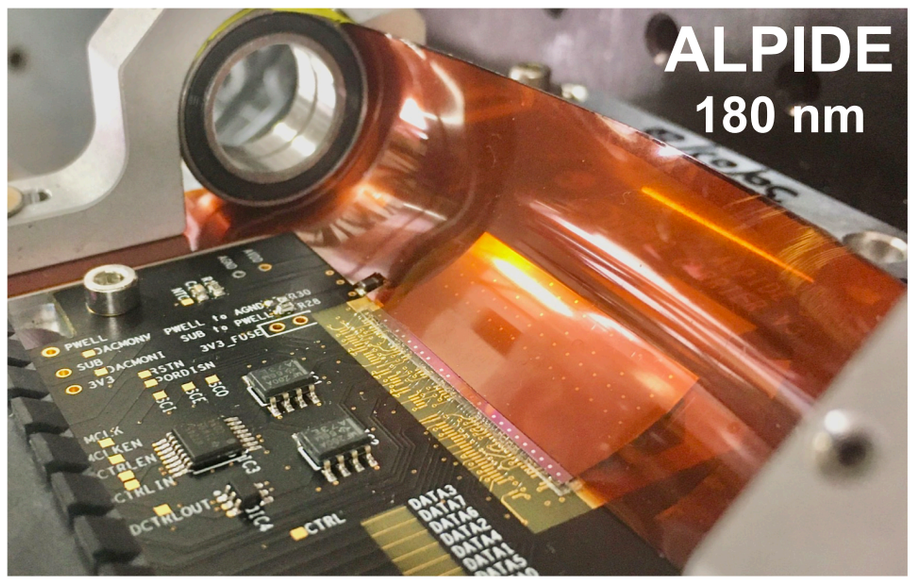

» Laboratory and test beam measurements (Jun 2020) allow to conclude that **chip (180 nm CMOS) performance doesn't change after bending**
- Pixel matrix threshold distribution does not change when sensor is bent
- Efficiency above 99.9% at a threshold of 100 e^-

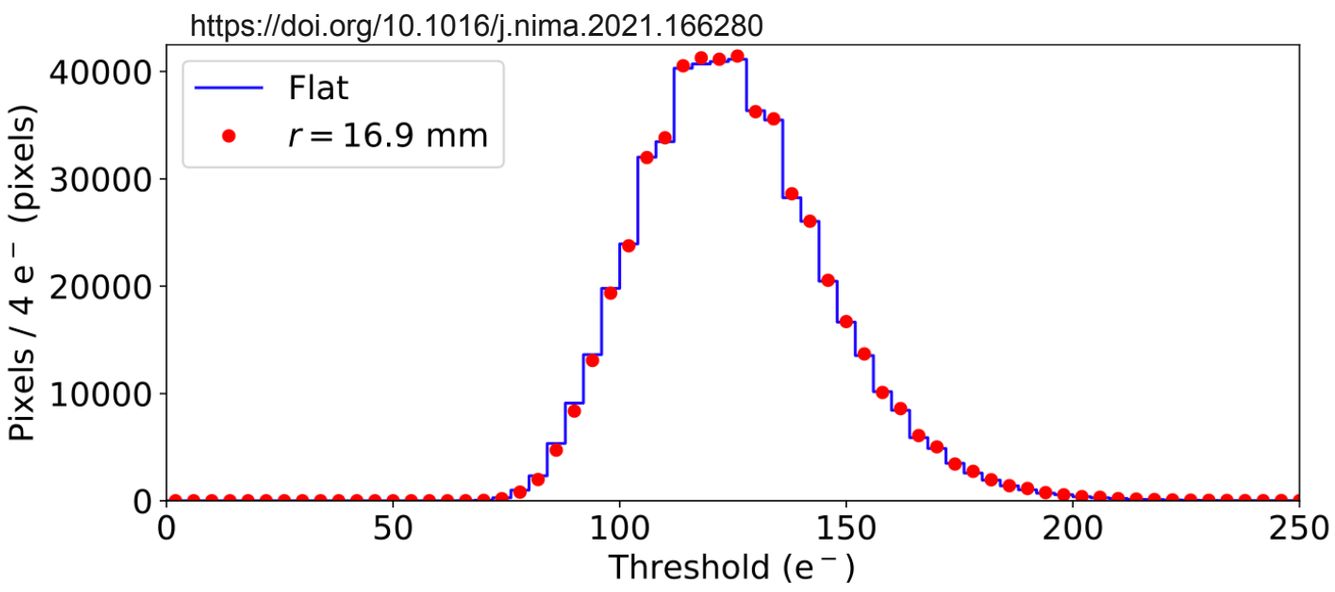

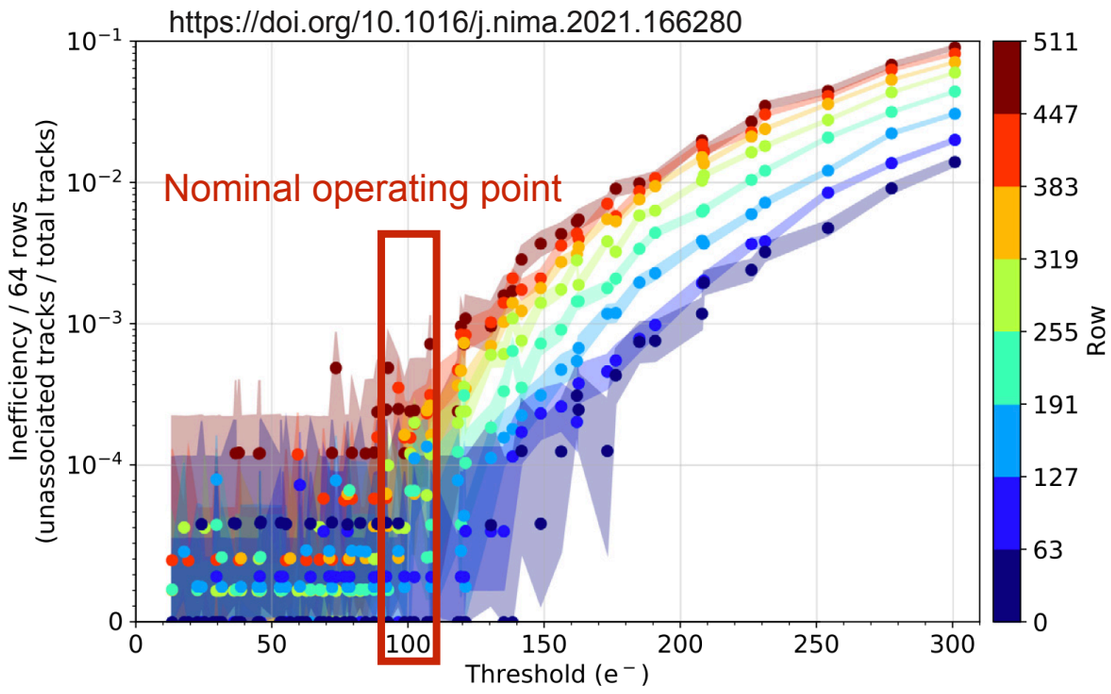

Bending effect on MAPS

» Laboratory and test beam measurements (Jun 2020) allow to conclude that **chip (180 nm CMOS) performance doesn't change after bending**
- Pixel matrix threshold distribution does not change when sensor is bent
- Efficiency above 99.9% at a threshold of 100 e^-

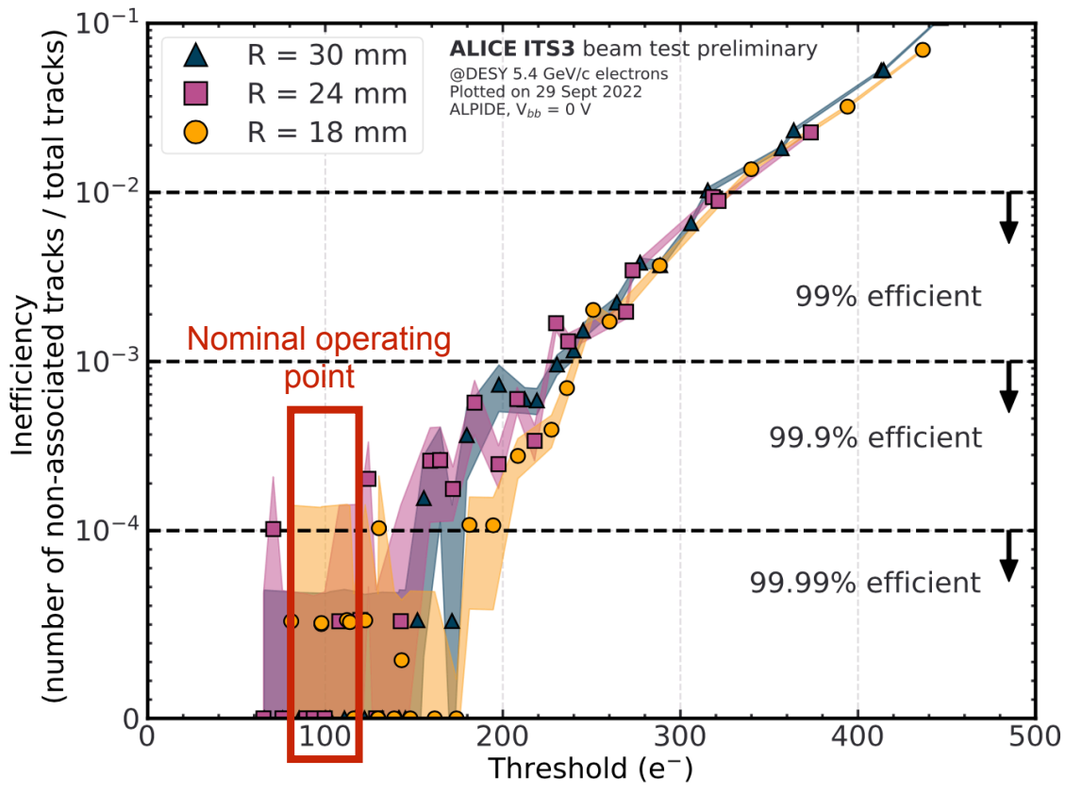

Bending effect on MAPS

» Comparison between flat and bent MLR1 (65 nm) sensors (both APTS and DPTS) ongoing
- Bending procedure developed and proximity board adapted to bent configuration
- Few samples prepared and under measurements in laboratory with ^{55}Fe source

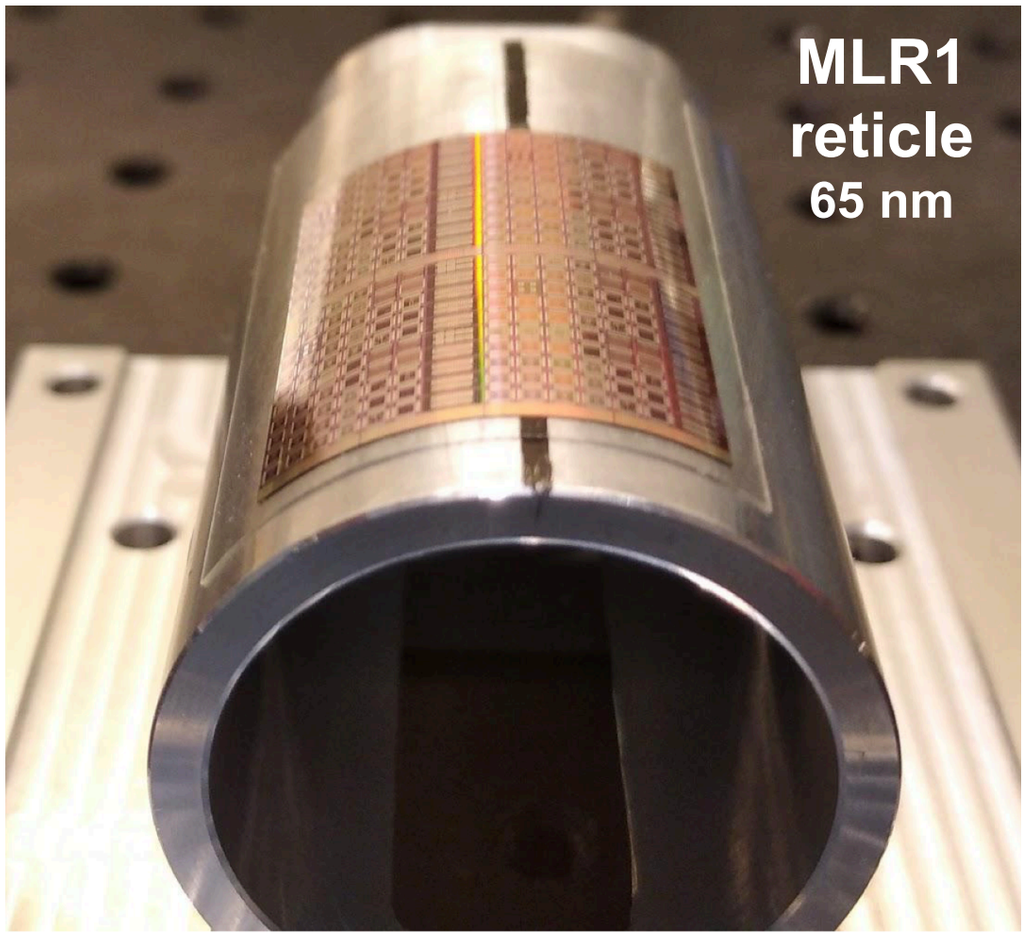

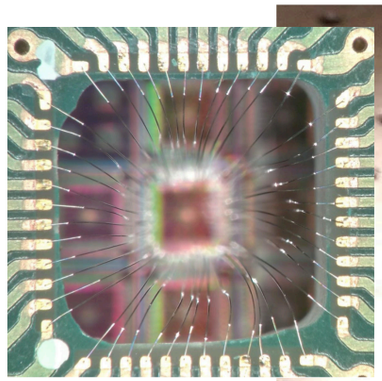

Board

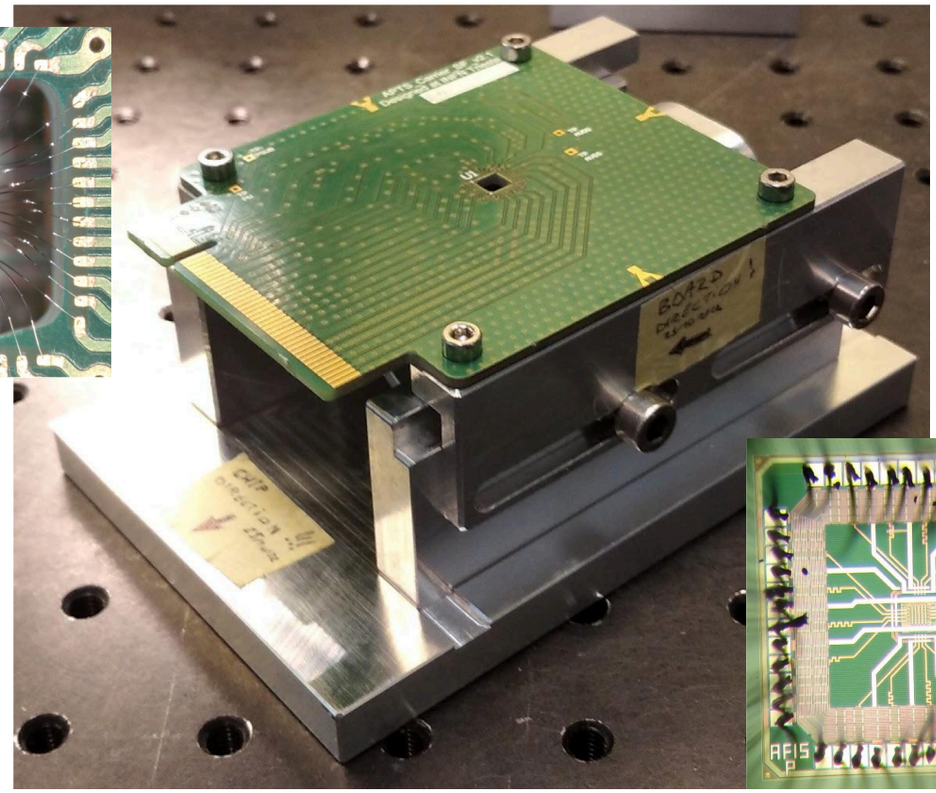

Sensor

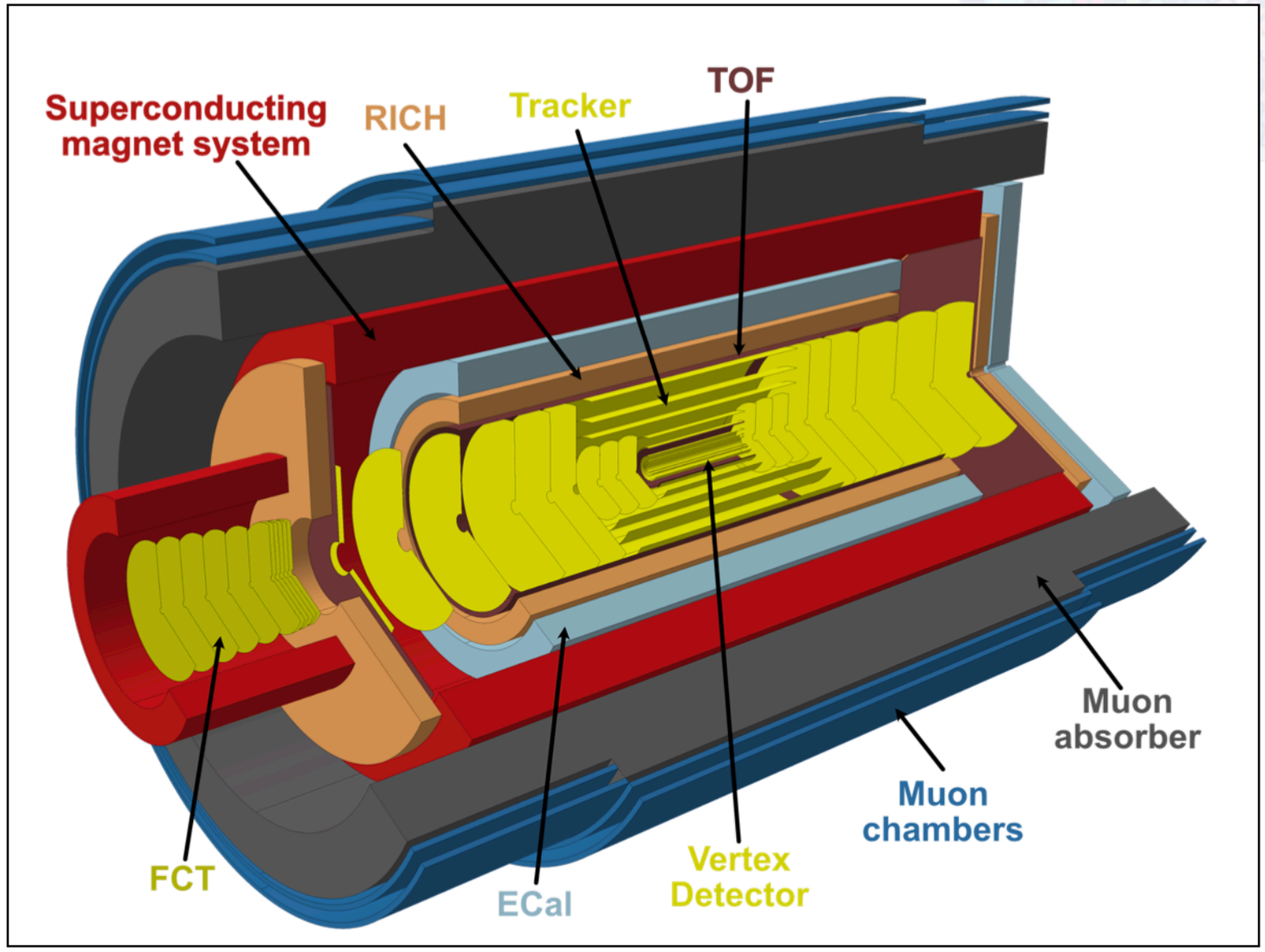

ALICE3: a silicon sensor based experiment

ALPIDE leap ITS3 developments ALICE3 developments

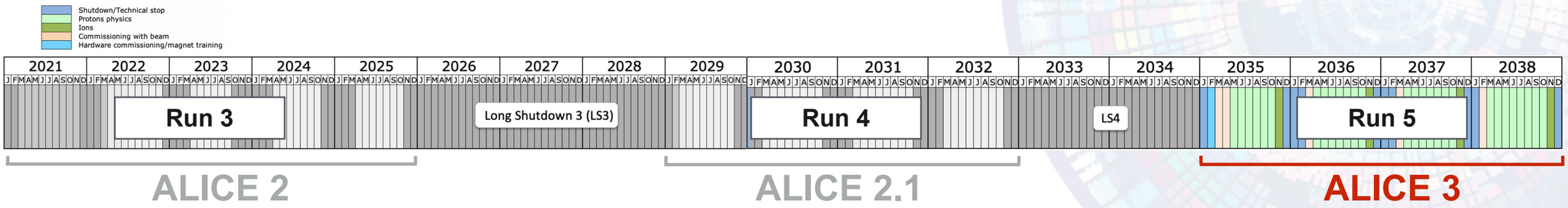

A next generation LHC HI (soft-QCD experiment) giving unprecedented insight into QGP

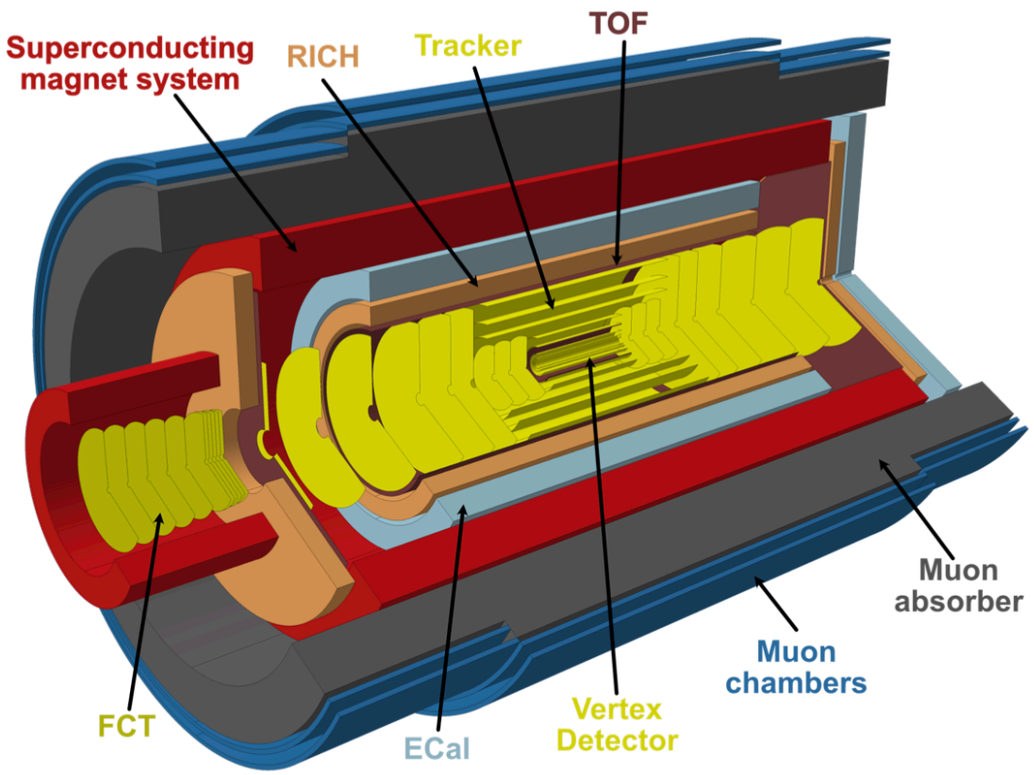

Compact all-silicon nearly massless detector!

» Core will be a 70 m² MAPS tracker
- *innermost layers* based on wafer-scale silicon sensors in vacuum and retractible
- *outer tracker* based on modules

» Extensive particle identification, including time-of-flight based detector
- silicon based sensor with timing resolution of ~20 ps
- technology choices include MAPS

Expression of Interest (2019): https://arxiv.org/abs/1902.01211
LoI (2022) [LHCC-2022-009]: https://cds.cern.ch/record/2803563?ln=fr

Outer tracker

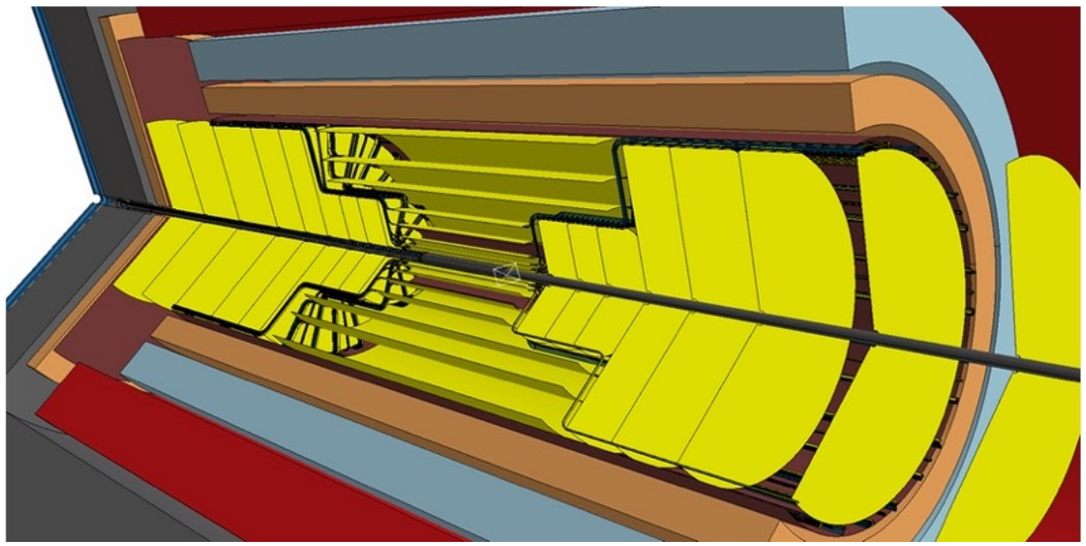

Total MAPS surface ~70 m²

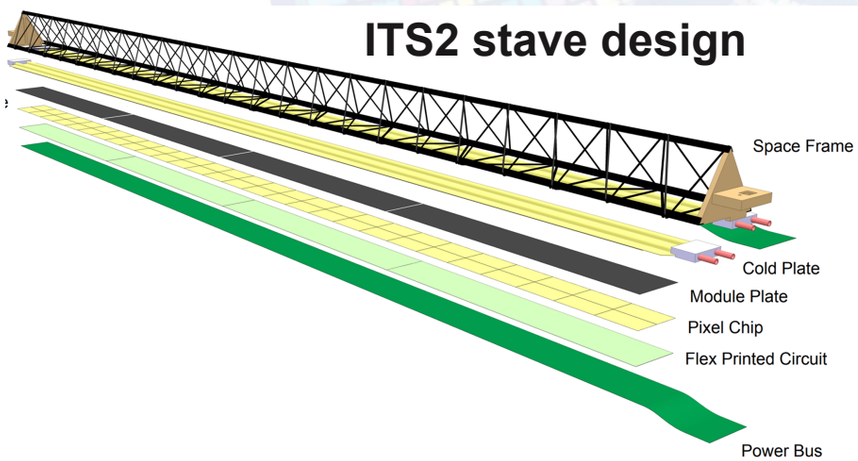

LEGO like interlocking concept

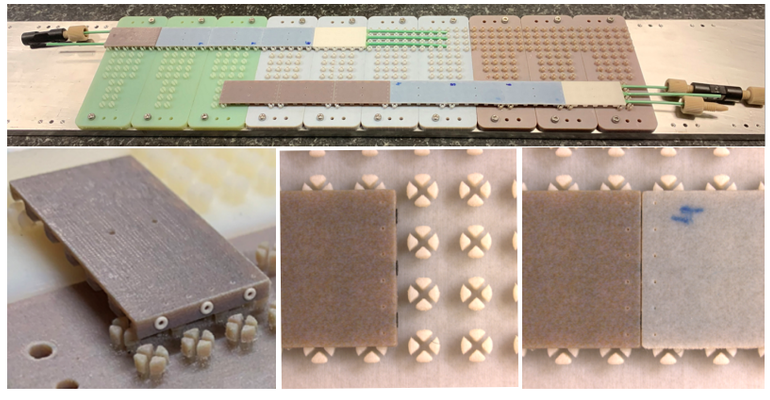

- » Stave based layers, like ITS2, but one order of magnitude larger surface
- » Module (O(10 x 10 cm²)) concept based on industry-standard processes for assembly and testing
- » Basic requirements
  - large coverage: ±4η
  - high-spatial resolution: ≈ 10 μm
  - very low material budget X/X_0 (per layer): ≲ 1%

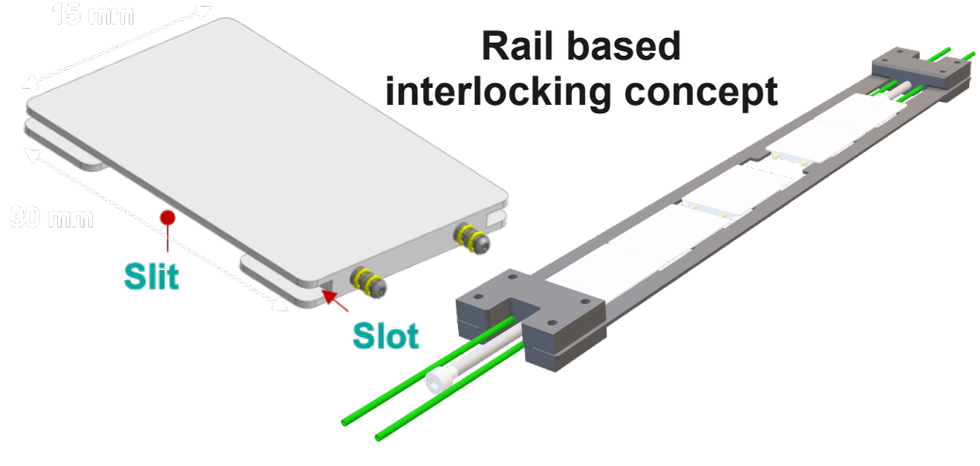

Rail based interlocking concept

Inner tracker - IRIS tracker

» Based on wafer-scale, ultra-thin, curved MAPS

» Basic requirements
- radial distance from interaction point: 5 mm (inside beam pipe, retractible configuration)
- unprecedented spatial resolution: ≈ 2.5 μm
- unprecedented low material budget X/X_0 (per layer): ≲ 0.1%
- radiation tolerance: ≈ 10^{16} 1 MeV n_{eq}/cm^2 + 200 Mrad
- hit rates up to: 94 MHz/cm^2

» R&D will largely leverage on the ITS3 developments and push improvements on a number of fronts

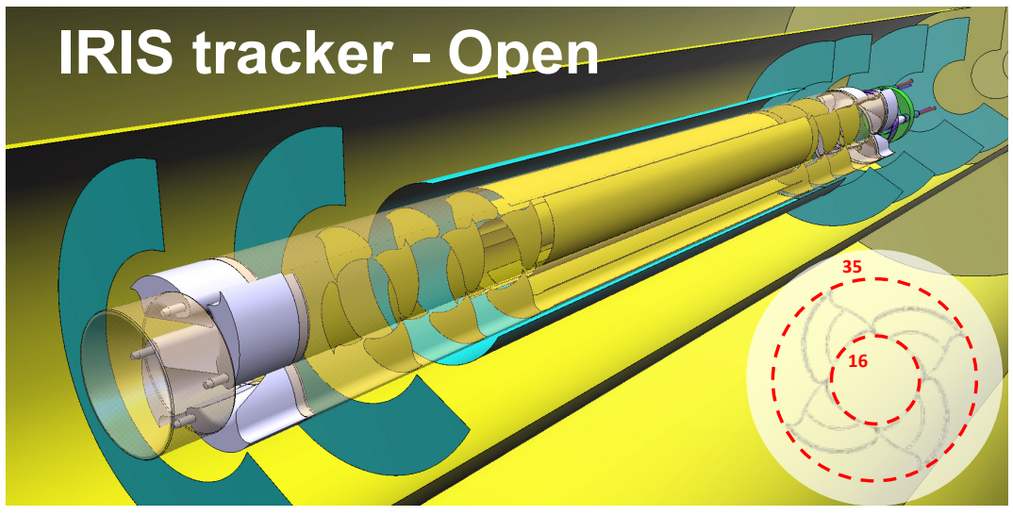

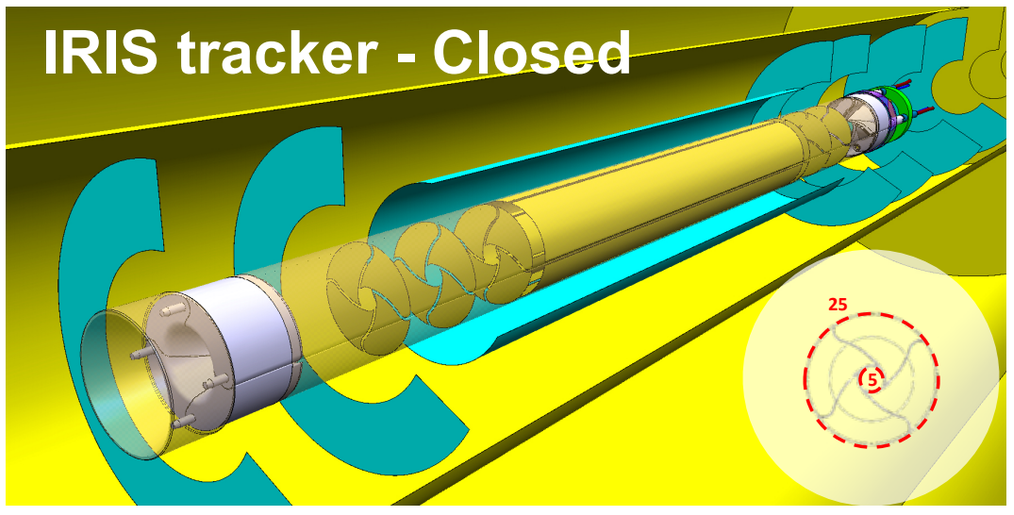

Inner tracker - IRIS tracker

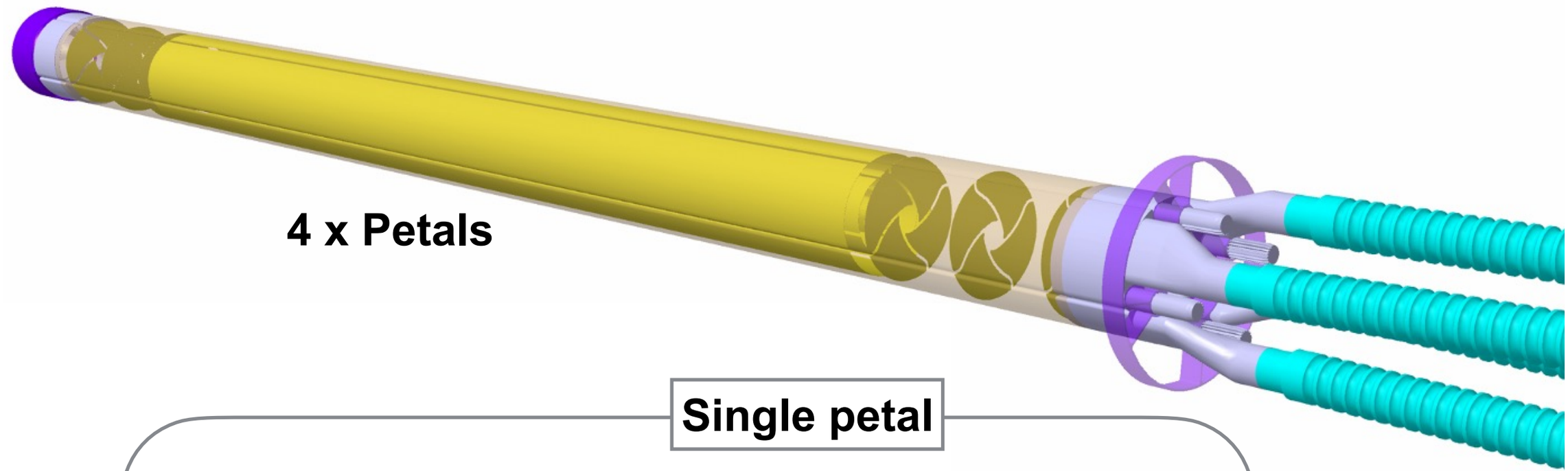

Single petal

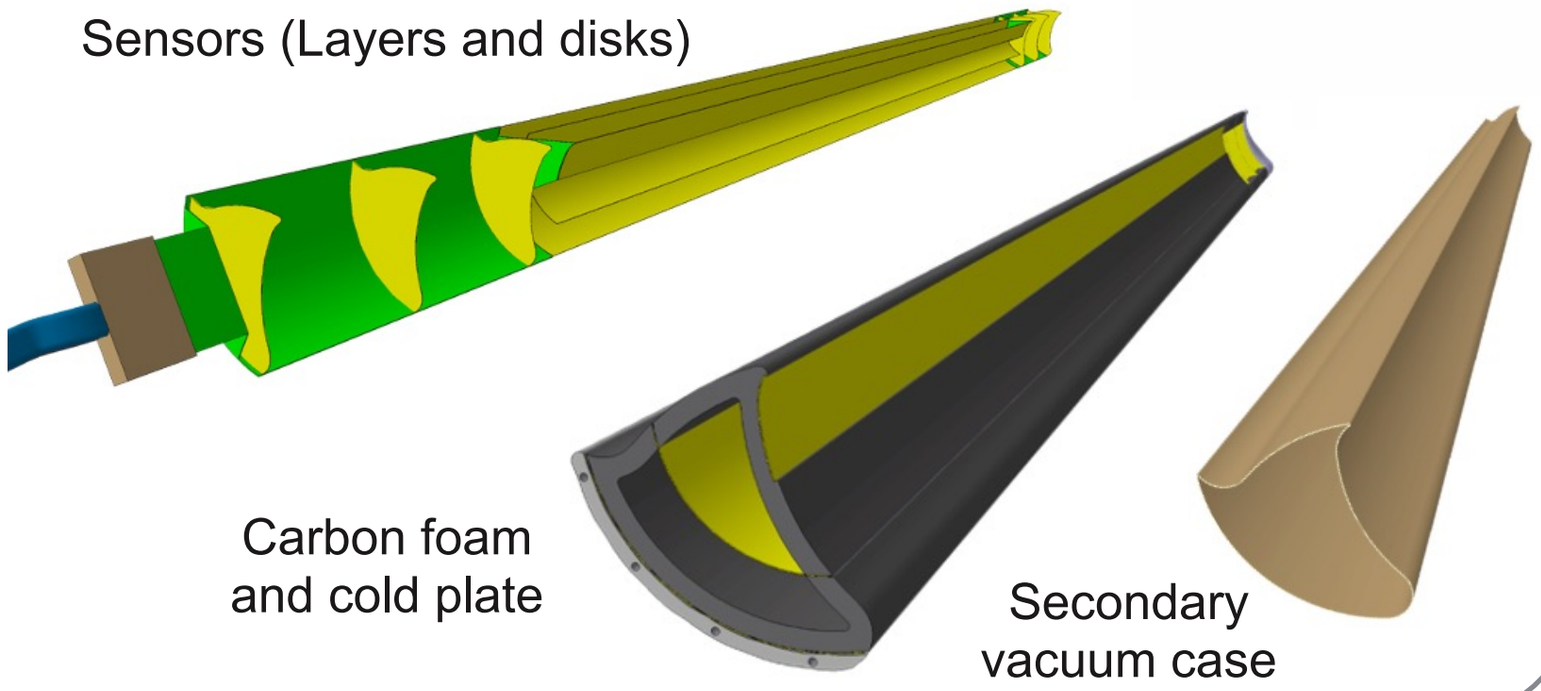

Inner tracker - IRIS tracker

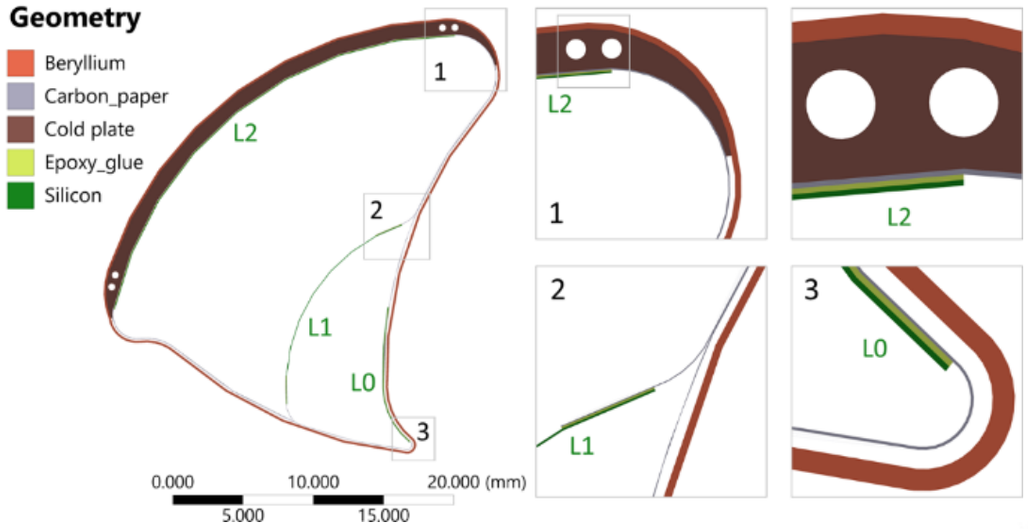

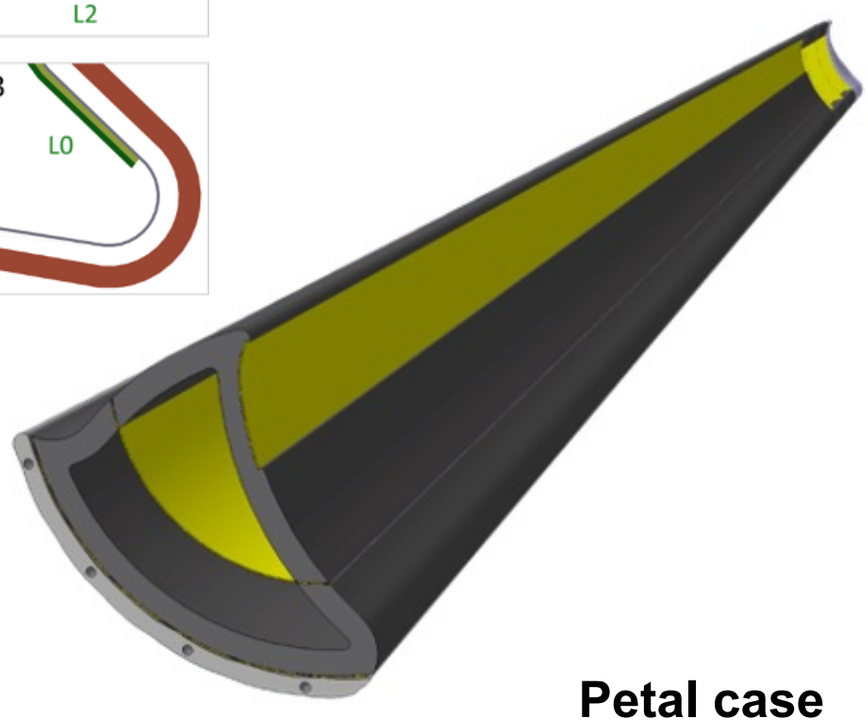

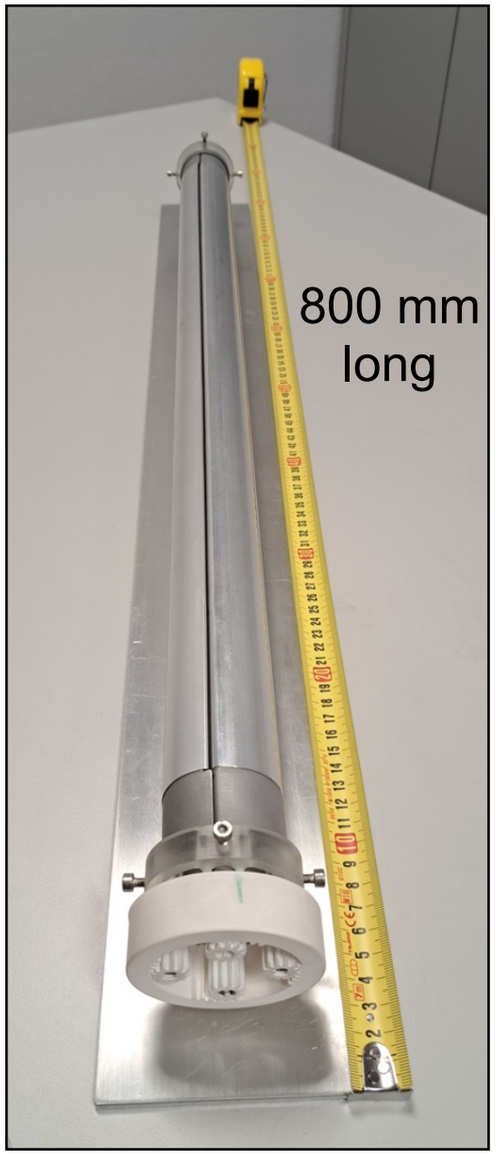

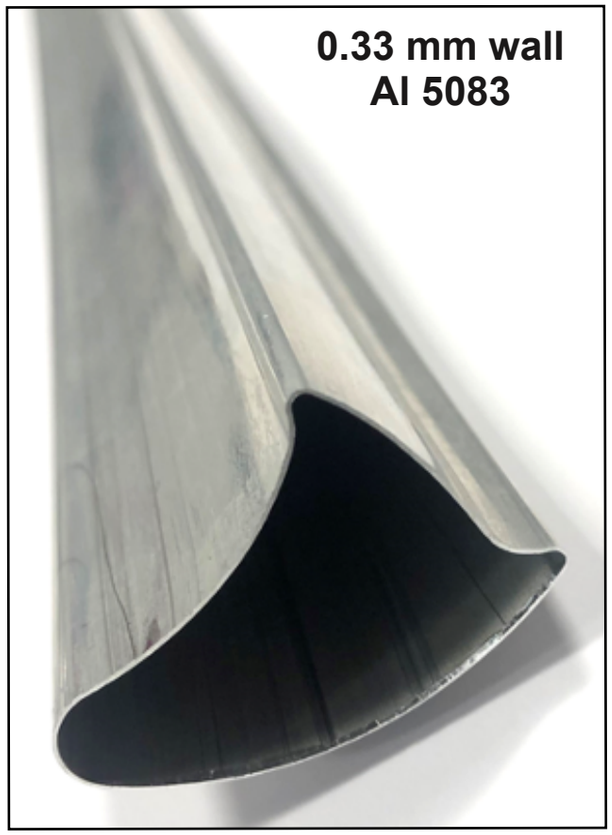

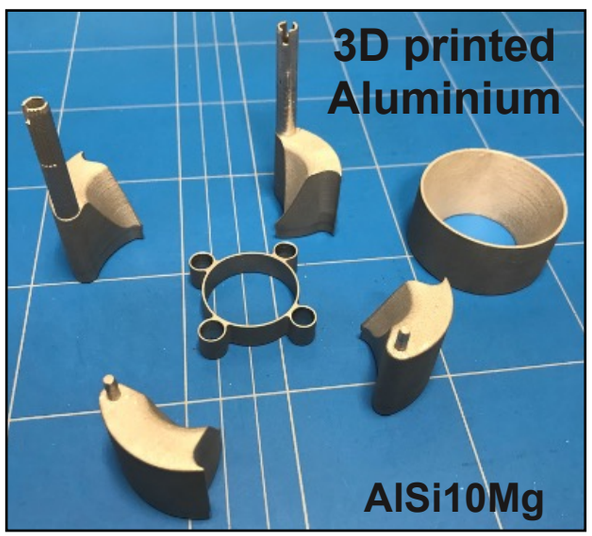

Petal case bread board model

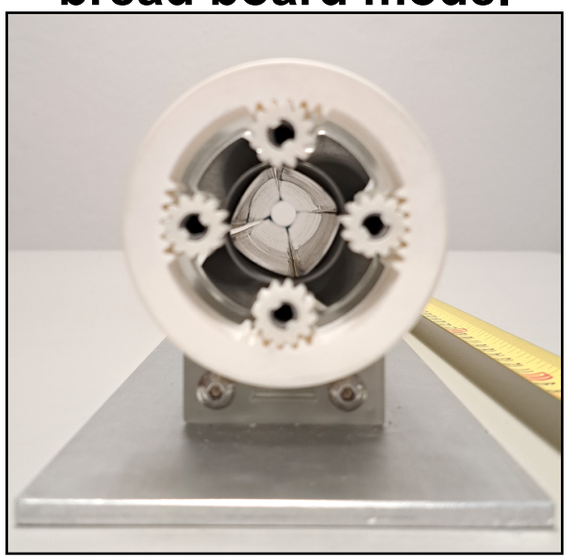

Timing performance for TOF

» TOF separation power $\propto L/\sigma_{TOF}$
- distance and time resolution crucial

» 2 barrel + 1 forward layers
- outer TOF at R ≈ 85 cm
- inner TOF at R ≈ 19 cm
- forward TOF at z ≈ 405 cm

» Sensor basic requirements
- timing resolution: ≈ 20 ps
- material budget X/X_0 (per layer): 1-3%
- power consumption: < 50 mW/cm²

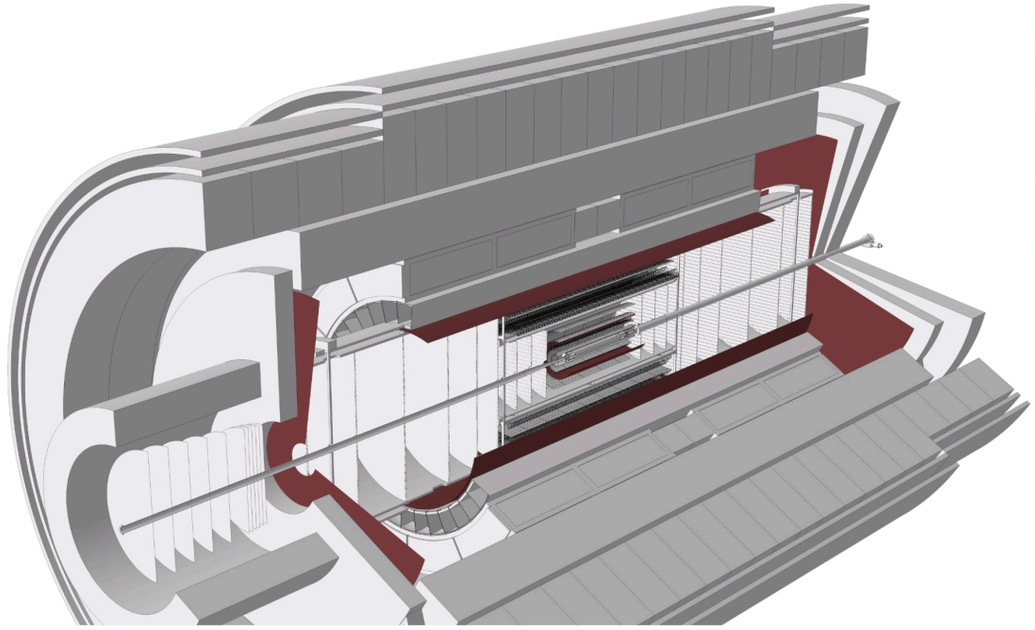

Total TOF surface ~45 m²

SiPM

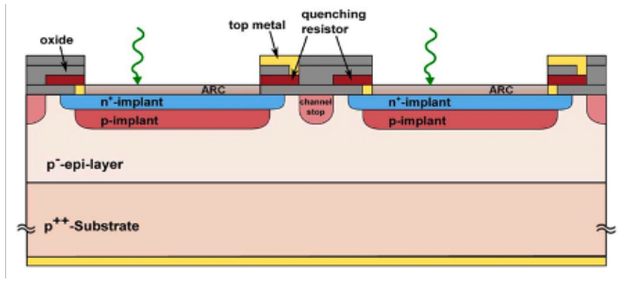

- Timing resolution: ≈ 20 ps only for photons
- Feasibility to be demonstrated with charged particles

L-GAD

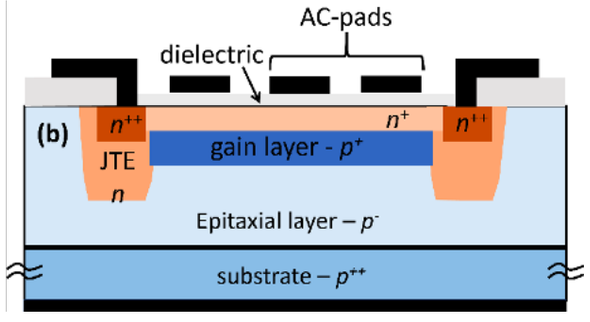

- Timing resolution of ≈ 30 ps demonstrated with 50 µm up to (1-2) 10^{15} 1 MeV n_{eq}/cm^2
- Thinner LGADs produced by different manufacturers

HV DEPLETED MAPS

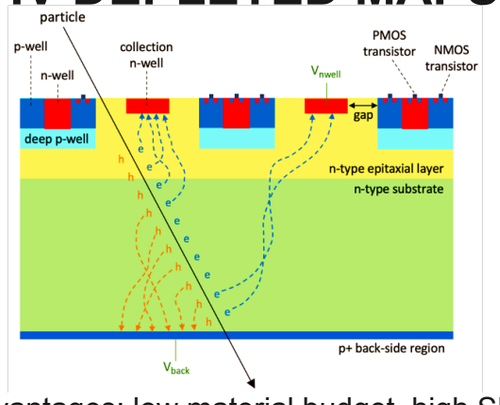

- Advantages: low material budget, high SNR
- Investigation on innovative design to proof timing performance

Timing performance for TOF - MAPS

» Several monolithic projects targeting enhanced timing resolution

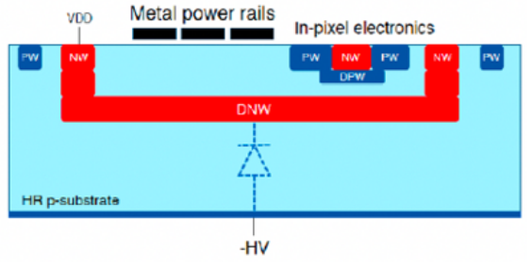

Y. Degerli et al., 2020 JINST 15 P06011

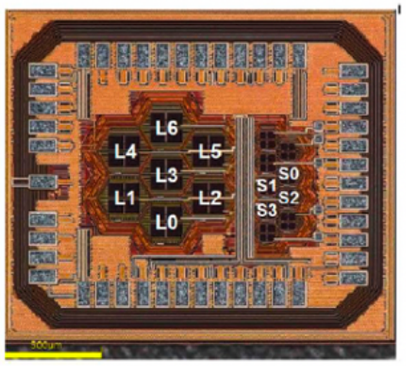

G. Iacobucci et al., 2019 JINST 14 P11008

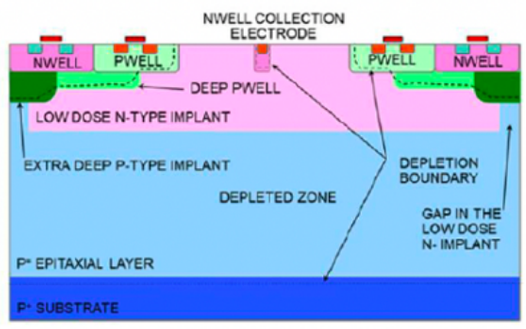

T. Kugathasan et al., Nucl. Inst. Meth. A Vol. 979, Nov. 2020

» Project with application in ALICE

ARCADIA sensor

- Developed between INFN and LFoundry
- 110 nm CMOS, 6 metal layers
- Adding gain layer (gain 10-20) to reach **20 ps** resolution
- First prototype received in January 2023
  - pixel size: 250 x 100 μm^2
  - diode area: 220 x 70 μm^2
  - sensor capacitance: 127 fF
  - electronics size: 280 x 8 μm^2
  - active thickness: 50 µm
- Test beam campaign ongoing, results in Q4 2023

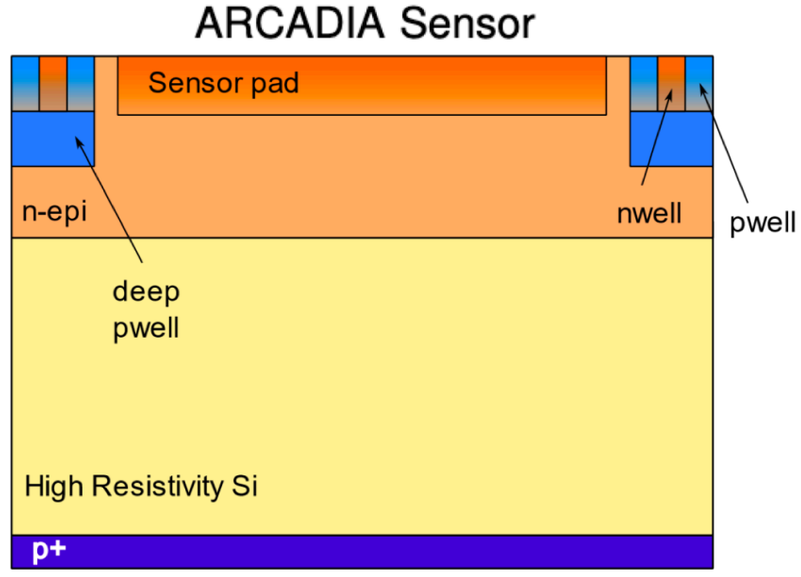

L. Pancheri, 2022

IEEE TRANSACTIONS ON ELECTRON DEVICES, VOL. 67, NO. 6, JUNE 2020

Summary

- **CMOS sensors in 180 nm technology successfully used for trackers**
  - used in ALICE (ITS2, MFT), sPHENIX and considered for other experiments (modified process)
  - limited by slow charge collection
  - process modification needed → many development ongoing
- **Future developments rely on wafer scale sensors (ITS3, ALICE 3)**
  - 65 nm TPSCo technology validated
  - first successful contact and readout of ER1 stitched sensor prototype (MOSS)
  - next stitched sensor submission (ER2), ITS3 requirements compatible, in preparation
- **Extensive R&D ongoing**
  - bending of wafer scale sensors
  - characterization of 65 nm bent structures
  - mechanical support and cooling studies
  - conceptual design of industry-standard processes for module assembly and test
  - MAPS with high timing performance development

Backup

Backup

Evolution of the ALICE Inner Tracking System from LHC Run1 to the future

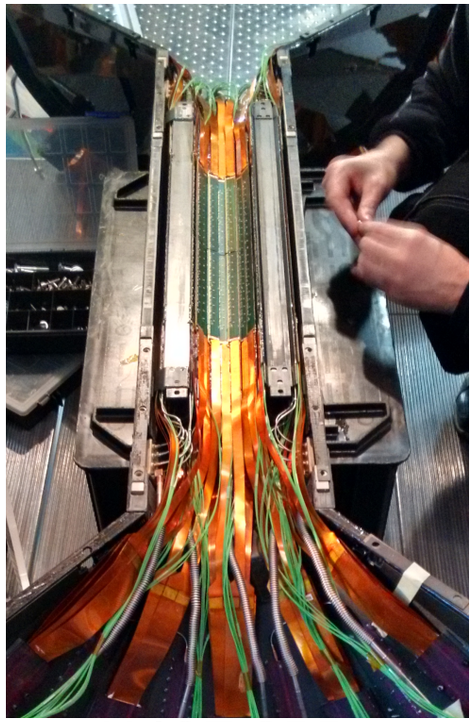

ALICE SPD

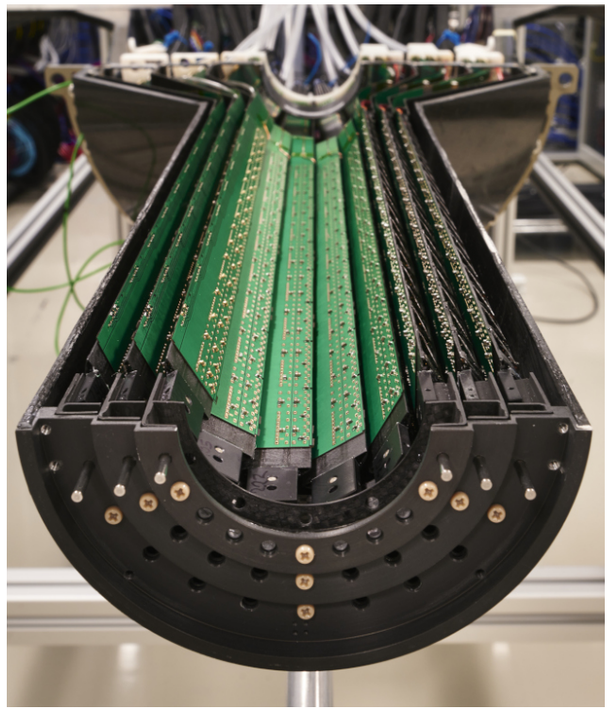

ALPIDE ITS2 (IB)

ALPIDE ITS3

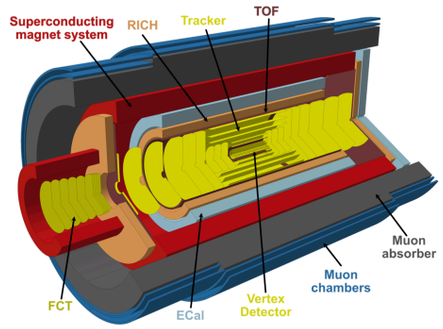

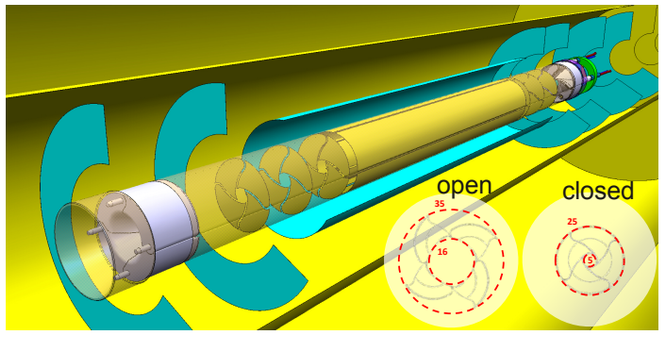

ALICE 3 Tracker + IRIS

Detector	Technology	Innermost layer radius (cm)	X/X_0 (%) for lighter layer	Total surface (m^2)	Operation
SPD	hybrid	3.9	1.14	0.21	Run 1+2
ITS2 + MFT	MAPS	2.2	0.35	O(10)	Run 3 + (4)
ITS3	MAPS	1.8	<0.1	0.24	Run 4
ALICE 3 tracker + IRIS	MAPS	0.5 (closed)	<0.1	O(70)	> Run 4

Hybrid vs Monolithic sensors

Characteristics of a sensor for tracking/vertexing

» High space point resolution (~10 μm)
» High detection efficiency (~100%) and low fake-hit rate
» Low material budget (< 0.1%)
» Low power density (→ material budget) ⇅
» Time resolution
» Radiation hardness (HL-LHC ~2×10^{16} 1 MeV n_{eq}/cm^2)

Hybrid sensor

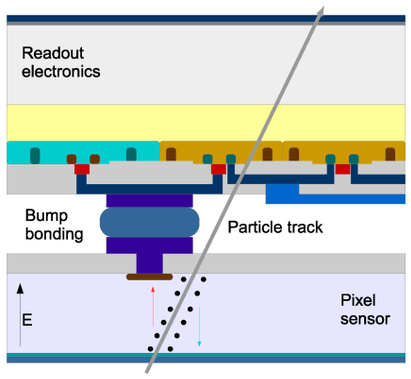

» **pro** - optimisation of readout and electronics
» **pro** - large signal
» **cons** - large material budget
» **cons** - large power consumption

Monolithic sensor

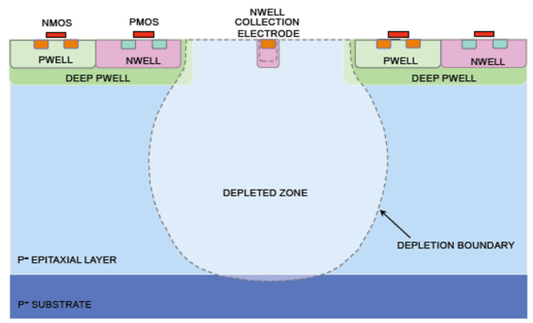

» **pro** - standard CMOS readout integration
» **pro** - low material budget
» **pro** - low power consumption
» **pro** - low noise
» **cons** - small signal
» **cons** - limited radiation tolerant
» **cons** - slow (charge collection by diffusion)

Backup

First MAPS based HEP detector

» First application of MAPS technology in a collider environment for STAR HFT PXL detector @RHIC/BNL (2014) → **Mimosa28**

- developed by IPHC Strasbourg
- pixel sizes: 20.7 × 20.7 μm²
- matrix: 928 × 960 pixels (890k)
- CMOS technology: twin well, AMS 0.35 μm
- readout: rolling-shutter fashion in 185.6 μs
- power budget: 170 mW/cm²

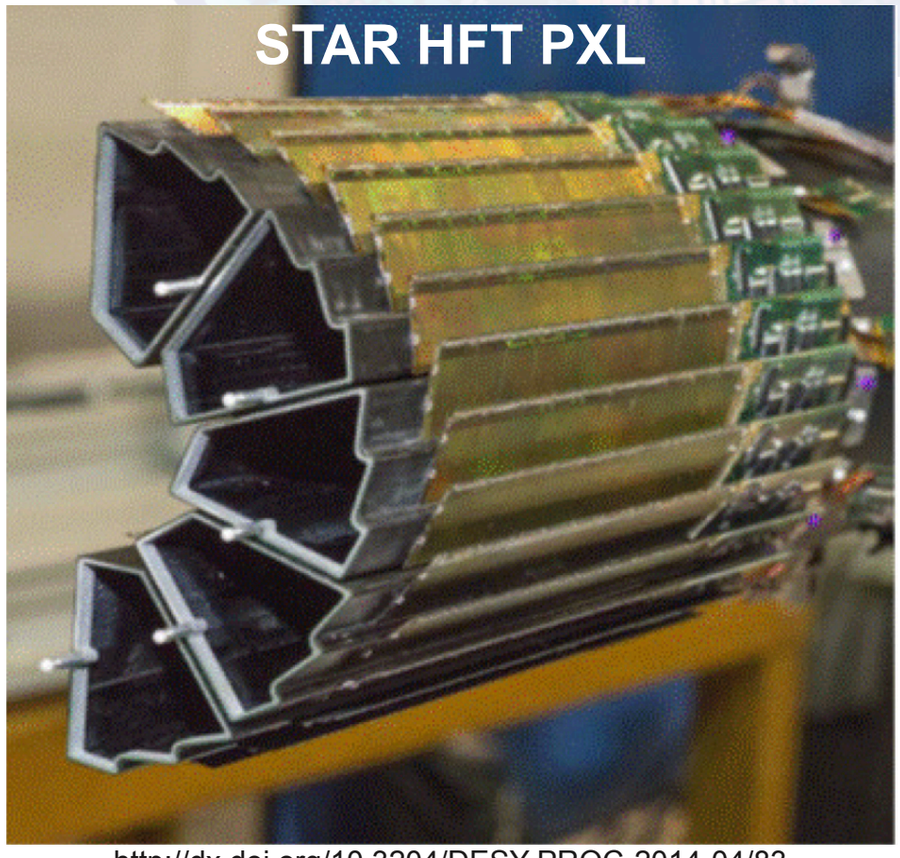

http://dx.doi.org/10.3204/DESY-PROC-2014-04/83

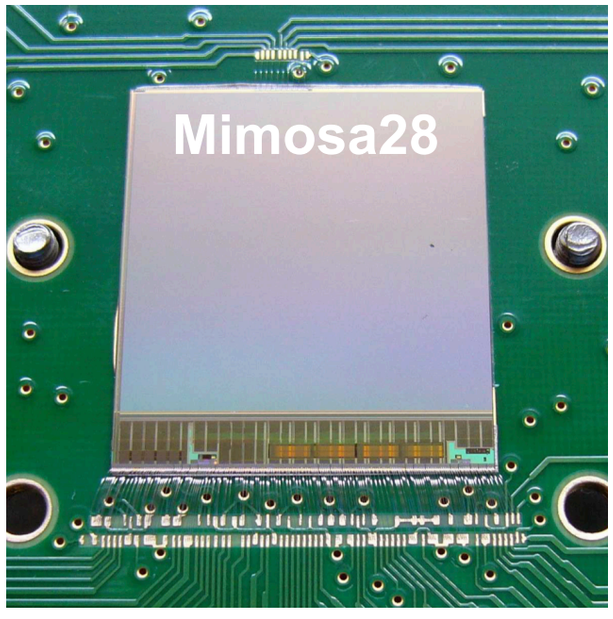

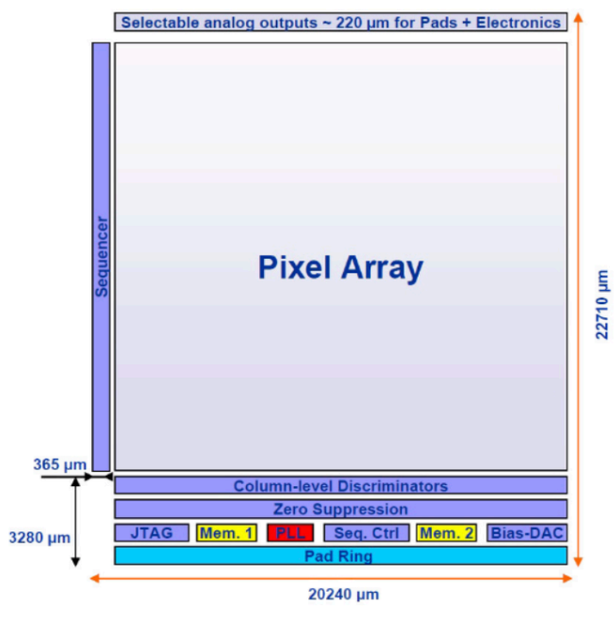

Backup

Technology improvements: toward fully depleted sensor

Four splits implemented in the 65 nm MLR1

- **split 1** - with the standard process without modifications
- **split 2** - with first modification of the deep p-well to improve isolation between circuitry and sensor to prevent punch-through between deep n-well and circuitry,
- **split 3** - adding to split 2 deep n-well adjustment in the pixel to allow full depletion
- **split 4** - adding to split 3 an additional deep p-well modification to prevent potential wells created by the additional in-pixel circuitry

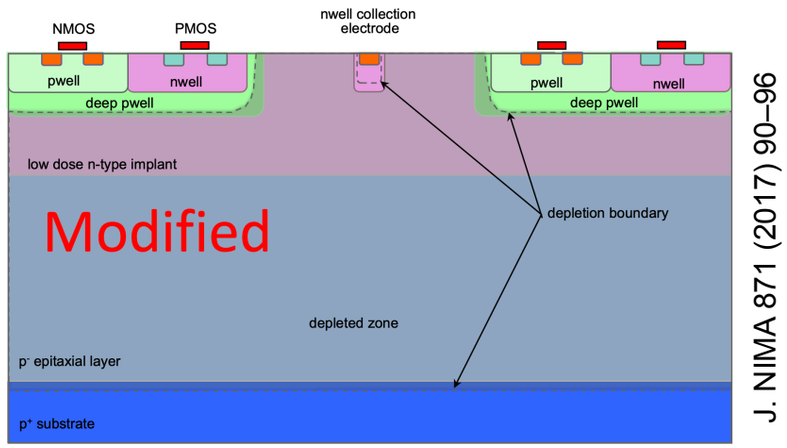

J. NIMA 871 (2017) 90–96

https://doi.org/10.22323/1.420.0083

Backup

65 nm CMOS technology: first prototypes characterization

APTS

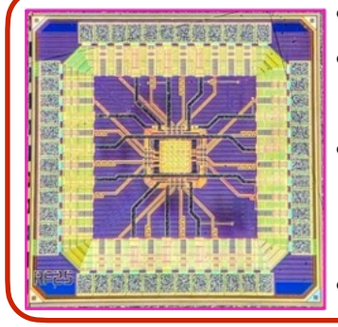

- 6x6 pixel matrix
- Direct analogue readout of central 4x4 submatrix
- Two types of output drivers:
  1. **Traditional source follower (APTS-SF)**
  2. Very fast OpAmp (APTS-OA)
- 4 pixel pitches: 10, 15, 20, 25 µm

» Moving from *Standard* to *Modified with gap* process, the fraction of charge collected by the seed pixel increases

^{55}Fe signal amplitude for different processes

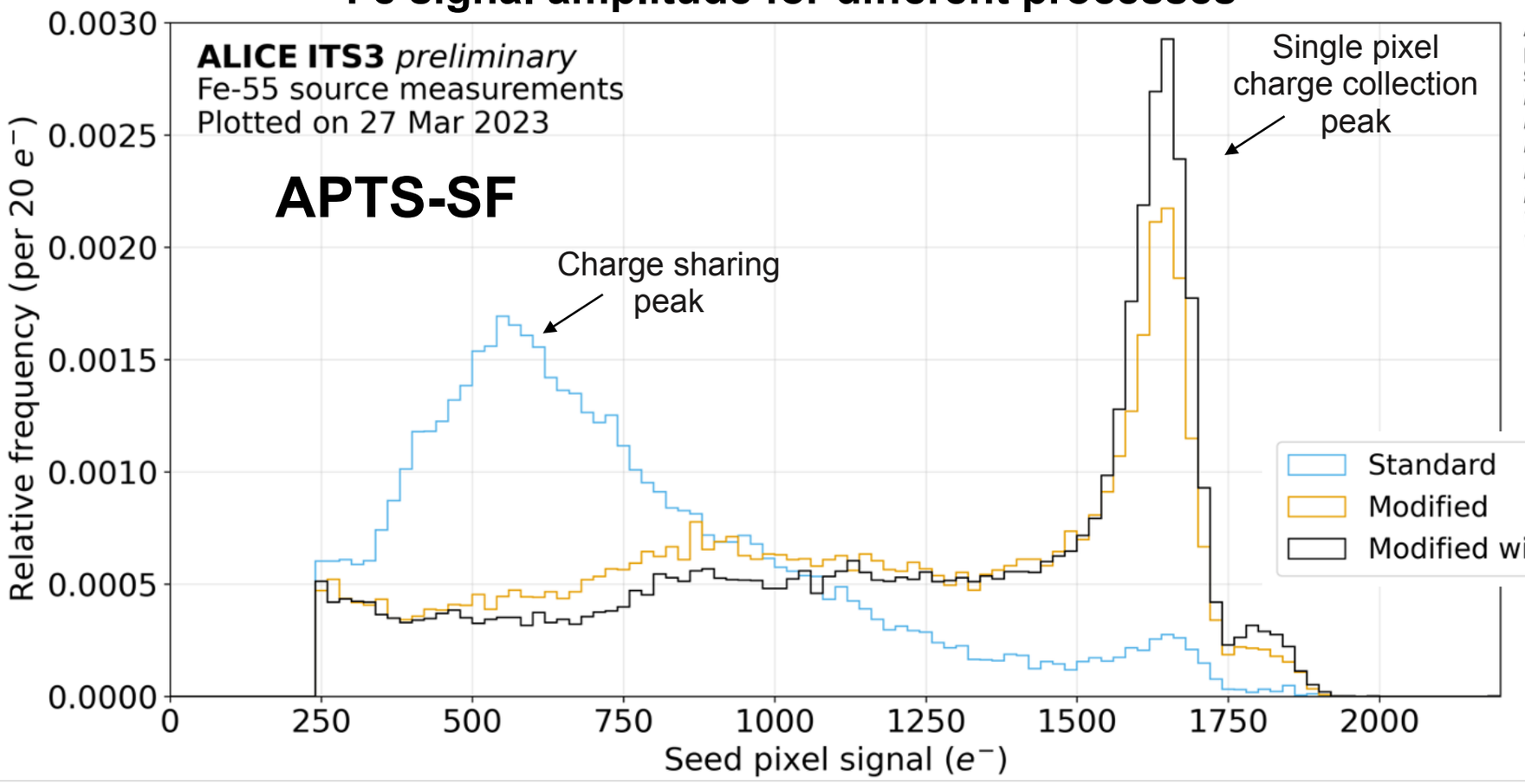

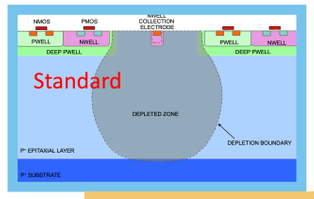

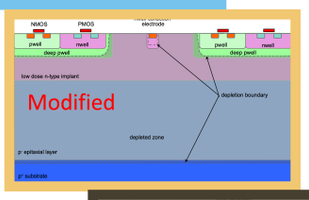

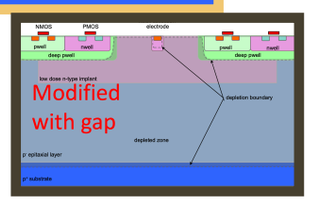

Backup

65 nm CMOS technology: first prototypes characterization

APTS

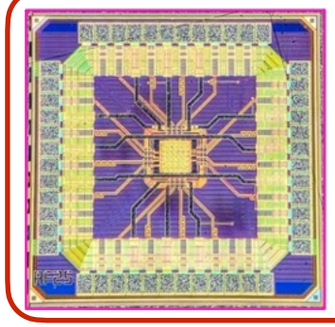

- 6x6 pixel matrix
- Direct analogue readout of central 4x4 submatrix
- Two types of output drivers:
  1. **Traditional source follower (APTS-SF)**
  2. Very fast OpAmp (APTS-OA)
- 4 pixel pitches: 10, 15, 20, 25 µm

» Moving from *Standard* to *Modified with gap* process, the efficiency degrading limit (< 99%) moves to higher threshold

Detector efficiency for different processes

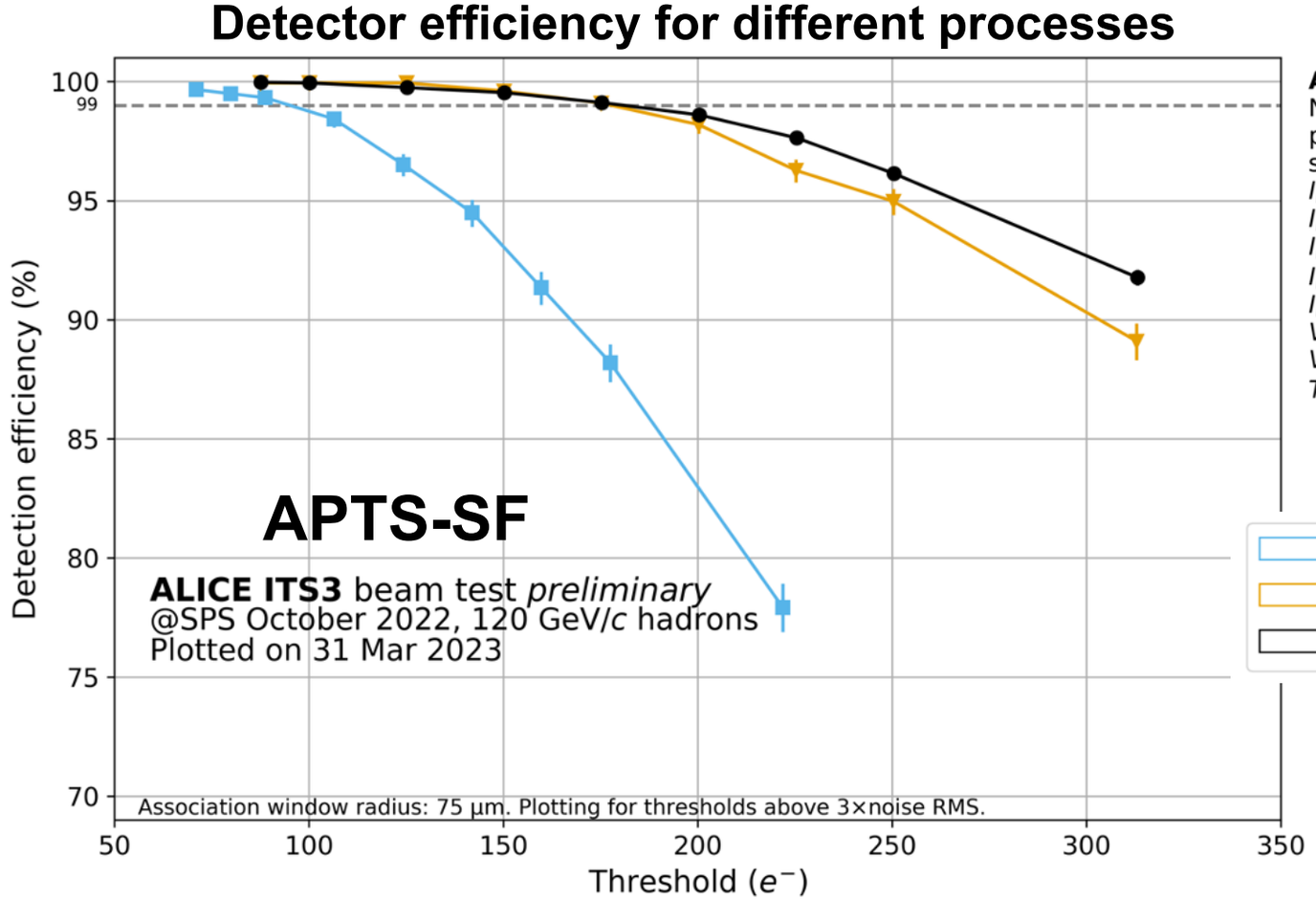

APTS SF
Non-irradiated
pitch: 15 µm
split: 4
$I_{reset} = 100$ pA
$I_{biasn} = 5$ µA
$I_{biasp} = 0.5$ µA
$I_{bias4} = 150$ µA
$I_{bias3} = 200$ µA
$V_{reset} = 500$ mV
$V_{pwell} = V_{sub}$=-1.2 V
$T = 20$ °C

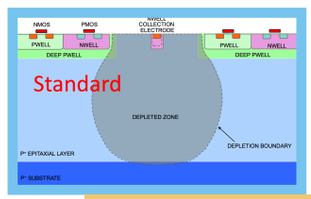

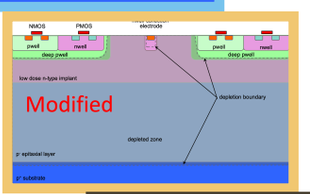

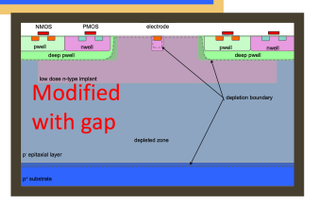

Backup

65 nm CMOS technology: first prototypes characterization

APTS

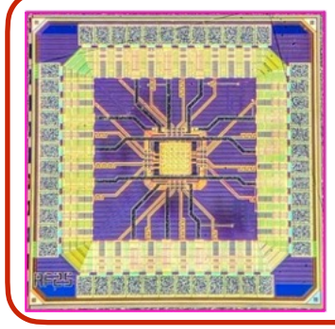

- 6x6 pixel matrix
- Direct analogue readout of central 4x4 submatrix
- Two types of output drivers:
  1. **Traditional source follower (APTS-SF)**
  2. Very fast OpAmp (APTS-OA)
- 4 pixel pitches: 10, 15, 20, 25 µm

» For *Modified with gap* process charge collection doesn't depend on pixel pitch

^{55}Fe signal amplitude for different pixel pitch

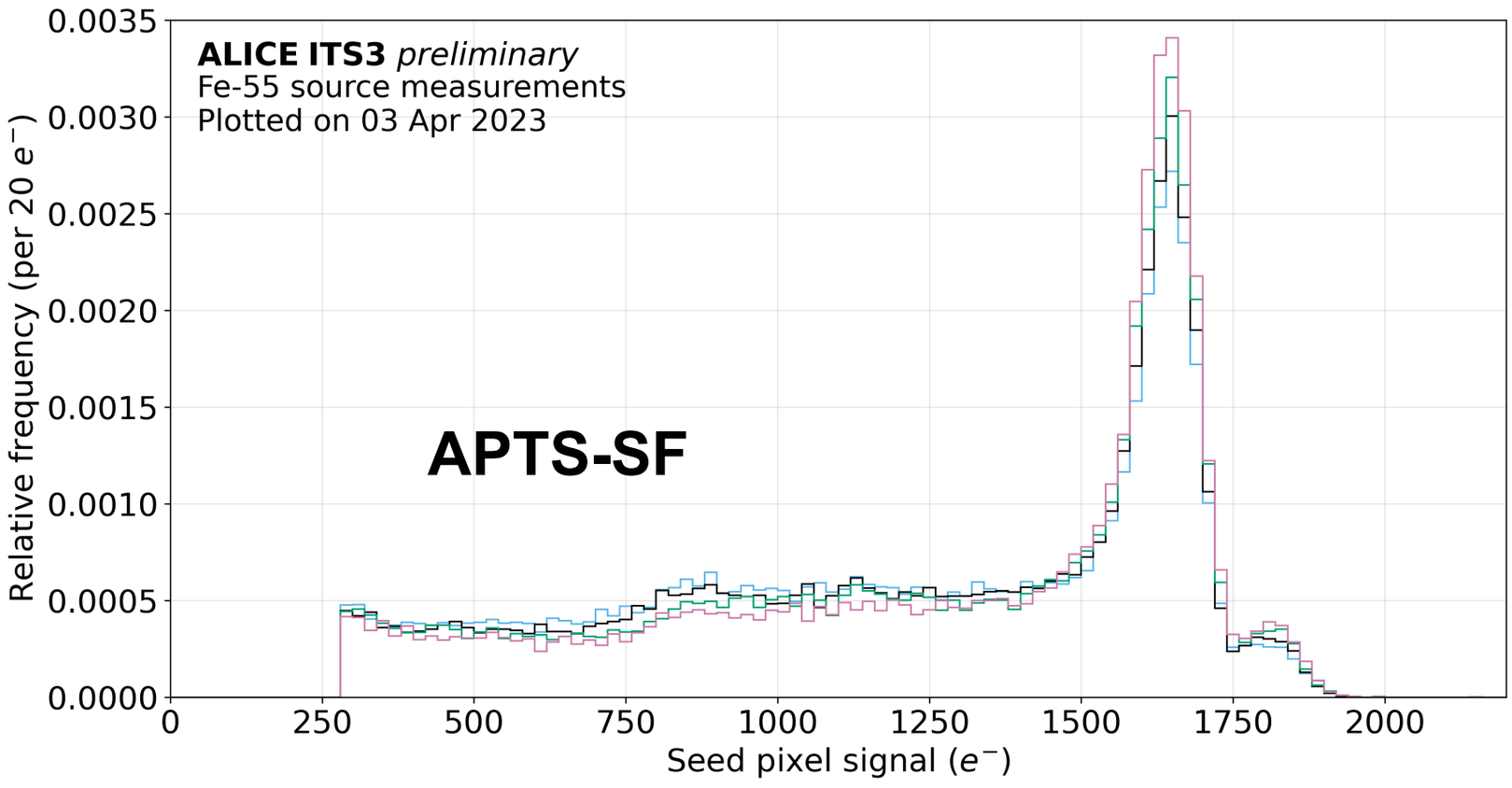

APTS SF
type: modified with gap
split: 4
$I_{reset} = 100\,pA$
$I_{biasn} = 5\,\mu A$
$I_{biasp} = 0.5\,\mu A$
$I_{bias4} = 150\,\mu A$
$I_{bias3} = 200\,\mu A$
$V_{reset} = 500\,mV$
$V_{sub} = V_{pwell} = -1.2\,V$

Pitch = 10 µm
Pitch = 15 µm
Pitch = 20 µm
Pitch = 25 µm

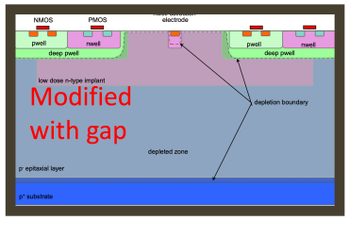

65 nm CMOS technology: first prototypes characterization

DPTS

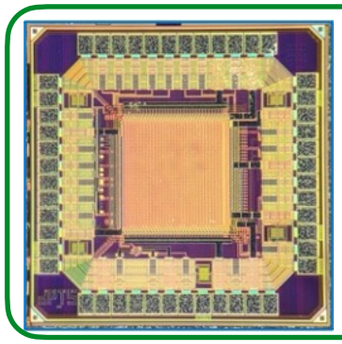

- 32x32 pixel matrix
- Asynchronous digital readout
- Time-over-threshold information
- Pixel pitch: 15 µm

» Non-ionising irradiation leads to a decrease in the detection efficiency

Detector efficiency and FHR for different irradiation level

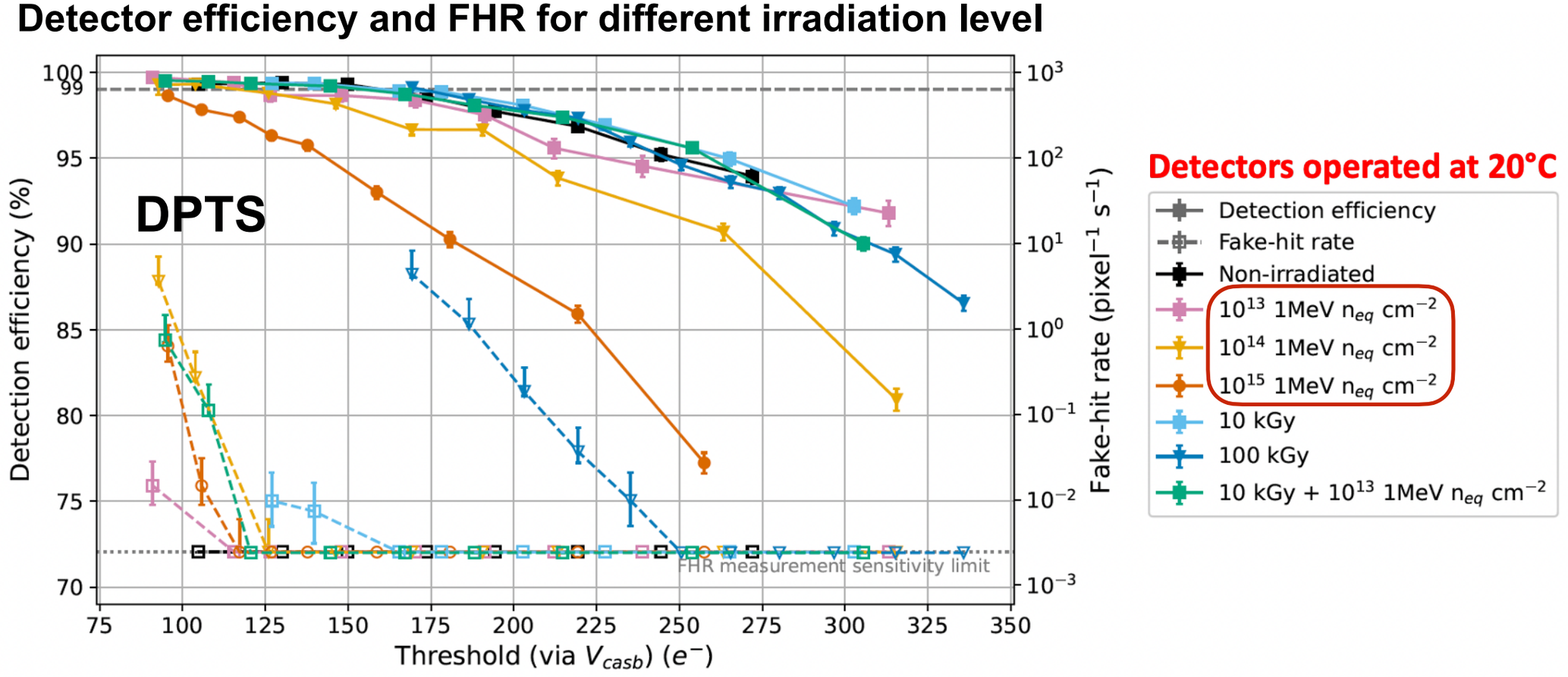

Gianluca Aglieri Rinella et al. arXiv:2212.08621v2

Backup

65 nm CMOS technology: first prototypes characterization

DPTS

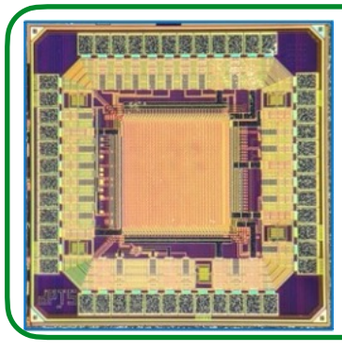

- 32x32 pixel matrix
- Asynchronous digital readout
- Time-over-threshold information
- Pixel pitch: 15 µm

» Non-ionising irradiation leads to a decrease in the detection efficiency

» Ionising irradiation leads to an increase in the fake-hit rate

Detector efficiency and FHR for different irradiation level

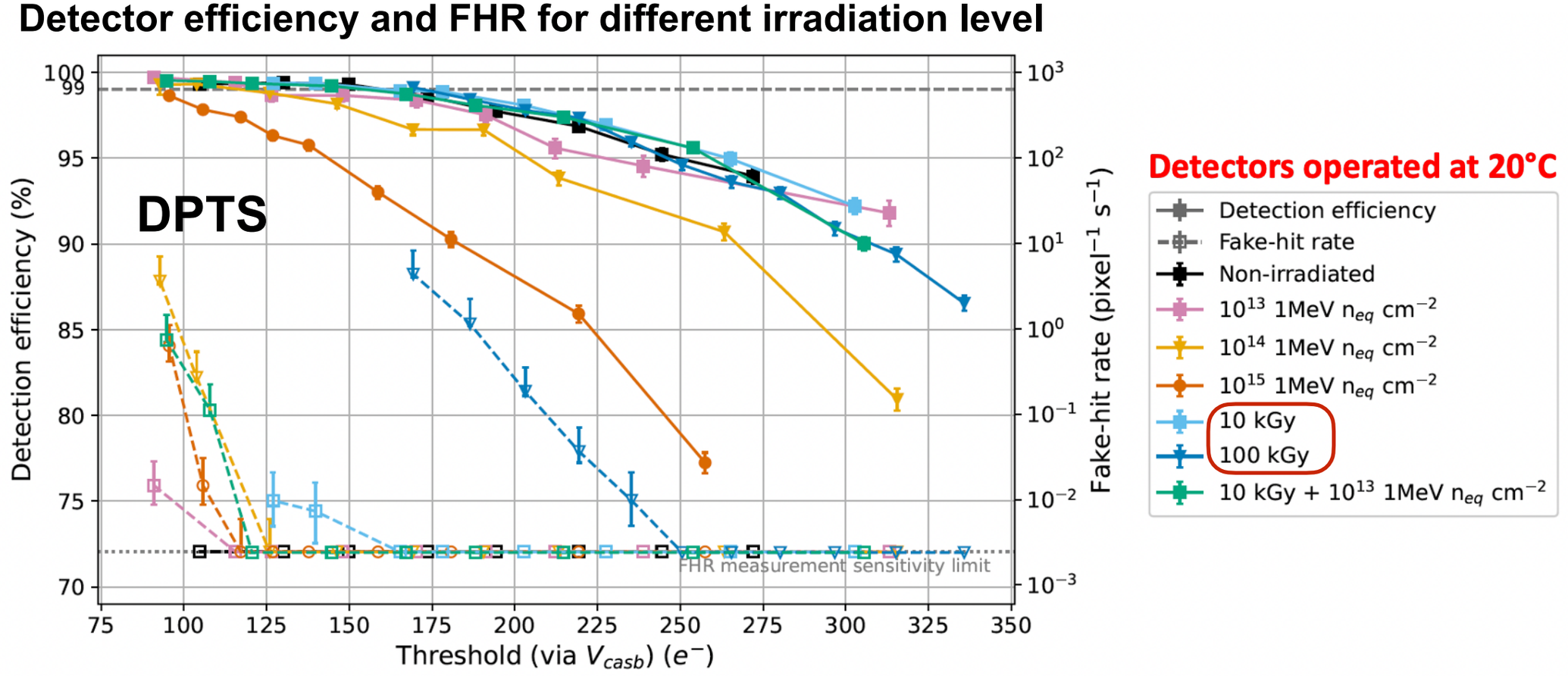

Gianluca Aglieri Rinella et al. arXiv:2212.08621v2

65 nm CMOS technology: first prototypes characterization

DPTS

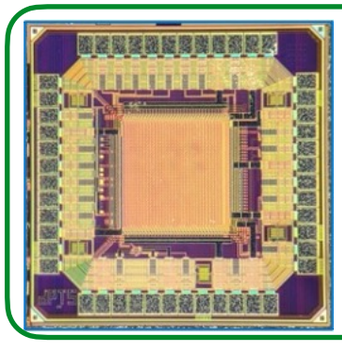

- 32x32 pixel matrix
- Asynchronous digital readout
- Time-over-threshold information
- Pixel pitch: 15 µm

» Non-ionising irradiation leads to a decrease in the detection efficiency

» Ionising irradiation leads to an increase in the fake-hit rate

» 10^{15} 1 MeV n_{eq} cm^{-2} can be operated at the temperature of +20ºC (99% efficiency)

Detector efficiency and FHR for different irradiation level

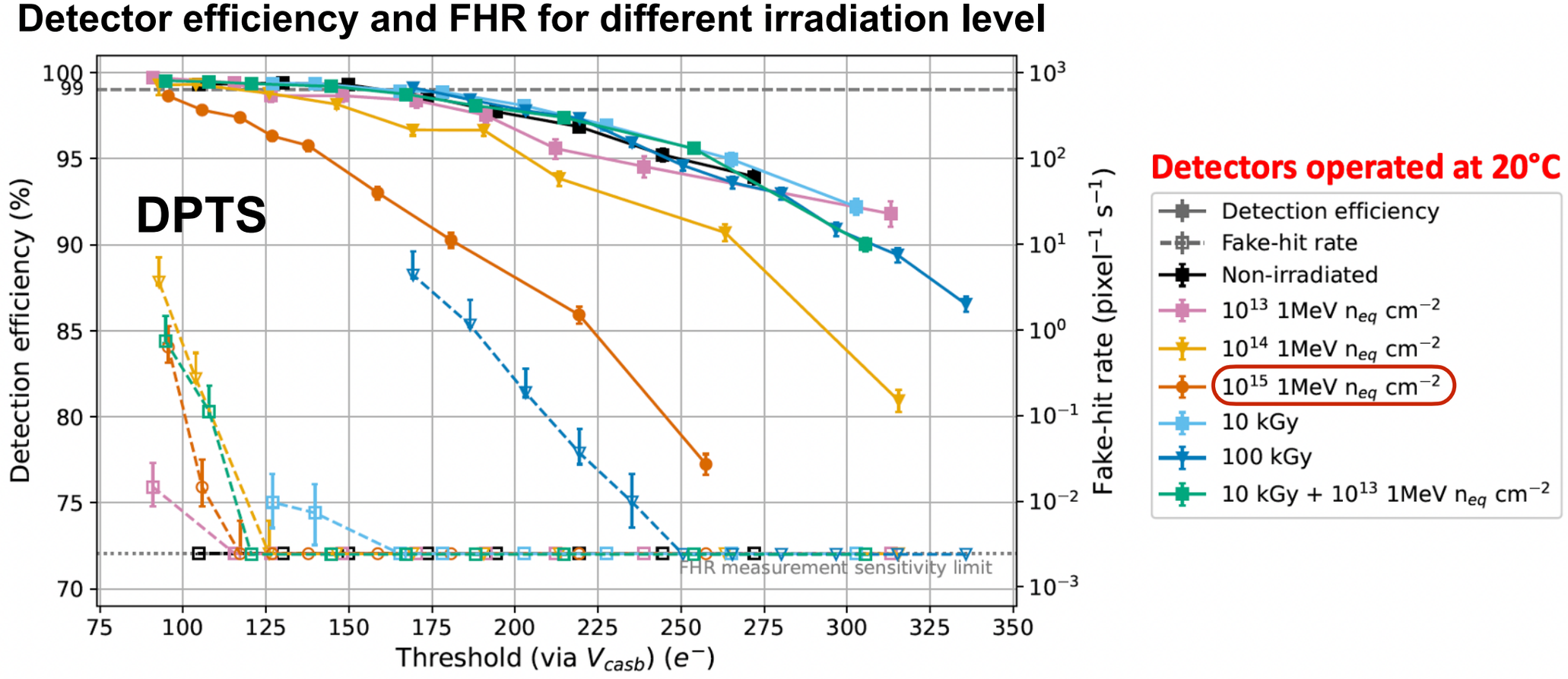

Gianluca Aglieri Rinella et al. arXiv:2212.08621v2

65 nm CMOS technology: first prototypes characterization

DPTS

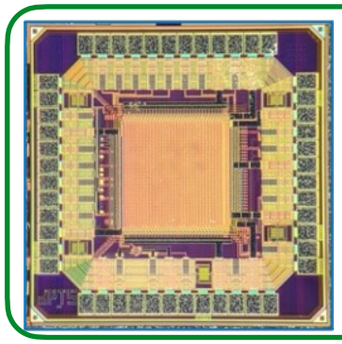

- 32x32 pixel matrix
- Asynchronous digital readout
- Time-over-threshold information
- Pixel pitch: 15 μm

» Non-ionising irradiation leads to a decrease in the detection efficiency

» Ionising irradiation leads to an increase in the fake-hit rate

» 10^{15} 1 MeV n_{eq} cm^{-2} can be operated at the temperature of +20ºC (99% efficiency)

» detection efficiency decreases when the particle track is further away from the collection diode

Detector efficiency and FHR for different irradiation level

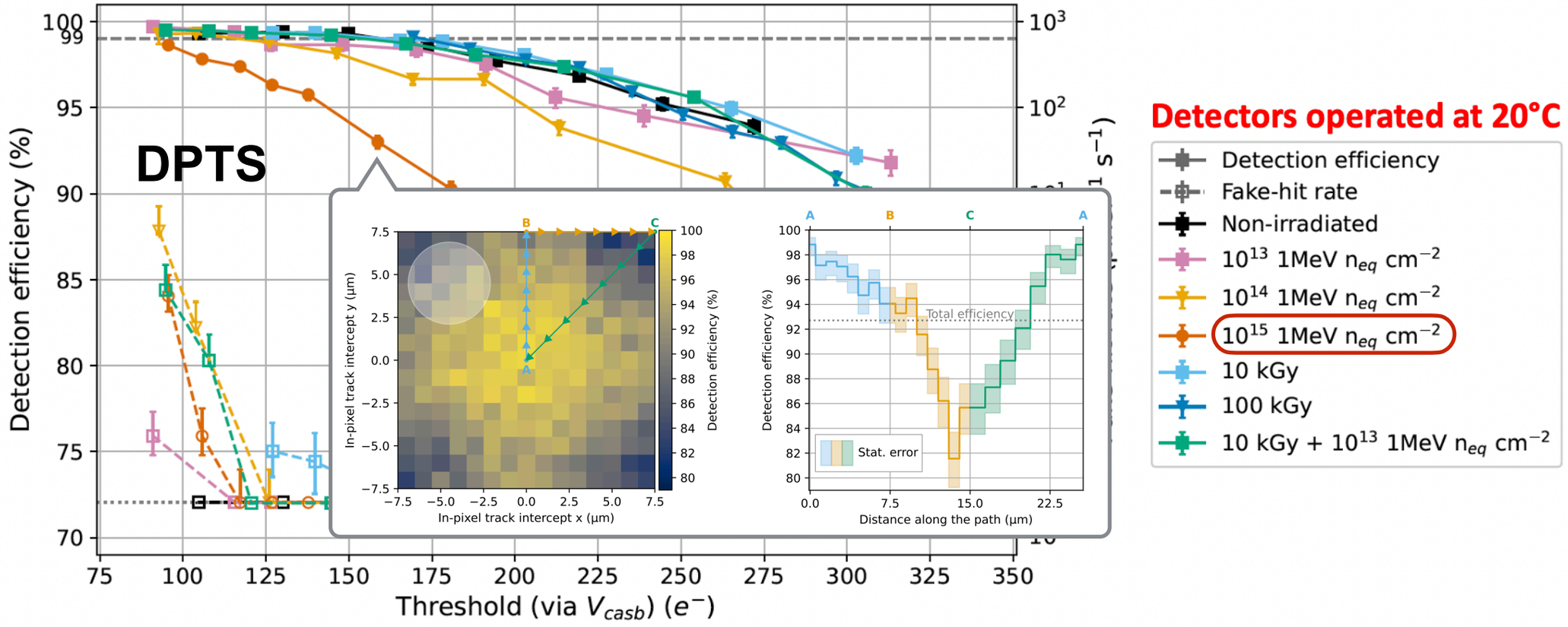

Gianluca Aglieri Rinella et al. arXiv:2212.08621v2

Backup

65 nm CMOS technology: first prototypes characterization

DPTS

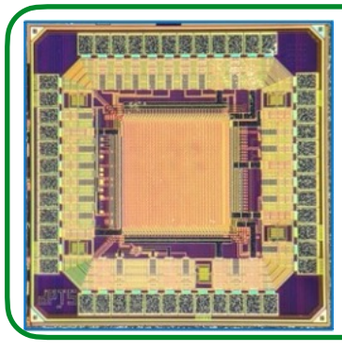

- 32x32 pixel matrix
- Asynchronous digital readout
- Time-over-threshold information
- Pixel pitch: 15 μm

» Non-ionising irradiation leads to a decrease in the detection efficiency

» Ionising irradiation leads to an increase in the fake-hit rate

» 10^{15} 1 MeV n_{eq} cm^{-2} can be operated at the temperature of +20ºC (99% efficiency)

» detection efficiency decreases when the particle track is further away from the collection diode

Detector efficiency and FHR for different irradiation level

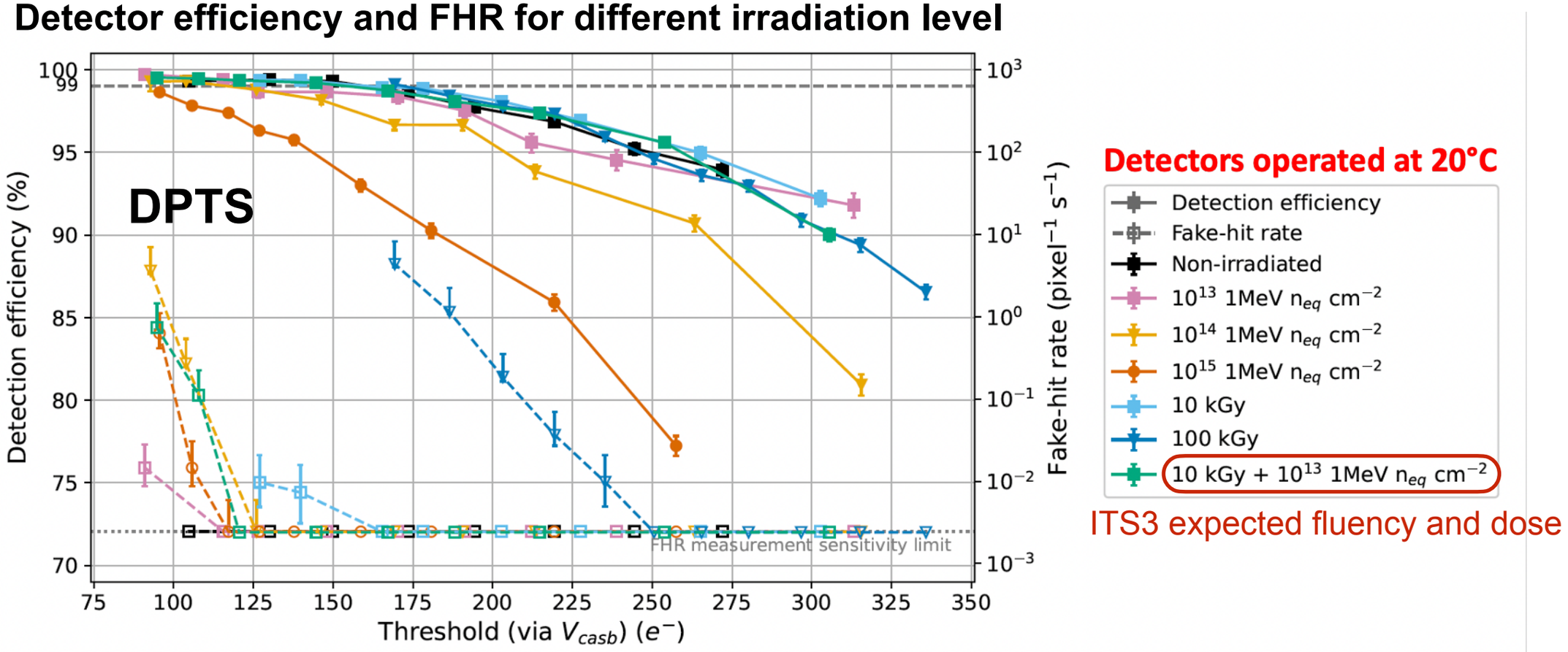

ITS3 expected fluency and dose

Gianluca Aglieri Rinella et al. arXiv:2212.08621v2

Backup

65 nm CMOS technology: first prototypes characterization

DPTS

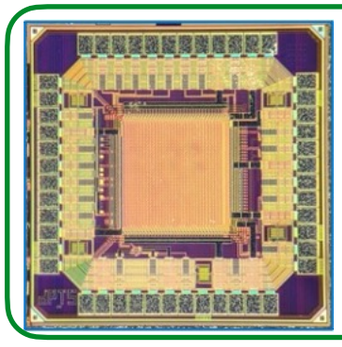

- 32x32 pixel matrix
- Asynchronous digital readout
- Time-over-threshold information
- Pixel pitch: 15 µm

Sketch of the beam test telescope

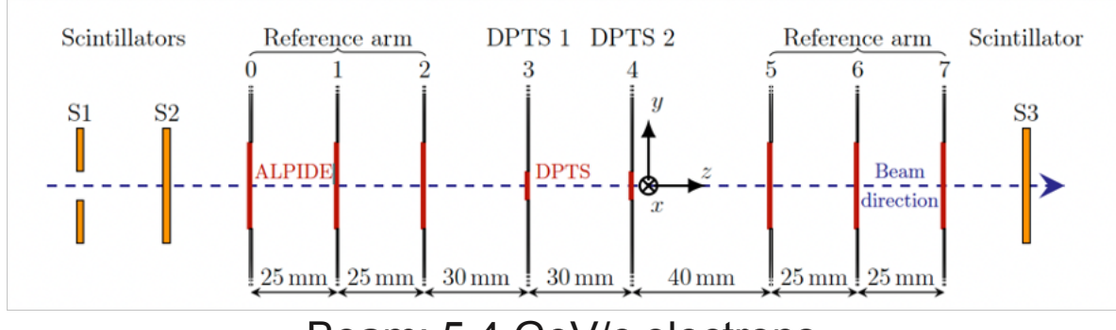

Beam: 5.4 GeV/c electrons
Trigger by scintillators or one of the two DPTS

DPTS timing resolution

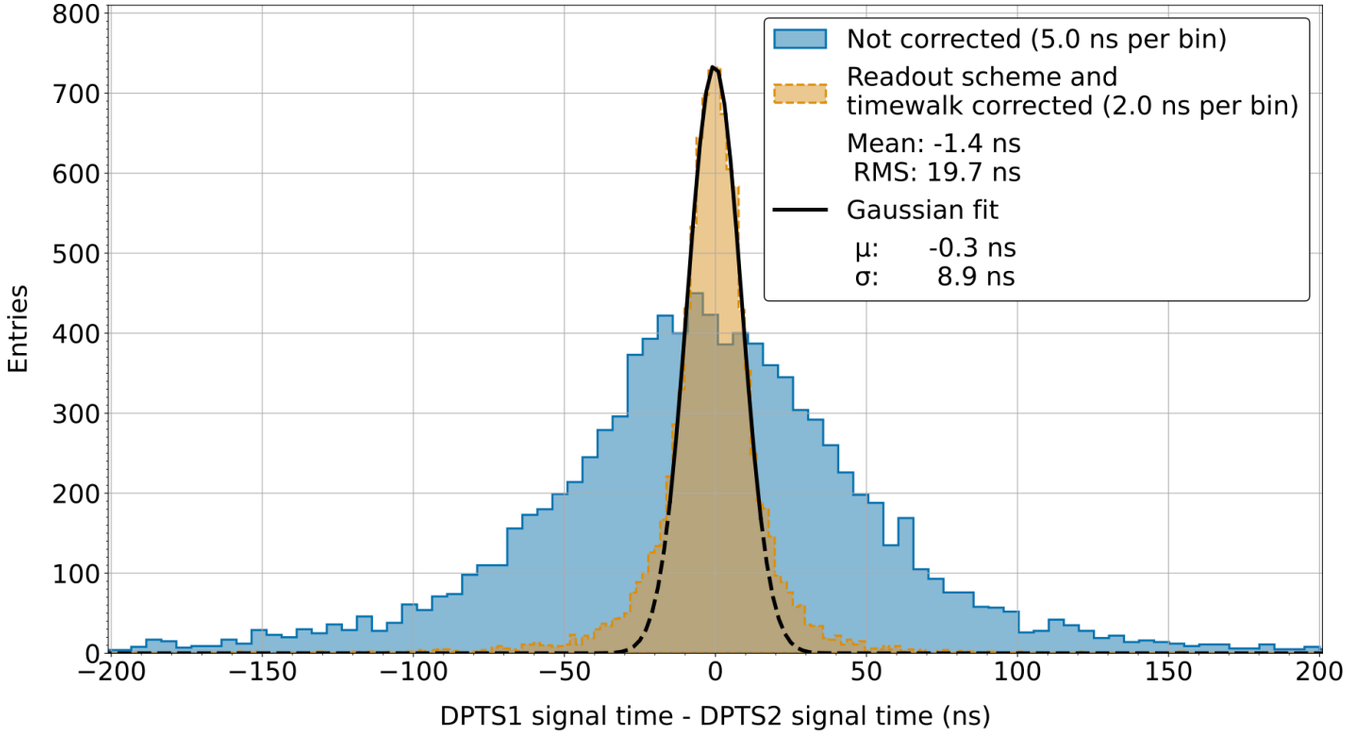

» Time residual distributions of two DPTSs with no corrections (blue) and with readout scheme and time walk corrections applied (orange)

» Timing resolution:

$\sigma_{gauss}/\sqrt{2} = 6.3 \pm 0.1$ ns

» FE parameters not optimised for timing performance (I_{bias} = 10 nA)

Gianluca Aglieri Rinella et al. arXiv:2212.08621v2

Backup

65 nm CMOS technology: first prototypes characterization

APTS

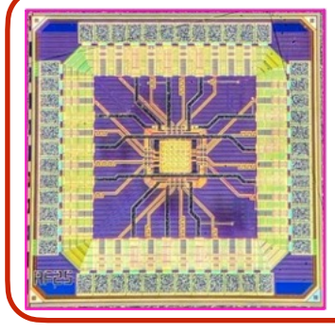

- 6x6 pixel matrix
- Direct analogue readout of central 4x4 submatrix
- Two types of output drivers:
  1. Traditional source follower (APTS-SF)
  2. **Very fast OpAmp (APTS-OA)**
- 4 pixel pitches: 10, 15, 20, 25 µm

APTS-OA timing response: standard vs modified with gap

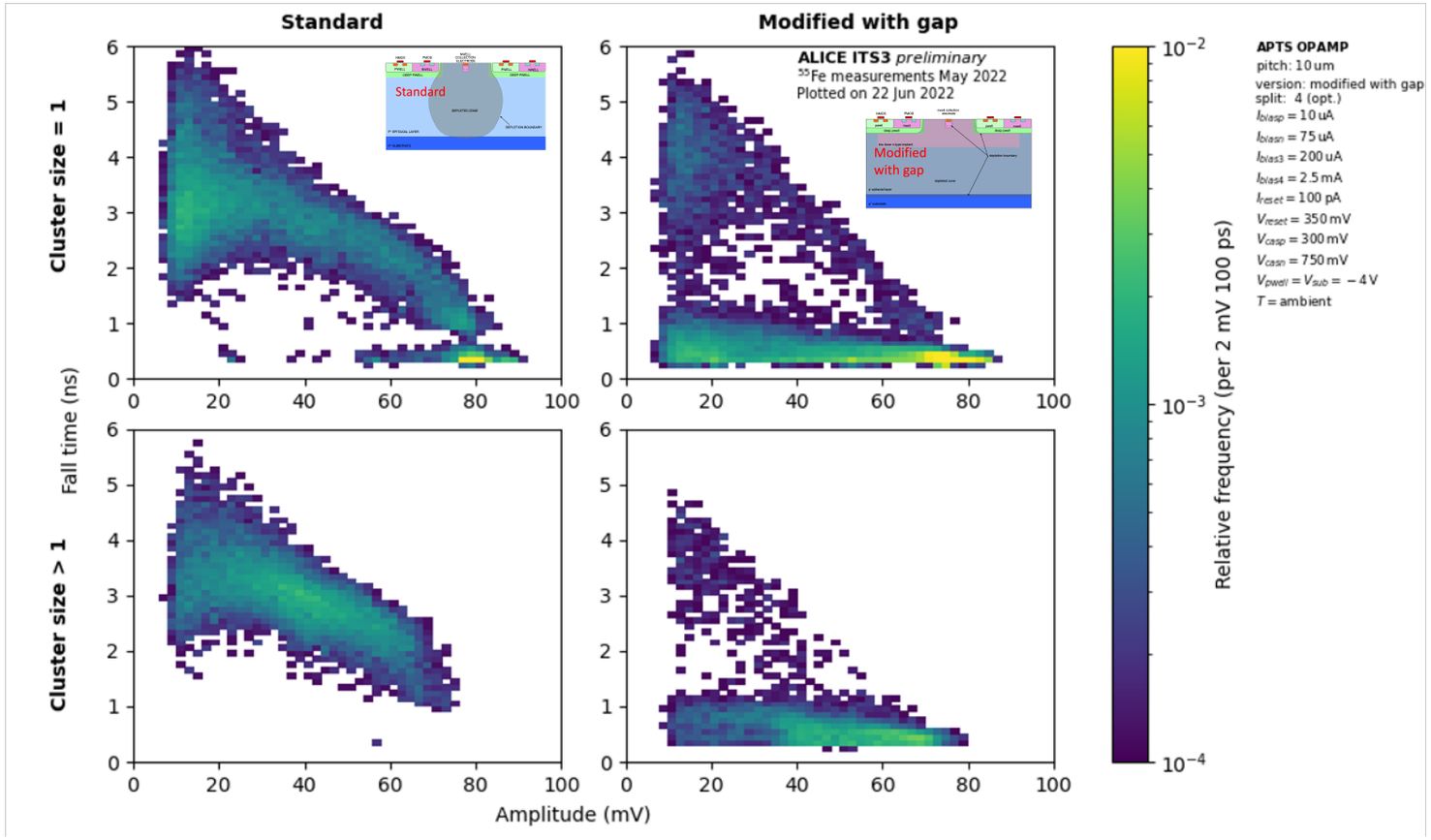

» Fast readout allows to estimate the charge collection time via signal fall time

» In *modified with gap* process charge collection is faster and amplitude in larger

Backup

65 nm CMOS technology: first prototypes characterization

APTS

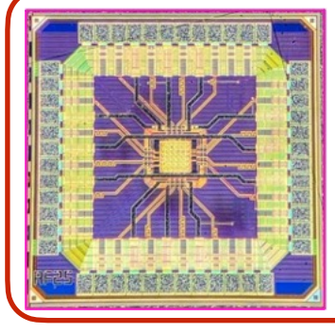

- 6x6 pixel matrix
- Direct analogue readout of central 4x4 submatrix
- Two types of output drivers:
  1. Traditional source follower (APTS-SF)
  2. **Very fast OpAmp (APTS-OA)**
- 4 pixel pitches: 10, 15, 20, 25 µm

APTS-OA timing response

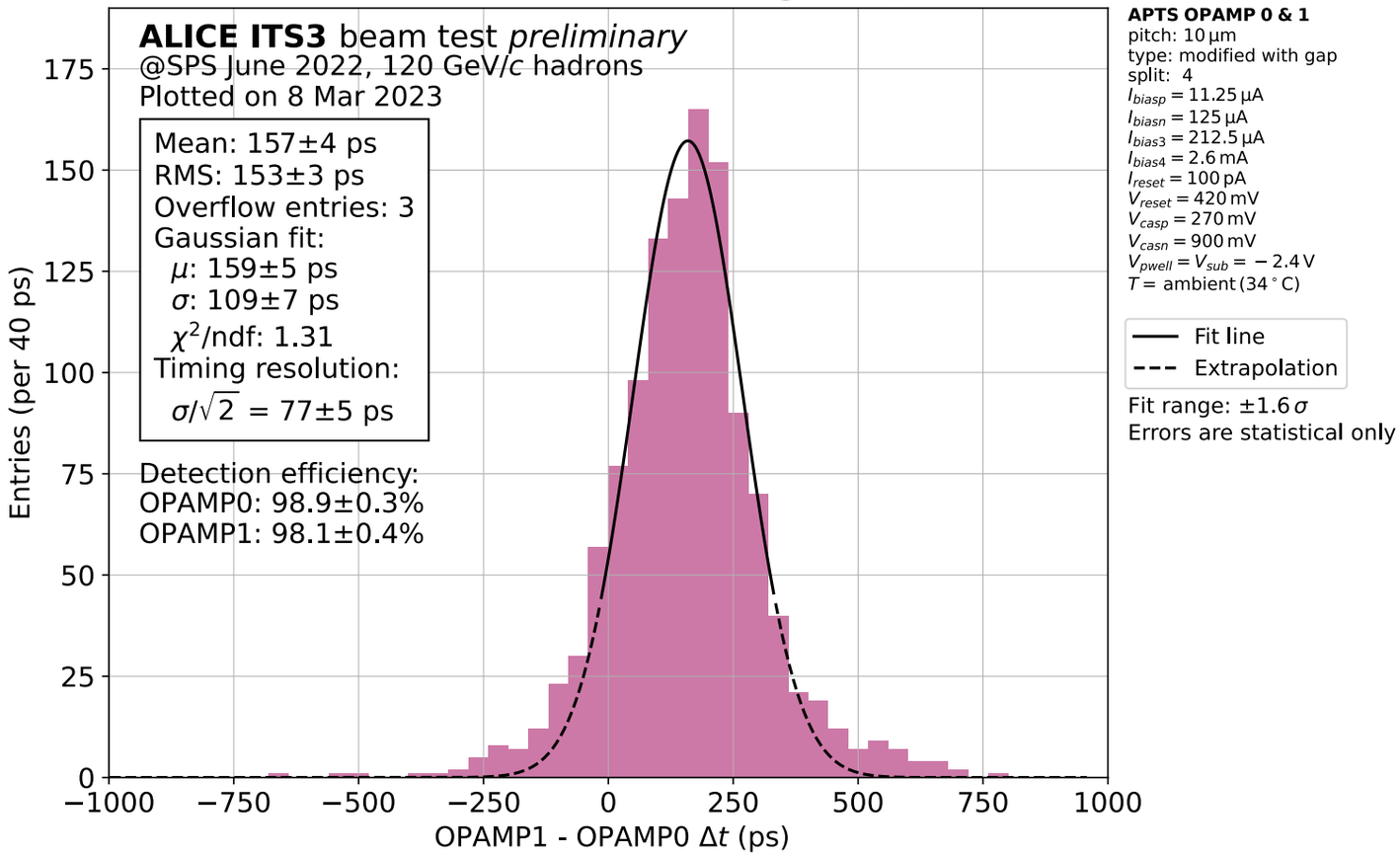

- CFD Time stamp $t = t_{10\%CFD}$
- Time difference $\Delta t = t_{OPAMP1} - t_{OPAMP0}$ distribution fitted with a Gaussian function
- Efficiency on both OPAMP plane ~99% (at threshold 5.5 mV = 150e)
- **Time resolution: 77 ± 5 ps** without time walk/jitter corrections

Backup

R&D activities - ALPIDE chip bending

» MAPS at thickness used in current detectors (~50 μm) are quite flexible

» Large benefit from going even a bit thinner: the bending force scales with thickness to the third power

» The breaking point moves to smaller bending radii when going thinner

» Project goal thicknesses and desired bending radii are in a “not breaking” regime

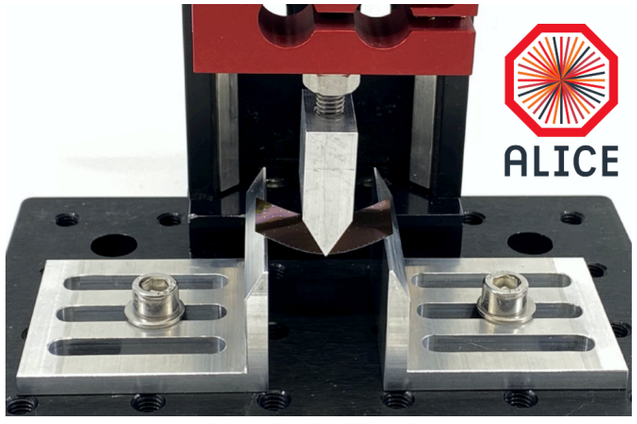

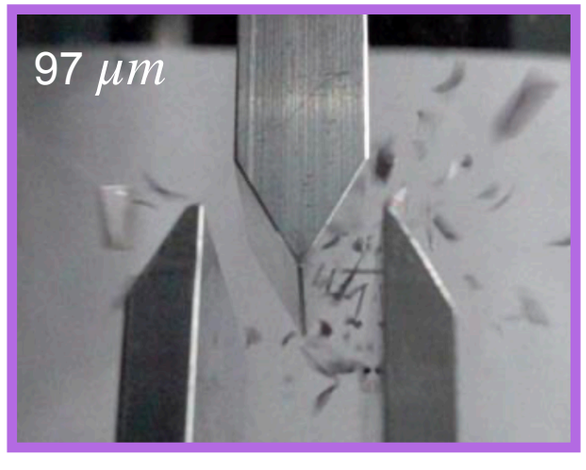

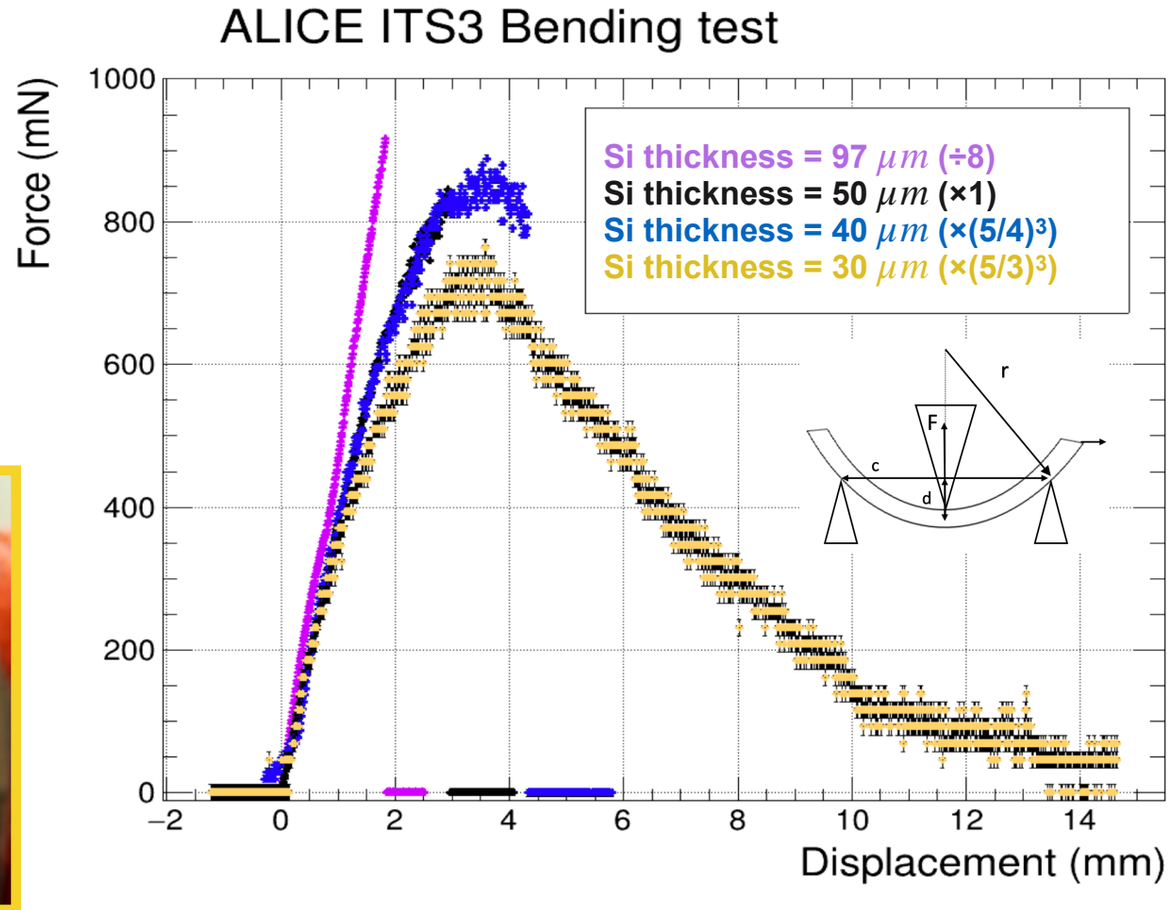

R&D activities - Wafer-scale silicon bending

» Developed procedure allows silicon bending in a repeatable reliable way

» Bending tool: tensioned mylar foil wrapping around a cylindrical mandrel

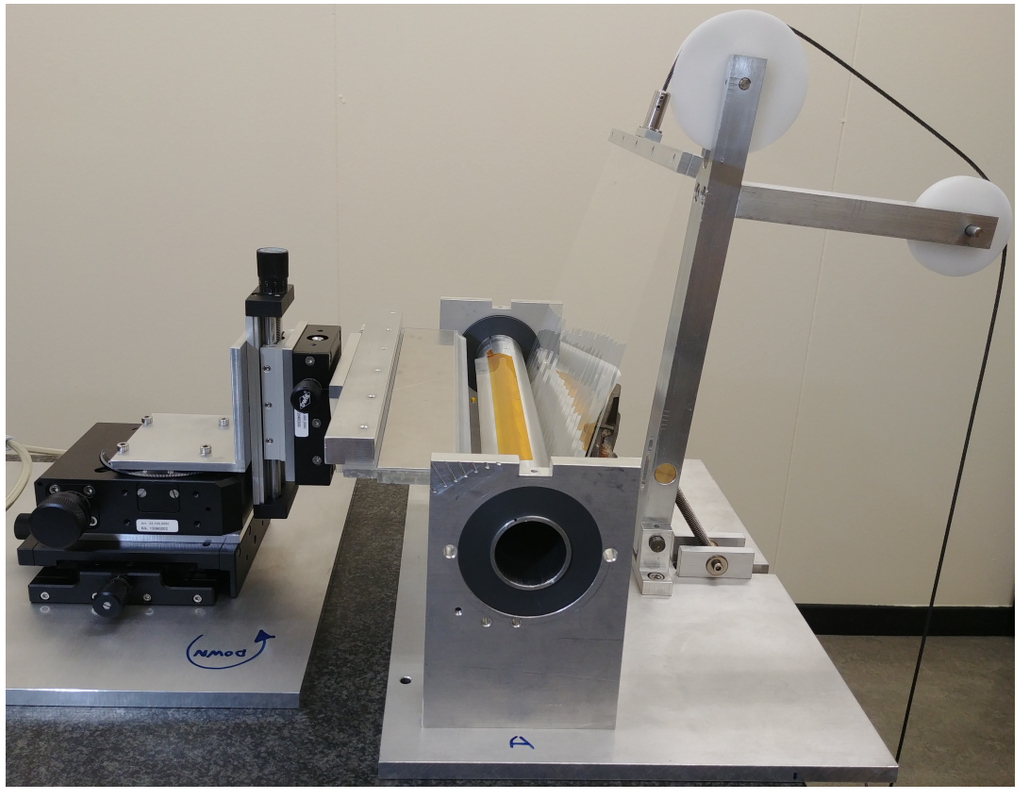

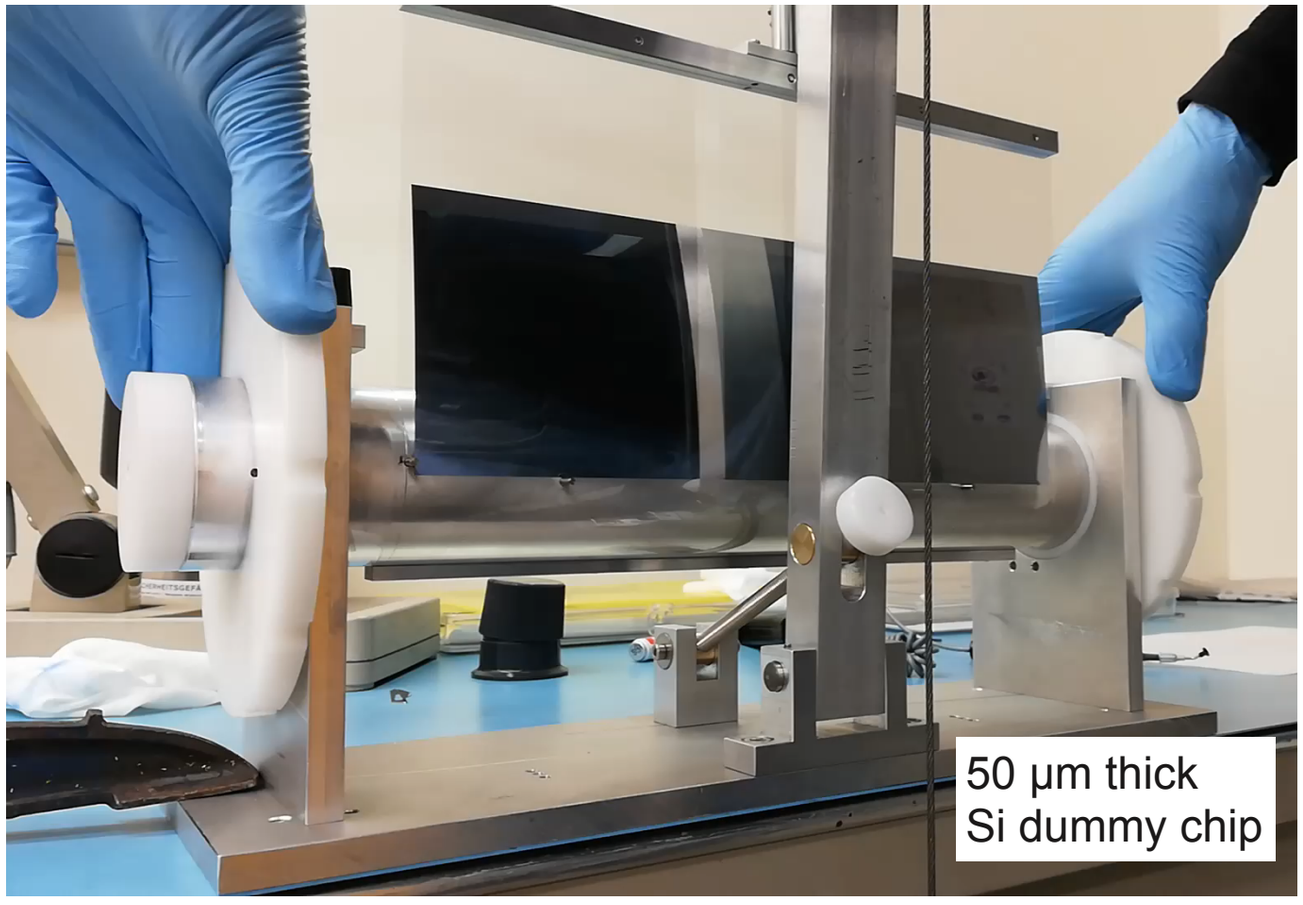

Backup

R&D activities - Carbon foam characterisation

» Different foams characterised for machinability and thermal properties

ERG DUOCEL
0.06 kg/dm³
0.033 W/m·K

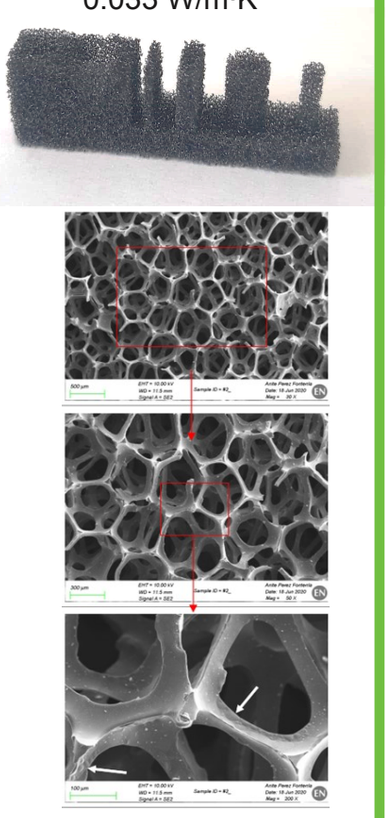

ALLCOMP LD
0.2-0.26 kg/dm³
>17 W/m·K

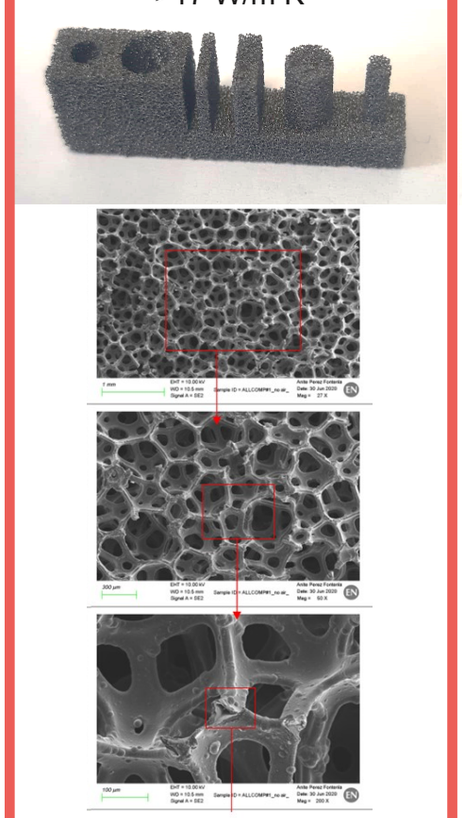

ALLCOMP HD
0.45-0.68 kg/dm³
85-170 W/m·K

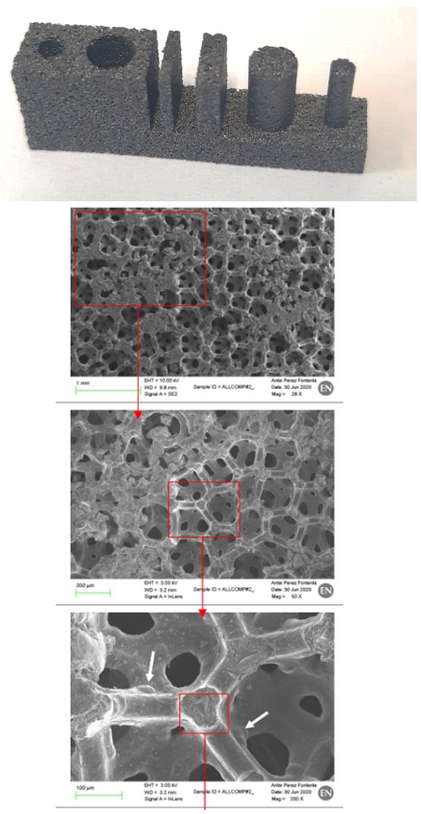

Longerons and wedge ← ERG DUOCEL
Support

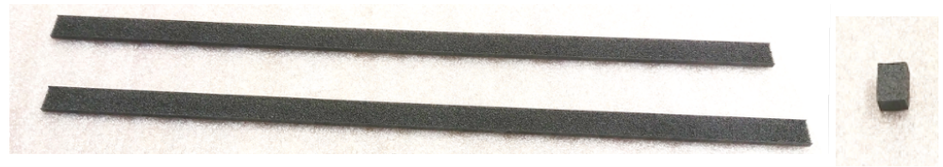

Half-ring ← ALLCOMP LD
Support + Cooling

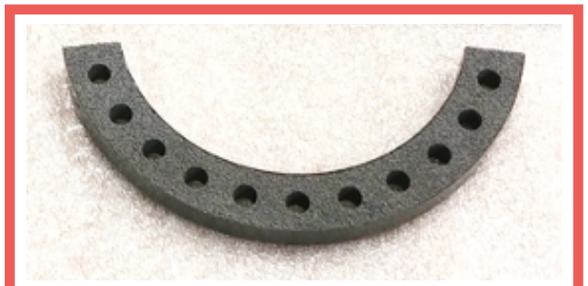

Fleece to reduce glue

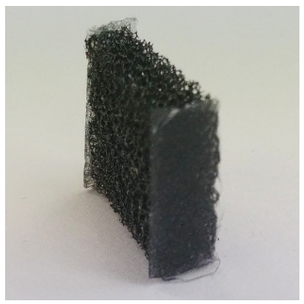

Backup

R&D activities - Carbon foam characterisation

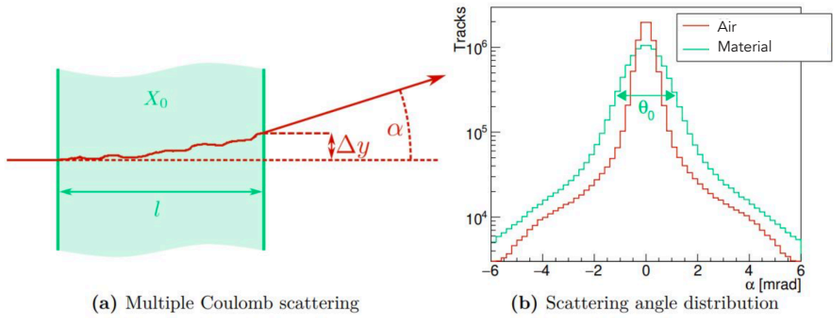

(a) Multiple Coulomb scattering (b) Scattering angle distribution

Taken from [Paul Schütze, 2019, Dissertation]

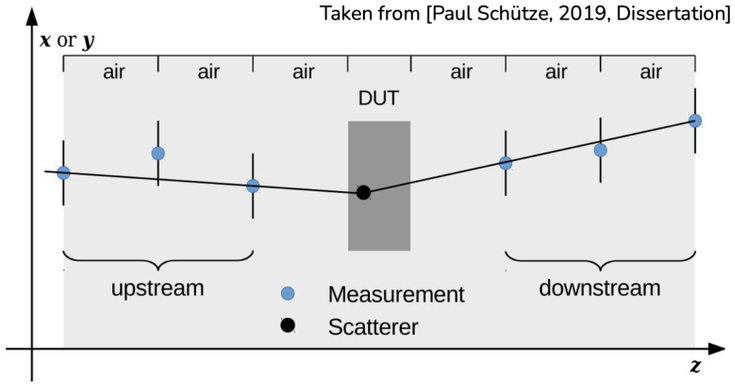

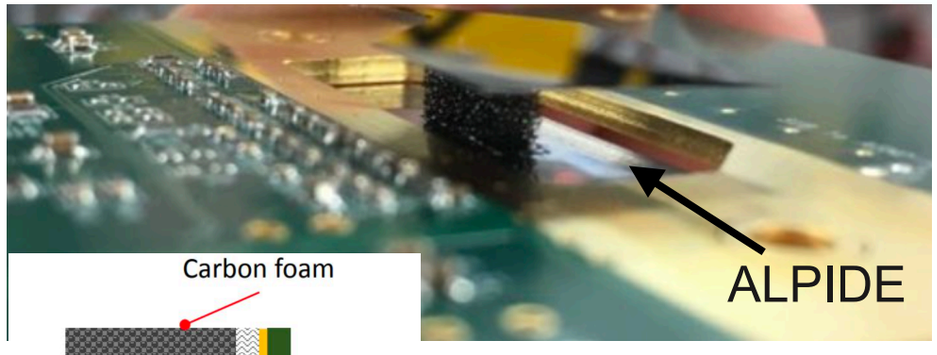

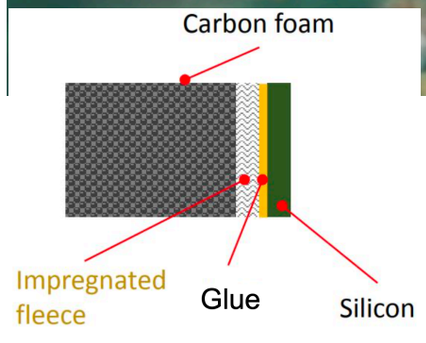

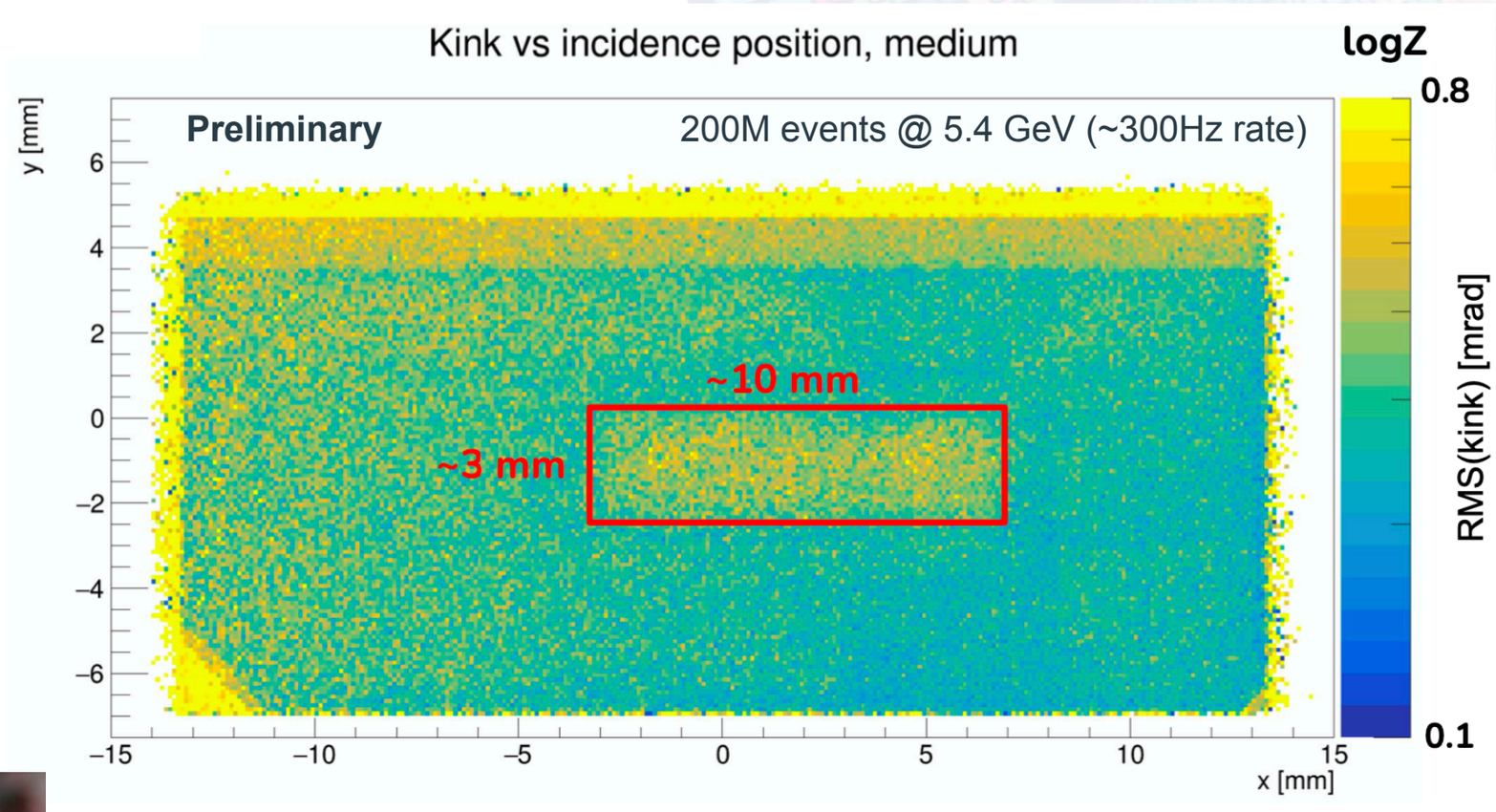

» Analysis of the kink angle distributions at the position of a scatterer

» Material budget image: represents the widths of the scattering angle distribution of all particles traversing a given bin

Backup

R&D activities - Layer assembly procedure

» Different options under study (including vacuum clamping)
» Currently working solution based on adhesive caption tape

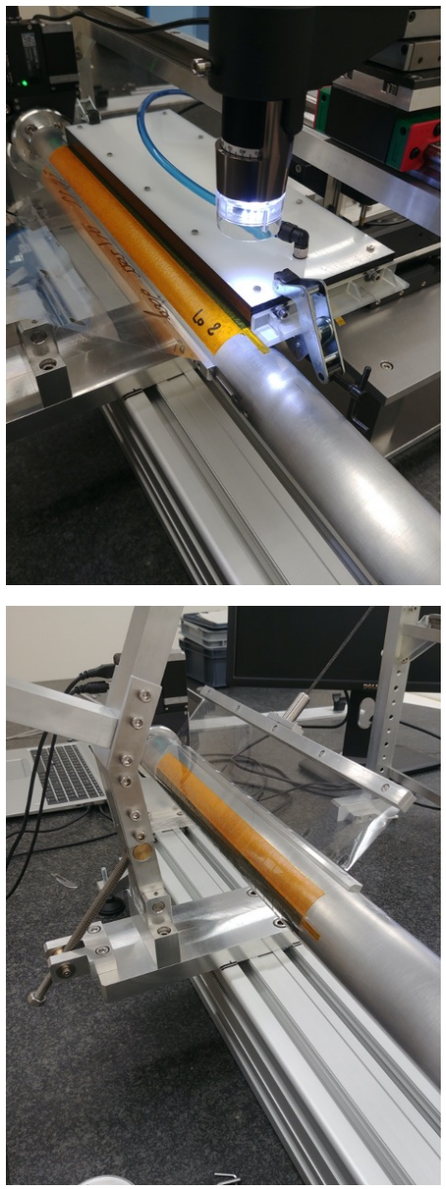
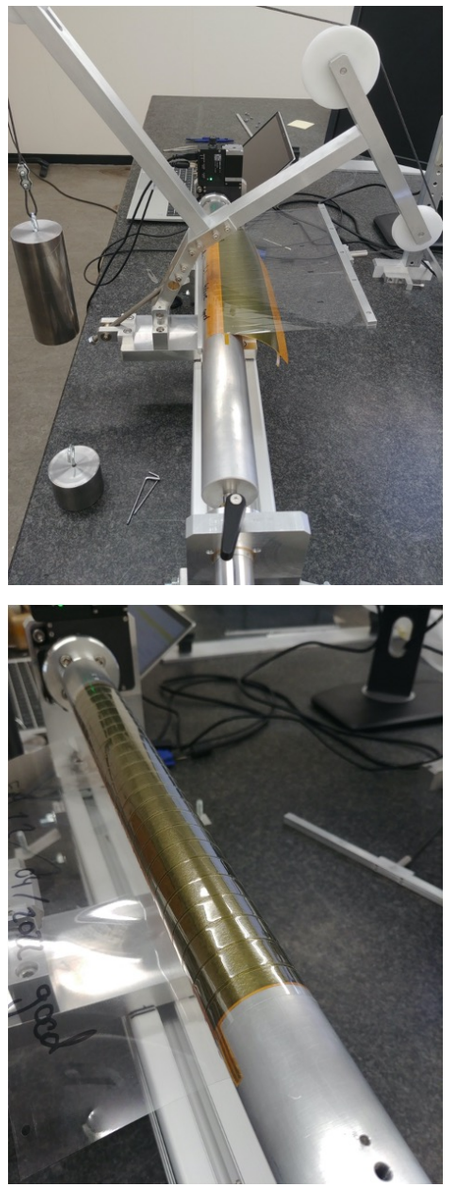

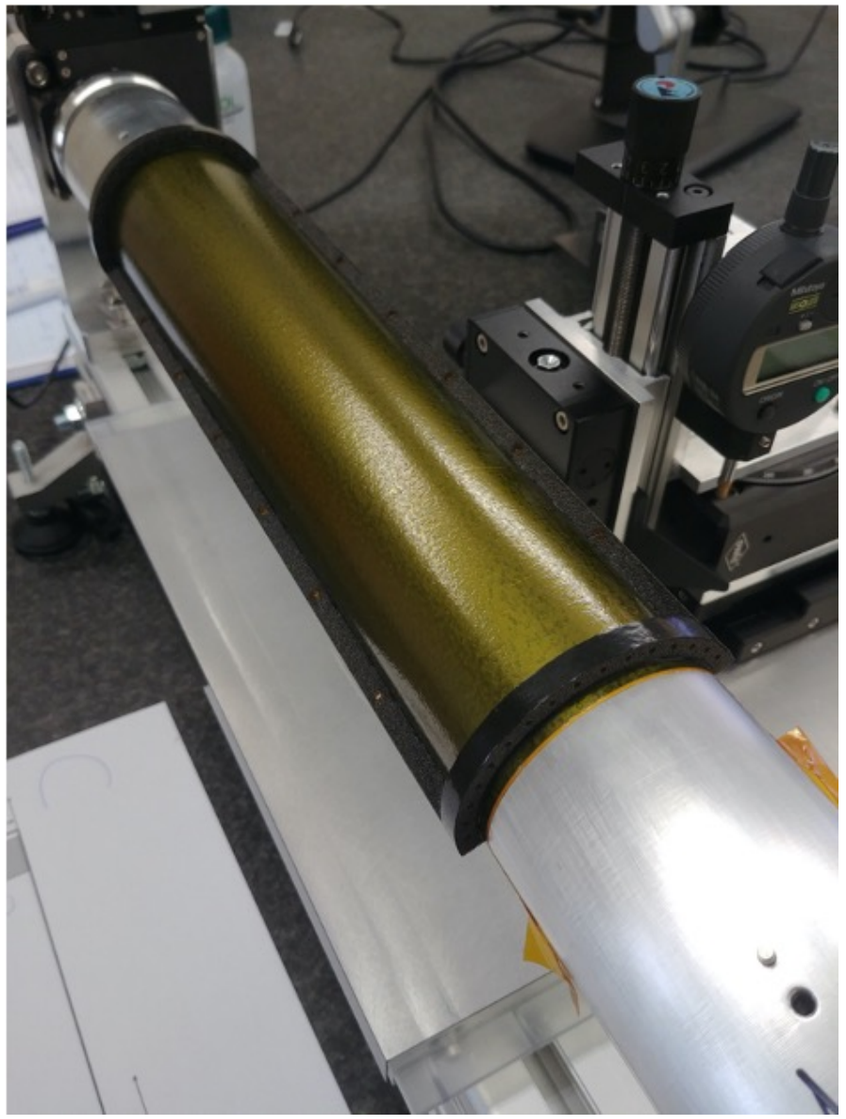

Backup

R&D activities - Layer assembly procedure

» Different options under study (including vacuum clamping)
» Currently working solution based on adhesive caption tape

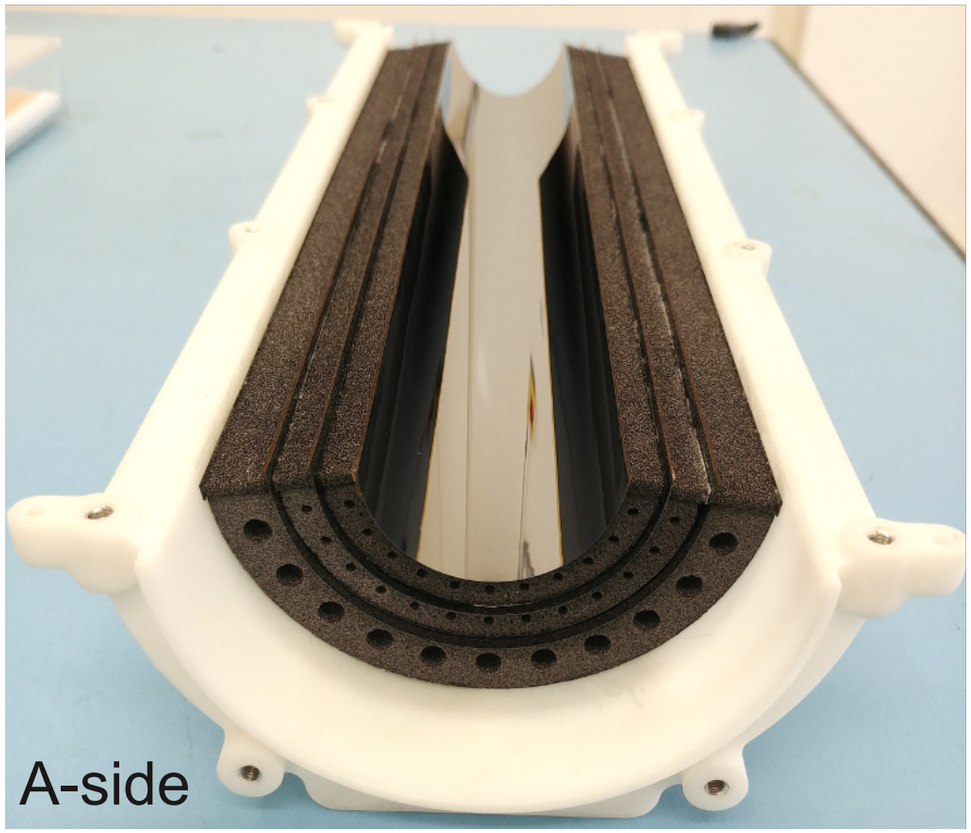

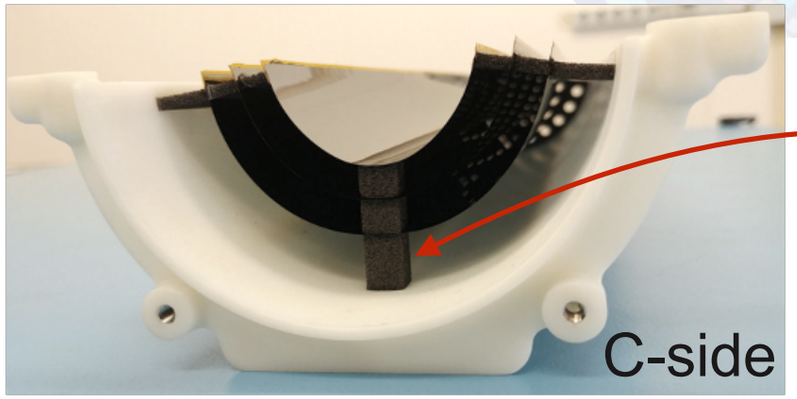

Wedges replaced with half-ring due to excessive deformation from cylindrical shape

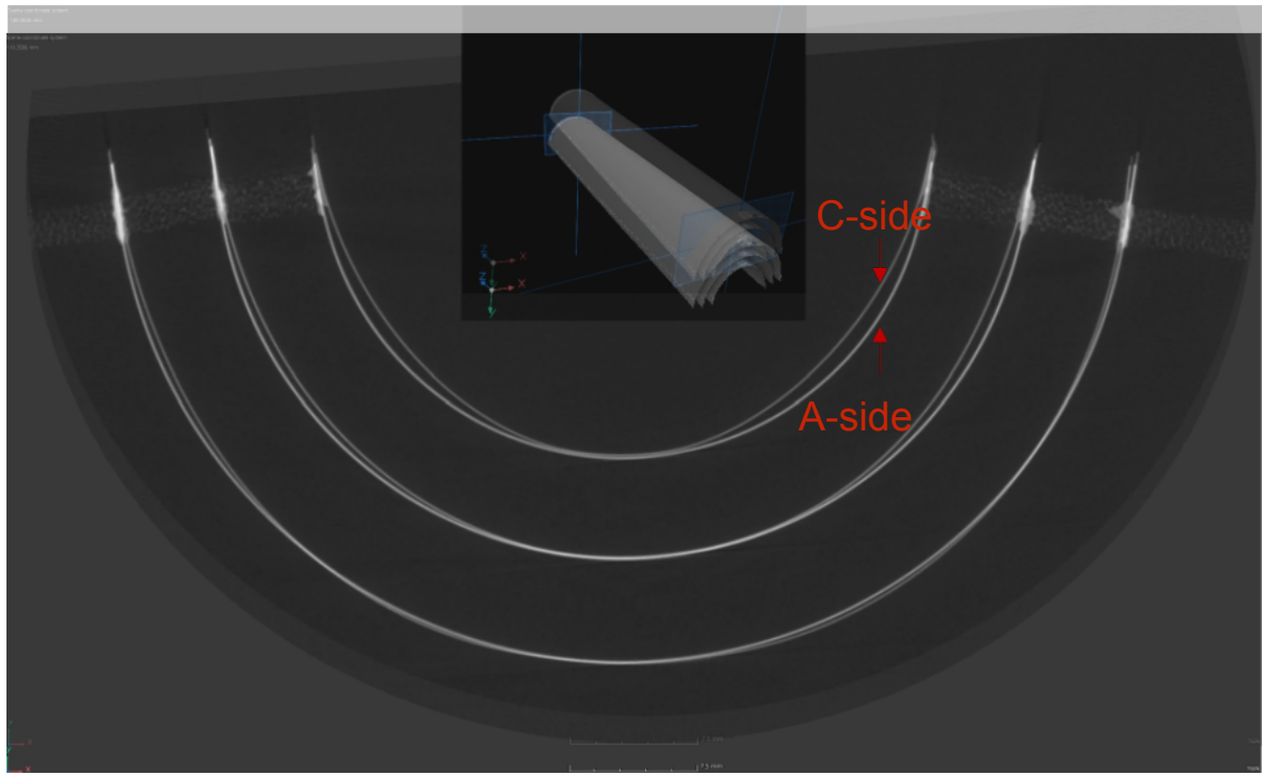

Backup

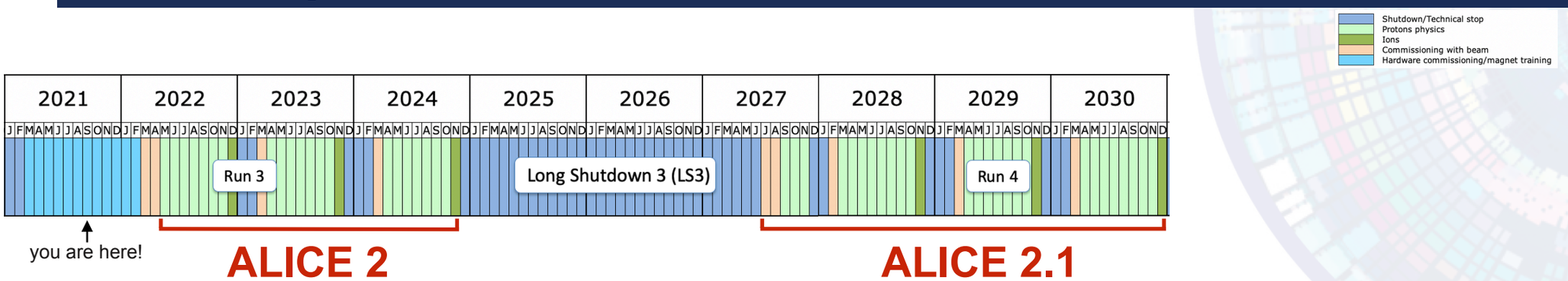

Data taking strategy

» **Record large minimum-bias data sample**

→ read out all Pb-Pb interactions up to maximum LHC collision rate of 50 kHz (was ~1 kHz in the central barrel)

→ increase Pb-Pb Run 2 minimum-bias sample by factor 50-100

Colliding System	Integrated luminosity	Comment
Pb-Pb @ $\sqrt{s_{NN}}$ = 5 - 5.5 TeV	13 nb^{-1}	Plus pp reference data
p-Pb @ $\sqrt{s_{NN}}$ = 8 - 8.8 TeV	0.6 pb^{-1}	Plus pp reference data
pp @ $\sqrt{s}$ = 14 TeV	200 pb^{-1}	Focus on high multiplicity and rare signals

» **Improve tracking efficiency and resolution at low-p_T**

→ increase tracking granularity

→ reduce material thickness

» **Preserve Particle IDentification (PID)**

→ consolidate and speed-up main ALICE PID detectors

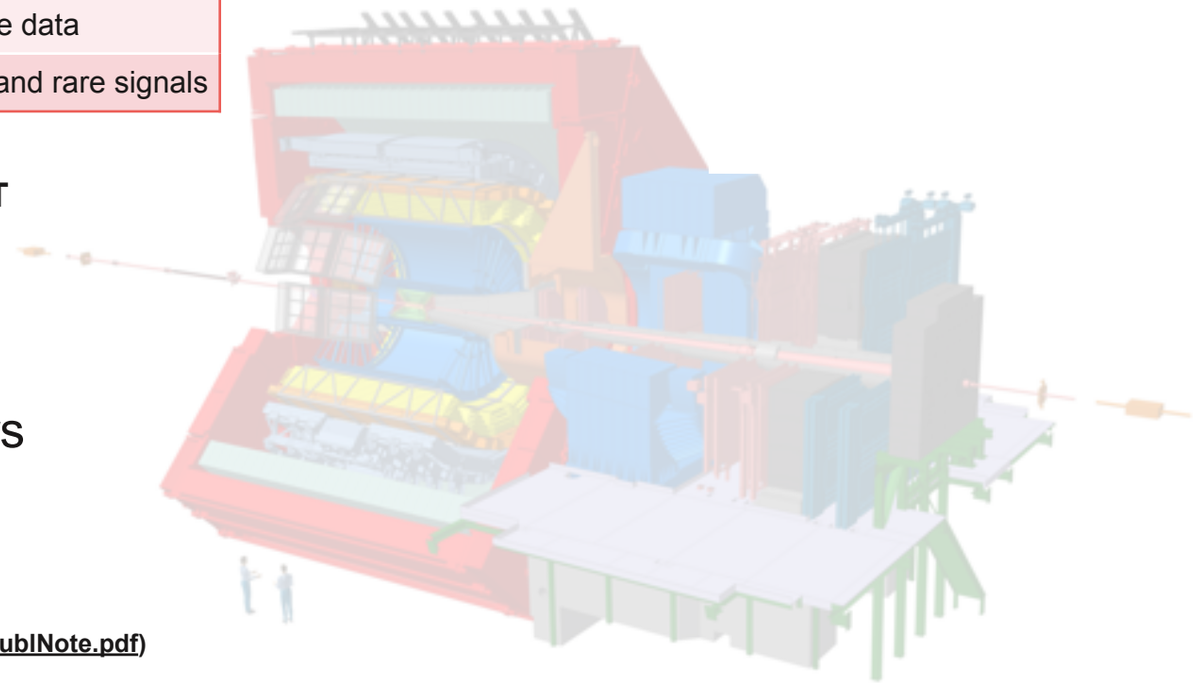

Programme is presented in CERN Yellow Report (https://arxiv.org/abs/1812.06772)
Future high-energy pp programme with ALICE (https://cds.cern.ch/record/2724925/files/ALICE_HEpp_PublNote.pdf)
LHC schedule

Backup

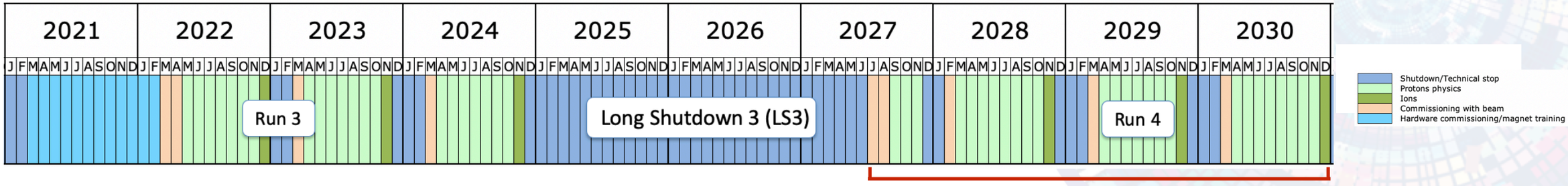

ALICE 2.1

Expression of Interest

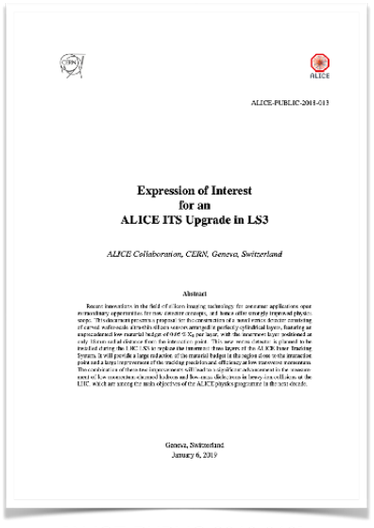

ALICE-PUBLIC-2018-013

Expression of Interest for an ALICE ITS Upgrade in LS3

ALICE Collaboration, CERN, Geneva, Switzerland

Abstract

Geneva, Switzerland
January 6, 2019

[ALICE-PUBLIC-2018-013]
https://cds.cern.ch/record/2644611

Letter of Intent

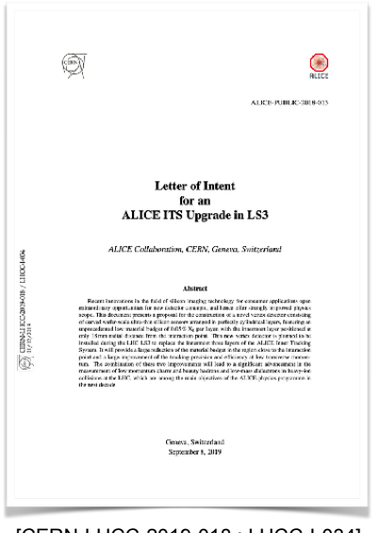

ALICE-PUBLIC-2019-015

Letter of Intent for an ALICE ITS Upgrade in LS3

ALICE Collaboration, CERN, Geneva, Switzerland

Abstract

Geneva, Switzerland
September 9, 2019

[CERN-LHCC-2019-018 ; LHCC-I-034]
https://cds.cern.ch/record/2703140/

LHCC 139 (Sep 2019)

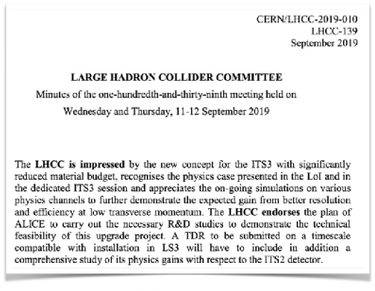

CERN/LHCC-2019-010
LHCC-139
September 2019

LARGE HADRON COLLIDER COMMITTEE

Minutes of the one-hundredth-and-thirty-ninth meeting held on
Wednesday and Thursday, 11-12 September 2019

The **LHCC is impressed** by the new concept for the ITS3 with significantly reduced material budget, recognises the physics case presented in the LoI and in the dedicated ITS3 session and appreciates the on-going simulations on various physics channels to further demonstrate the expected gain from better resolution and efficiency at low transverse momentum. The **LHCC endorses** the plan of ALICE to carry out the necessary R&D studies to demonstrate the technical feasibility of this upgrade project. A TDR to be submitted on a timescale compatible with installation in LS3 will have to include in addition a comprehensive study of its physics gains with respect to the ITS2 detector.

"The LHCC is **impressed** by the new concept for the ITS3…"

Project setup (spring 2020)

- Project leaders
- Work packages conveners
- Institutes joining

LHCC 142 (Jun 2020)

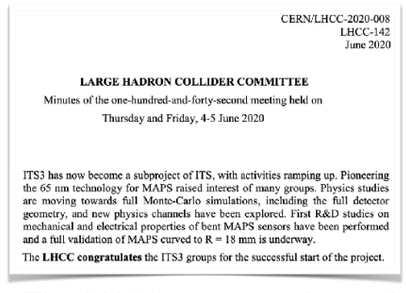

CERN/LHCC-2020-008
LHCC-142
June 2020

LARGE HADRON COLLIDER COMMITTEE

Minutes of the one-hundred-and-forty-second meeting held on
Thursday and Friday, 4-5 June 2020

ITS3 has now become a subproject of ITS, with activities ramping up. Pioneering the 65 nm technology for MAPS raised interest of many groups. Physics studies are moving towards full Monte-Carlo simulations, including the full detector geometry, and new physics channels have been explored. First R&D studies on mechanical and electrical properties of bent MAPS sensors have been performed and a full validation of MAPS curved to R = 18 mm is underway.

The **LHCC congratulates** the ITS3 groups for the successful start of the project.

"The LHCC **congratulates** the ITS3 groups for the successful start of the project."

Oct 2018 — **Sep 2019** — **Sep 2019** — **Dec 2019** — **Spring 2020** — **Jun 2020**

Backup

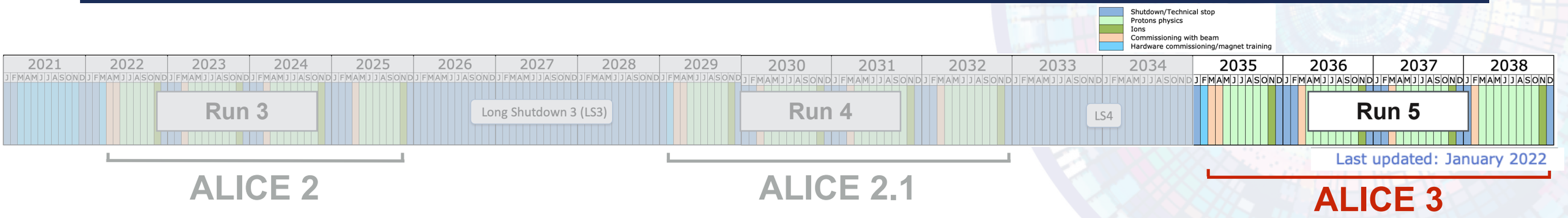

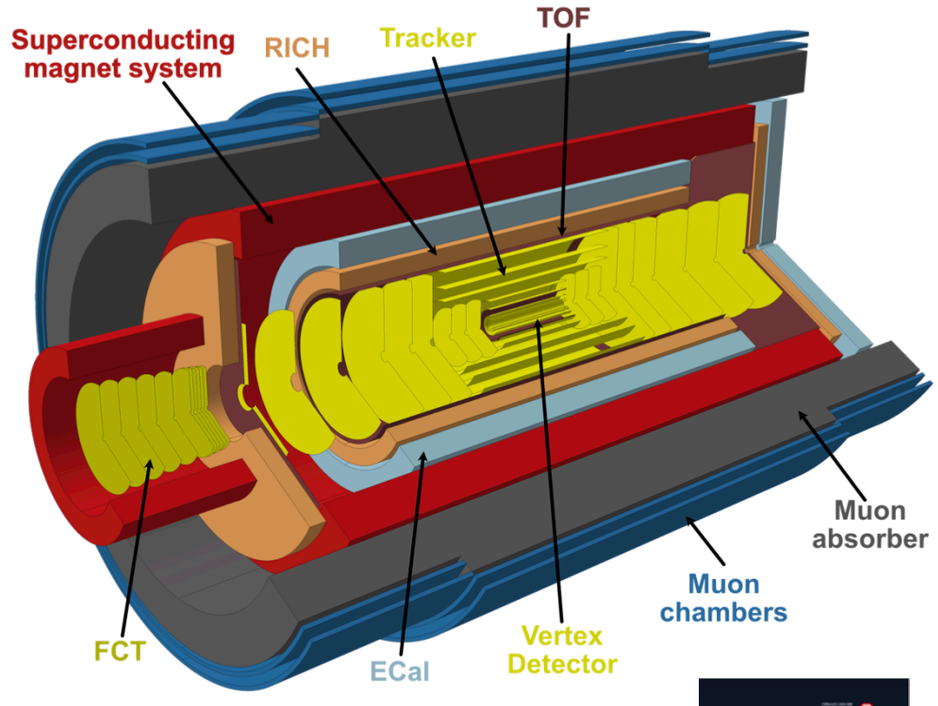

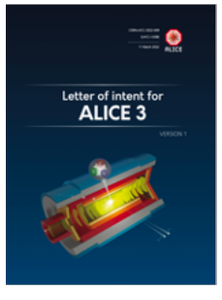

Physics program

» **Charm and beauty hadrons correlation** over a wide rapidity range

» Systematic measurements of **multiply heavy-flavoured hadrons** (expected enhanced production from the QGP)

» Production and behaviour of the **charmed exotic states** in the QGP and their structure

» **Multi-differential measurements of electromagnetic radiation** from the QGP (probe early evolution and restoration of chiral symmetry)

» Measurements of **net-quantum number fluctuations** over a wide rapidity range (constrain susceptibilities of QGP and to test the realisation of a cross-over phase transition)

Expression of Interest (2019): https://arxiv.org/abs/1902.01211
LoI (2022) [LHCC-2022-009]: https://cds.cern.ch/record/2803563?ln=fr